

AD-A242 089



2 *Um*

ESL-TR-90-12

# HIGH-INTENSITY COMPRES- SIVE STRESS WAVE PROPAGA- TION THROUGH UNSATURATED SANDS

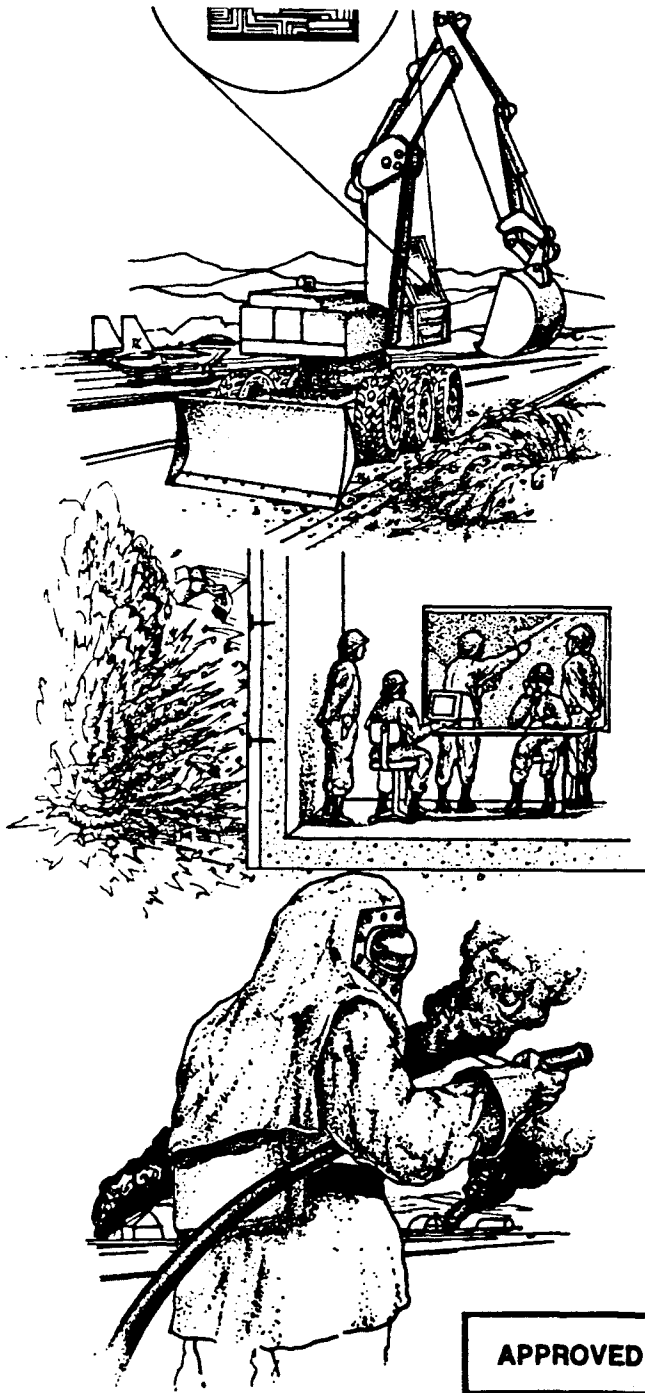
S.J. PIERCE AND W.A. CHARLIE

GEOTECHNICAL ENGINEERING PROGRAM  
COLORADO STATE UNIVERSITY  
FORT COLLINS COLORADO 80523

SEPTEMBER 1990

FINAL REPORT

MAY 1989 — SEPTEMBER 1989



DTIC  
ELECTE  
OCT 30 1991  
S D

91-14419



APPROVED FOR PUBLIC RELEASE: DISTRIBUTION UNLIMITED



**ENGINEERING RESEARCH DIVISION**  
Air Force Engineering & Services Center  
**ENGINEERING & SERVICES LABORATORY**  
Tyndall Air Force Base, Florida 32403



91 10 29 019

NOTICE

PLEASE DO NOT REQUEST COPIES OF THIS REPORT FROM  
HQ AFESC/RD (ENGINEERING AND SERVICES LABORATORY).  
ADDITIONAL COPIES MAY BE PURCHASED FROM:

NATIONAL TECHNICAL INFORMATION SERVICE  
5285 PORT ROYAL ROAD  
SPRINGFIELD, VIRGINIA 22161

FEDERAL GOVERNMENT AGENCIES AND THEIR CONTRACTORS  
REGISTERED WITH DEFENSE TECHNICAL INFORMATION CENTER  
SHOULD DIRECT REQUESTS FOR COPIES OF THIS REPORT TO:

DEFENSE TECHNICAL INFORMATION CENTER  
CAMERON STATION  
ALEXANDRIA, VIRGINIA 22314

REPORT DOCUMENTATION PAGE				Form Approved OMB No. 0704 0188	
1a REPORT SECURITY CLASSIFICATION UNCLASSIFIED			1b RESTRICTIVE MARKINGS NA		
2a SECURITY CLASSIFICATION AUTHORITY NA			3 DISTRIBUTION/AVAILABILITY OF REPORT Approved for Public Release Distribution Unlimited		
2b DECLASSIFICATION/DOWNGRADING SCHEDULE NA					
4 PERFORMING ORGANIZATION REPORT NUMBER(S)  210-9MG-075			5 MONITORING ORGANIZATION REPORT NUMBER(S)  ESL-TR-90-12		
6a NAME OF PERFORMING ORGANIZATION Geotechnical Engineering Program		6b OFFICE SYMBOL (If applicable)	7a NAME OF MONITORING ORGANIZATION Headquarters, Air Force Engineering and Services Center		
6c ADDRESS (City, State, and ZIP Code) Colorado State University Fort Collins, Colorado 80523			7b ADDRESS (City, State, and ZIP Code) HQ AFESC/RDCM Tyndall AFB, FL 32403-6001		
8a NAME OF FUNDING/SPONSORING ORGANIZATION Air Force Office of Scientific Research		8b OFFICE SYMBOL (If applicable)	9 PROCUREMENT INSTRUMENT IDENTIFICATION NUMBER  F49620-87-0004		
8c ADDRESS (City, State, and ZIP Code) Bolling AFB, DC 20332			10 SOURCE OF FUNDING NUMBERS		
		PROGRAM ELEMENT NO	PROJECT NO	TASK NO	WORK UNIT ACCESSION NO
11 TITLE (Include Security Classification)  High Intensity Compressive Stress Wave Propagation Through Unsaturated Sands					
12 PERSONAL AUTHOR(S) S. J. Pierce and W. A. Charlie					
13a TYPE OF REPORT Final		13b TIME COVERED FROM 8905 TO 8909		14. DATE OF REPORT (Year, Month, Day) September 1990	
15 PAGE COUNT					
16 SUPPLEMENTARY NOTATION This research was conducted under the Research Initiation Program.					
17 COSATI CODES			18 SUBJECT TERMS (Continue on reverse if necessary and identify by block number)		
FIELD	GROUP	SUB-GROUP	Unsaturated Sands, Compressive Stress Waves, Dynamic Testing		
19 ABSTRACT (Continue on reverse if necessary and identify by block number) High amplitude split-Hopkinson pressure bar laboratory tests were performed on confined specimens of 20-30 Ottawa and Eglin sands. Triaxial confining stresses of zero and 310 kPa were used, and the samples were subjected to a constant incident stress. Samples were compacted dry, then saturated, then desaturated by use of the pressure plate method. For saturation levels increasing from zero to 80 percent, the compressive wave velocity and stress transmission ratio values decreased slightly for both confining stresses. Quasi-static constrained modulus were found to vary in a similar manner. Previous researchers have shown that for specimens compacted moist, the values of wave velocity, stress transmission ratio and quasi-static constrained modulus increase as the saturation level increases from zero to approximately 30 percent, and then decreases with any further increase in saturation. Several specimens were compacted moist in this research and the results show similar trends. The difference in trends is directly related to the moisture content of the sand during compaction.					
20 DISTRIBUTION/AVAILABILITY OF ABSTRACT <input checked="" type="checkbox"/> UNCLASSIFIED/UNLIMITED <input type="checkbox"/> SAME AS RPT <input type="checkbox"/> DTIC USERS			21 ABSTRACT SECURITY CLASSIFICATION UNCLASSIFIED		
22a NAME OF RESPONSIBLE INDIVIDUAL Steven T. Kuennen, 1LT, USAF			22b TELEPHONE (Include Area Code) (904) 283-4932		22c OFFICE SYMBOL HQ, AFESC/RDCM

## PREFACE

This report was submitted as a final report to Universal Energy Systems, Inc. 4401 Dayton-Xenia Road, Dayton, Ohio 45432. This research was funded by the Air force Office of Scientific Research, Bolling AFB, Wash DC 20332, Contract F49620-87-0004, under the Research Initiation Program and was monitored by the Air Force Engineering and Services Laboratory, Tyndall AFB, Florida 32403-6001.


This dissertation is being published in its original format by this laboratory because of its interest to the worldwide scientific and engineering community. This dissertation covers work performed between May 1989 and August 1989. HQ AFESC/RDCM project officers were Dr C. Ross and Capt S. Kuennen.

This report has been reviewed by the Public Affairs Office and is releasable to the National Information Service (NTIS). At NTIS it will be available to the general public, including foreign nationals.

This report has been reviewed and is approved for publication.



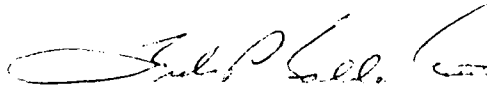
STEVEN T. KUENNEN, Capt, USAF  
Project Officer



NEIL H. FRAVEL, Lt Col, USAF  
Chief, Engineering  
Research Division



LOREN M. WOMACK, GM-14  
Chief, Air Base Structural  
Materials Branch



FRANK P. GALLAGHER III, Col, USAF  
Director, Engineering and  
Services Laboratory

## TABLE OF CONTENTS

<u>Chapter</u>	<u>Page</u>
ABSTRACT.....	iii
ACKNOWLEDGEMENTS.....	v
LIST OF TABLES.....	x
LIST OF FIGURES.....	xi
LIST OF SYMBOLS.....	xvii
I. INTRODUCTION.....	1
A. Statement of Problem.....	1
B. Objectives.....	2
II. LITERATURE REVIEW.....	4
A. Wave Propagation Theory.....	4
B. Split-Hopkinson Pressure Bar Development.....	8
1. Hopkinson Bar.....	9
2. Davis Bar.....	11
3. Kolsky Apparatus.....	12
C. Capillarity and Unsaturated Soil Mechanics.....	14
1. Capillarity.....	14
2. Unsaturated Soil Mechanics.....	19
D. Compaction of Unsaturated Cohesionless Soils.....	23
E. Compressibility and Wave Propagation Through Confined Soils.....	28
1. Compressibility.....	28
2. Wave Propagation.....	34
3. Comparisons Between Compressibility and Wave Velocity.....	47
F. Additional Useful Unsaturated Soils Research.....	49
G. Summary of Previous Research.....	52

III. EXPERIMENTAL PROCEDURES.....	54
A. Equipment Utilized.....	54
1. Description of Split-Hopkinson Pressure Bar...	54
2. Sample Container.....	58
3. Data Recording System.....	61
4. Description of Soil Saturation-Desaturation Equipment.....	64
5. Quasi-Static Confined Compression Apparatus...	64
B. Procedures.....	65
1. Sample Preparation.....	65
2. Sample Saturation and Desaturation.....	65
3. Split-Hopkinson Pressure Bar Tests.....	67
4. Quasi-Static Compression Tests.....	68
5. Capillary Pressure-Desaturation Curves.....	68
IV. EXPERIMENTAL RESULTS.....	71
A. Physical Properties.....	71
B. Split-Hopkinson Pressure Bar Test Results.....	74
C. Quasi-Static Stiffness Tests.....	79
D. Capillary Pressure-Desaturation Curves.....	86
V. ANALYSIS OF RESULTS.....	91
A. Present Investigation.....	91
1. General Observations.....	91
2. Prediction of Wave Velocities Based on Quasi- Static Modulus.....	93
3. Prediction of Wave Velocity Based on Constant Modulus.....	96
4. Constrained Modulus in Terms of $(\sigma - u_a)$ and $(u_a - u_w)$ .....	97
B. Comparison With the Results Obtained from Previous Investigations.....	102
1. Effects of Confining Stress.....	102
2. Effects of Saturation.....	105
3. Effects of Loading Rate.....	106
4. Model Comparisons.....	106
5. Results Obtained by Ross et al. (1988).....	111

VI.	SUMMARY, CONCLUSIONS, AND RECOMMENDATIONS.....	118
	A. Summary.....	118
	B. Conclusions.....	119
	C. Recommendations for Further Research.....	122
VII.	REFERENCES.....	123

Approved For	
NHS - CT421	
OTIC - 64c	
Unannounced	
Justification	
By	
Distribution	
Approved For Use	
Date	Approved For
A-1	6/1/64



## LIST OF TABLES

<u>Table</u>	<u>Page</u>
2 1    Maximum Variation in Shear Modulus with Changes in Saturation and Confining Stress (Wu et al., 1984).....	51
4.1    Physical Properties of 20-30 Ottawa Sand.....	72
4.2    Physical Properties of Eglin Sand.....	72
4.3    SHPB Test Results for 20-30 Ottawa Sand Under Zero Confining Stress.....	77
4.4    SHPB Test Results for 20-30 Ottawa Sand Under 310 kPa Confining Stress.....	77
4.5    SHPB Test Results for Eglin Sand Under Zero Confining Stress.....	78
4.6    SHPB Test Results for Eglin Under 310 kPa Confining Stress.....	78
4.7    Quasi-Static Constrained Modulus Values for 20-30 Ottawa Sand at Various Saturation Levels.....	88
4.8    Quasi-Static Constrained Modulus Values for Eglin Sand at Various Saturation Levels.....	88
5.1    Equations For Multiple Regression Analysis Planes for Ottawa and Eglin Sands, Based on Total Applied Stress, Pore Pressure, and Constrained Modulus.....	102



## LIST OF FIGURES

<u>Figure</u>	<u>Page</u>
2.1 Stress Wave Propagating Through Three Materials.....	7
2.2 Apparatus Developed by Hopkinson (Hopkinson, 1914).....	10
2.3 Apparatus Developed by Davies (Davies, 1948).....	10
2.4 Kolsky Apparatus (Kolsky, 1963).....	13
2.5 Sand Grains Held Together Due to Capillarity (Holtz and Kovacs, 1981).....	15
2.6 Bulking in Sand (Holtz and Kovacs, 1981).....	15
2.7 Capillary Pressure-Desaturation Curves (Corey, 1986)...	17
2.8 Drainage Versus Imbibition Schematic (Corey, 1986).....	17
2.9 Stress State Variables Versus Strain (Fredlund, 1986).....	22
2.10 Compaction Curve for Cohesionless Soils (Foster, 1962)..	24
2.11 Compaction Energy Versus Saturation (Ross, 1989).....	24
2.12 Theoretical Stress-Strain Curves for Different Lateral Confinement (Richart et al., 1970).....	30
2.13 Stress-Strain Curves For Sandy Silt at Various Saturation Levels (Hendron, et al., 1969).....	32
2.14 Variation of Compression Wave Velocity with Confining Stress for Steel Spheres (Duffy and Mindlin, 1957)...	32
2.15 Variation of Dry Density with Compactive Effort and Moisture Content for Vicksburg Loess (Martin, 1957).....	36
2.16 Variations of Wave Velocity with Confining Stress a. Dry, b. Saturated, c. Moist (Hardin, 1961).....	38
3.17 Variations of Wave Velocity with Confining Stress (Hardin, 1961; Stoll et al., 1965).....	41

2.18	Wave Velocity Versus Saturation for 20-30 Ottawa Sand (Ross et al., 1988).....	42
2.19	Transmission Ratio Versus Saturation for 20-30 Ottawa Sand (Ross et al., 1988).....	42
2.20	Wave Velocity Versus Saturation for Eglin Sand (Ross et al., 1988).....	43
2.21	Transmission Ratio Versus Saturation for Eglin Sand (Ross et al., 1988).....	43
2.22	Quasi-Static Stiffness Results for 20-30 Ottawa and Eglin Sands (Ross et al., 1988).....	45
2.23	Increase in Effective Stress Due To Capillarity for 20-30 Ottawa Sand (Ross et al., 1988).....	46
2.24	Increase in Effective Stress Due to Capillarity for Eglin Sand (Ross et al., 1988).....	46
2.25	Variations of Wave Velocity with Confining Stress for Monterey Sand Due To Static, Dynamic and Wave Propagation Methods (Moore, 1963).....	48
2.26	Gradations for Soil Types Used by Wu et al. (1984).....	50
2.27	Variations of Shear Modulus with Saturation Under Several Confining Stresses (Wu et al., 1984).....	50
3.1	Schematic of Split-Hopkinson Pressure Bar.....	55
3.2	Schematic of Axial Confining Stress Components a. Confining Piston, b. Confining Bracket.....	57
3.3	Schematic of Confining Pressure Apparatus.....	59
3.4	Schematic of Sample Container.....	60
3.5	Schematic of SHPB Data Recording System.....	62
3.6	Oscilloscope and Amplifiers Used on Conjunction with SHPB Data recording System.....	63
3.7	Standard Pressure Plate Apparatus.....	63
3.8	Quasi-Static Confined Compression Apparatus a. Load Cell and Sample Container, b. Strip-Chart Recorder.....	66

3.9	Specimen Container in Place Between Pressure Bars.....	69
4.1	Grain Size Distributions for 20-30 Ottawa and Eglin sands.....	73
4.2	Typical Oscilloscope Trace of Compression Wave as Recorded by Pressure Bar Strain Gages.....	75
4.3	Typical Oscilloscope Trace with Wave Transit Times.....	75
4.4	Wave Velocity Versus Saturation for 20-30 Ottawa Sand Under Zero Confining Stress.....	80
4.5	Wave Velocity Versus Saturation for 20-30 Ottawa Sand Under 310 kPa Confining Stress.....	80
4.6	Wave Velocity Versus Saturation for Eglin Sand Under Zero Confining Stress.....	81
4.7	Wave Velocity Versus Saturation for Eglin Sand Under 310 kPa Confining Stress.....	81
4.8	Transmission Ratio Versus Saturation 20-30 Ottawa Sand Under Zero Confining Stress.....	82
4.9	Transmission Ratio Versus Saturation for 20-30 Ottawa Sand Under 310 kPa Confining Stress.....	82
4.10	Transmission Ratio Versus Saturation for Eglin Sand Under Zero Confining Stress.....	83
4.11	Transmission Ratio Versus Saturation for Eglin Sand Under 310 kPa Confining Stress.....	83
4.12	Results For Eglin Sand Obtained by Ross et al. (1988) and Results for Samples Compacted Moist Using Sample Container in Current Investigation a. Wave Velocity, b. Transmission Ratio.....	84
4.13	Comparison of Eglin Sand Samples Compacted and Tested Both Moist and Dry a. Wave Velocity, b. Transmission Ratio.....	85
4.14	Typical Strip-Chart Recorder Load-Time History for Quasi-Static Tests.....	87
4.15	Quasi-Static Constrained Modulus Versus Saturation for 20-30 Ottawa Sand.....	89

4.16	Quasi-Static Constrained Modulus Versus Saturation for Eglin Sand.....	89
4.17	Capillary Pressure-Desaturation Curve for 20-30 Ottawa Sand and Eglin Sands.....	90
5.1	Wave Velocity Versus Saturation Results with Values Based on Quasi-Static Modulus for 20-30 Ottawa Sand Under Zero Confining Stress (Compacted Dry)....	94
5.2	Transmission Ratio Versus Saturation Results with Values Based on Quasi-Static Modulus for 20-30 Ottawa Sand Under Zero Confining Stress (Compacted Dry).....	94
5.3	Wave Velocity Versus Saturation Results with Values Based on Quasi-Static Modulus for Eglin Sand Sand Under Zero Confining Stress (Compacted Dry)....	95
5.4	Transmission Ratio Versus Saturation Results with Values Based on Quasi-Static Modulus for Eglin Sand Under Zero Confining Stress (Compacted Dry)....	95
5.5	Wave Velocity Versus Saturation Model Based on Constant Modulus for 20-30 Ottawa Sand under Zero Confining Stress (Compacted Dry).....	98
5.6	Wave Velocity Versus Saturation Model Based on Constant Modulus for 20-30 Ottawa Sand under 310 kPa Confining Stress (Compacted Dry).....	98
5.7	Wave Velocity Versus Saturation Model Based on Constant Modulus for Eglin Sand under Zero Confining Stress (Compacted Dry).....	99
5.8	Wave Velocity Versus Saturation Model Based on Constant Modulus for Eglin Sand under 310 kPa Confining Stress (Compacted Dry).....	99
5.9	Constrained Modulus Versus ( $\sigma - u_a$ ) and $u_a - u_w$ ) for 20-30 Ottawa Sand (Compacted Dry).....	101
5.10	Constrained Modulus Versus ( $\sigma - u_a$ ) and $u_a - u_w$ ) for Eglin Sand (Compacted Dry).....	101
5.11	Confining Stress Versus Wave Velocity for Results Obtained by Hardin (1961), Stoll et al. (1965), and the Current Investigation for 20-30 Ottawa Sand (Compacted Dry).....	104

5.12	Wave Velocity Versus Saturation Results with Model Proposed by Whitman (1970) for 20-30 Ottawa Sand Under Zero Confining Stress (Compacted Dry).....	108
5.13	Wave Velocity Versus Saturation Results with Model Proposed by Whitman (1970) for 20-30 Ottawa Sand Under 310 kPa Confining Stress (Compacted Dry).....	108
5.14	Wave Velocity Versus Saturation Results with Model Proposed by Whitman (1970) for Eglin Sand Under Zero Confining Stress (Compacted Dry).....	109
5.15	Wave Velocity Versus Saturation Results with Model Proposed by Whitman (1970) for Eglin Sand Under 310 kPa Confining Stress (Compacted Dry).....	109
5.16	Wave Velocity Versus Saturation Results with Model Proposed by Anderson and Hampton (1980) for 20-30 Ottawa Sand Under Zero Confining Stress (Compacted Dry).....	110
5.17	Wave Velocity Versus Saturation Results with Model Proposed by Anderson and Hampton (1980) for Eglin Sand Under Zero Confining Stress (Compacted Dry).....	110
5.18	Wave Velocity Values Obtained by Ross et al. (1988) and in the Current Investigation for Eglin Sand Under Zero Confining Stress.....	113
5.19	Stress Transmission Ratio Results Obtained by Ross et al. (1988) and in the Current Investigation for Eglin Sand Under Zero Confining Stress.....	113
5.20	Wave Velocity Values Obtained by Ross et al. (1988) and in the Current Investigation for Eglin Sand Under Zero and 310 kPa Confining Stress.....	117

## LIST OF SYMBOLS AND UNITS

- A = cylindrical explosive in Hopkinson bar schematic
- B = time piece in Hopkinson bar schematic
- B = bulk modulus (kPa)
- cm = centimeter
- C = incident bar in Hopkinson bar schematic
- $C_c$  = coefficient of curvature
- $C_c$  = compressibility of soil structure with respect to change in  $(\sigma - u_a)$  (1/kPa)
- $C_u$  = coefficient of uniformity
- $C_w$  = compressibility of soil structure with respect to change in capillary pressure (1/kPa)
- d = diameter of cylindrical material (m)
- $d_x$  = effective grain size diameter; x% of soil has size finer than this value (mm)
- D = constrained modulus (kPa)
- D = momentum trap in Hopkinson bar schematic
- $D_s$  = constrained modulus of mineral skeleton (kPa)
- e = void ratio
- E = Young's modulus (kPa)
- ft = feet
- g = acceleration due to gravity ( $9.81 \text{ m/sec}^2$ )

$G_s$  - specific gravity of mineral particle  
 $G_o$  - shear modulus (kPa)  
kg - kilogram  
kPa - kilo Pascals  
 $K$  - aggregate bulk modulus (kPa)  
 $K_o$  - coefficient of lateral stress under static conditions  
 $l$  - total length of material (m)  
 $m$  - mass  
 $m$  - meter  
mm - millimeter  
 $n$  - porosity  
 $N$  - Newton  
psi - pounds per square inch  
psf - pounds per square foot  
 $P_d$  - displacement pressure (kPa)  
 $P$  - hydrostatic pressure (kPa)  
 $P_c$  - capillary pressure (kPa)  
 $R^2$  - coefficient of determination  
 $r_m$  - radius of meniscus (m)  
s - second  
s - standard deviation  
 $S$  - saturation level (%)  
SHPB - Split-Hopkinson Pressure Bar

$S_r$  = residual saturation (%)  
 $t$  = time  
 $T$  = surface tension (kPa)  
 $u_a$  = pore air pressure (kPa)  
 $u_w$  = pore water pressure (kPa)  
 $V_c$  = compressional wave velocity (m/sec)  
 $w$  = water content (%)  
 $x$  = variable length (m)  
 $\bar{x}$  = mean  
 $z$  = variable length in vertical direction (m)  
 $\epsilon$  = strain (longitudinal)  
 $\epsilon_r$  = radial strain  
 $\epsilon_v$  = volumetric strain  
 $\epsilon_z$  = strain in z direction  
 $\mu s$  = microsecond ( $10^{-6}$  seconds)  
 $\rho$  = density of material ( $\text{kg/m}^3$ )  
 $\rho_t$  = total density of soil ( $\text{kg/m}^3$ )  
 $\rho_w$  = density of water ( $\text{kg/m}^3$ )  
 $\rho V_c$  = acoustic impedance ( $\text{kg/m}^2\text{-sec}$ )  
 $\sigma$  = total stress (kPa)  
 $\sigma'$  = effective stress (kPa)



- $\sigma_1$  - stress due to the incident stress wave (kPa)
- $\sigma_2$  - stress due to the reflected stress wave (kPa)
- $\sigma_D$  - average dynamic stress applied by SHPB (kPa)
- $\sigma_I$  - stress in incident material due to incident stress wave (kPa)
- $\sigma_o$  - isotropic confining stress (kPa)
- $\sigma_r$  - radial stress (kPa)
- $\sigma_R$  - stress in incident material due to reflected stress wave (kPa)
- $\sigma_T$  - stress in transmitting material due to transmitted stress wave (kPa)
- $\sigma'_T$  - stress transmitted into a third medium (kPa)
- $\sigma_z$  - total stress in z direction (kPa)
- $\gamma_d$  - dry unit weight ( $N/m^3$ )
- $\chi$  - saturation parameter

## I. INTRODUCTION

### A. STATEMENT OF PROBLEM

Compressive stress wave propagation through soils is of considerable interest to the armed forces, mining industry and in the area of geophysical investigations. Research on high amplitude, short duration compressive loadings is particularly important in understanding the soil-structure response of buried structures subjected to explosive-induced stress waves. Because the response of a structure is highly dependent on the dynamic properties of the soil, changes in the characteristics of the soil during construction and over time could greatly affect the behavior of the structure.

A substantial amount of research has been conducted in the area of compressive wave propagation and compressibility of dry or saturated sand. However, little has been done for unsaturated sands. This lack of research is especially evident for high amplitude loading conditions.

Previous studies and wave propagation theory have shown that there is a link between the saturation level and stiffness of soil. The soil stiffness is reflected in the values of compressive wave propagation velocity and the magnitude of the stress wave being transmitted through the soil. Currently there are no methods

available for predicting these parameters under large amplitude compressive stress wave loading conditions.

For two sands compacted in a similar manner to the same void ratio, but at different moisture contents, the static and dynamic properties of the sands will be different. It has been shown previously that the liquefaction potential, cyclic shear strength and permeability of sands are affected when different specimen compaction procedures are used. Therefore, before the compressive stress wave propagation parameters can be evaluated, an understanding of the effects of sample preparation technique is required.

### 3. OBJECTIVES OF THIS INVESTIGATION

The objective of this research is to determine how moisture content during compaction, saturation level and confining stress affect the values of wave velocity, stress transmission ratio and quasi-static constrained modulus for 20-30 Ottawa (ASTM C190) and Eglin sands. In order to achieve this objective, a split-Hopkinson pressure bar, located at Tyndall Air Force Base, Florida, was utilized to subject the sands to high amplitude, short duration compressive loadings. Quasi-static stiffness tests were performed to determine the relationship between the quasi-static and dynamic parameters of the two sands.

In this investigation saturation level and confining stress were varied. Samples were compacted dry to a constant void ratio, and the applied dynamic stress was held constant for both of the sands used.

During testing, samples were allowed to strain one-dimensionally under triaxial confining stresses of zero and 310 kPa.

The results obtained in this investigation have been compared to tests performed on the same two sands by Ross et al. (1988). Ross et al. used the same split-Hopkinson pressure bar, the same void ratio and range of saturation levels, and subjected the sands to identical dynamic stress and confining conditions as in this investigation. The only difference between the research performed by Ross et al. and the current investigation is that Ross et al. compacted the sand samples moist, while in this investigation, the samples were compacted dry, saturated, then desaturated by use of the pressure plate method. The results have also been compared to experimental results obtained by other investigators, and compared with several mathematical models developed for the determination of compressive wave velocities through soils.

## II. LITERATURE REVIEW

This chapter consists of five sections in which previous research has been reviewed and cited for its relevance and usefulness in the current investigation. The first section is a review of the wave propagation equations which are used in this study. The second section is a history of the evolution of the split-Hopkinson pressure bar. The third section is a brief review of the current state of knowledge in the area of capillarity and unsaturated soil mechanics. Section four is a summary of the most recent work in the area of compaction, and its effects on lateral stress and fabric development in sands. The final section is a review of compressibility and wave propagation research performed on unsaturated, cohesionless soils within the saturation ranges used in this investigation.

### A. WAVE PROPAGATION THEORY

The velocity of a wave as it propagates through a material can be theoretically determined from Newton's Second Law of Motion and elasticity theory if the applied stress is within the elastic limits of the material. Depending on the strain conditions allowed, one of the following equations can be used to determine the compression wave propagation velocity (Kolsky, 1963):

$$V_c = \left\{ \frac{E}{\rho} \right\}^{0.5} \quad (2.1)$$

$$V_c = \left\{ \frac{B}{\rho} \right\}^{0.5} \quad (2.2)$$

$$V_c = \left\{ \frac{D}{\rho} \right\}^{0.5} \quad (2.3)$$

where  $E$  is Young's Modulus,  $B$  is the Bulk modulus, and  $D$  is the constrained modulus. Equations 2.1 through 2.3 state that the compressive wave velocity is only a function of the stiffness and the density of the material. Total density is used in these equations when determining the propagation velocity through soils.

When a propagating wave comes to a boundary with a material of different acoustic impedance, a portion of the wave will be reflected back into the bar, and a portion will be transmitted into the second medium. Acoustic impedance is defined as the wave propagation velocity multiplied by the mass density of the material. Rinehart (1975) shows that the amount of stress reflected back into the first material can be determined by:

$$\sigma_R = \frac{\rho_2 V_{c2} - \rho_1 V_{c1}}{(\rho_2 V_{c2} + \rho_1 V_{c1})} \sigma_I \quad (2.4)$$

where  $\sigma_I$  and  $\sigma_R$  are the incident and reflected stresses, and the subscripts 1 and 2 denote the two mediums being considered. The values in the form  $\rho V_c$  are the acoustic impedances of the two materials. The amount of stress being transmitted into the second medium can be determined from:

$$\sigma_{T_2} = \frac{2\rho_2^V c_2}{(\rho_2^V c_2 + \rho_1^V c_1)} \sigma_{I_1} \quad (2.5)$$

where  $\sigma_T$  is the transmitted stress.

If several materials are in contact, such as Figure 2.1, the stress at each interface can be determined. Using equation 2.5 for the stress transmitted into material 2, and assuming no wave attenuation occurs through material 2, then the magnitude of the stress transmitted into the third medium can be determined by replacing the incident stress with the stress transmitted into medium 2 and changing the values for the acoustic impedances in equation 2.5:

$$\sigma'_{T_3} = \frac{2\rho_3^V c_3}{(\rho_2^V c_2 + \rho_3^V c_3)} \sigma_{T_2} \quad (2.6).$$

$\sigma'_T$  is the stress transmitted into the third medium. This process can be continued for any number of boundary conditions which are of interest.

If the special case occurs where the first and third mediums of Figure 2.1 are the same, but different than the second, a relationship between the incident pulse and the pulse transmitted into the third medium can be determined. If equations 2.5 and 2.6 are combined for this condition, the following equation is obtained:

$$\frac{\sigma'_{T_1}}{\sigma_{I_1}} = 4 \frac{\rho_1^V c_1 \rho_2^V c_2}{(\rho_2^V c_2 + \rho_1^V c_1)^2} \quad (2.7).$$

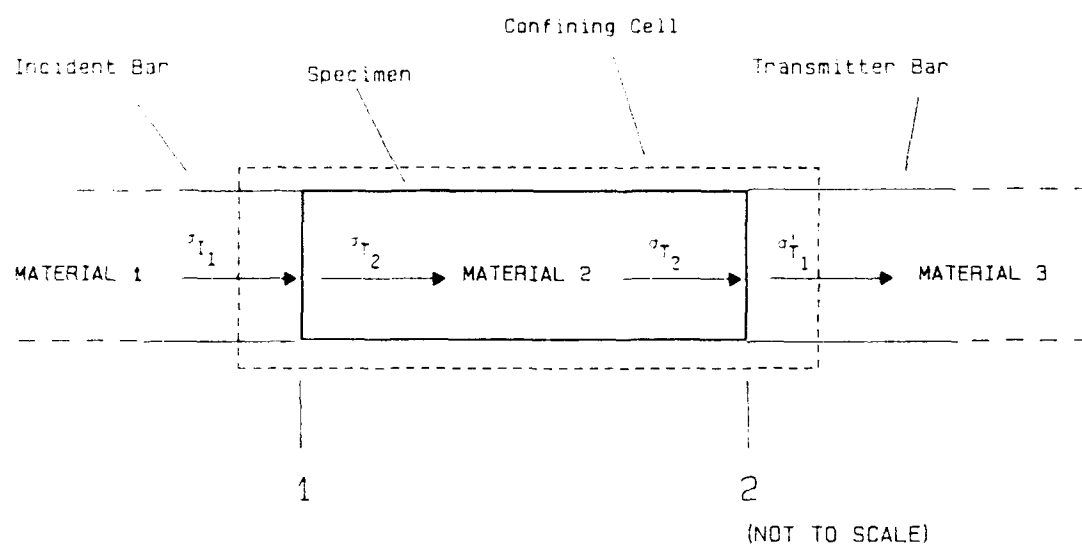


Figure 2.1 Stress Wave Propagating Through Three Materials



The value in equation 2.7 is referred to as the stress transmission ratio. Comparing equations 2.5 and 2.7, the magnitude of the stress transmitted into the third medium is approximately two times the magnitude of the stress in the second medium if the acoustic impedance of the second medium is considerably smaller than the first and third. This relationship is of particular importance in an investigation utilizing a split-Hopkinson pressure bar. In this investigation, a soil sample (medium 2) is placed between two steel bars (mediums 1 and 3).

#### B. SPLIT-HOPKINSON PRESSURE BAR DEVELOPMENT

The split-Hopkinson pressure bar (SHPB) was developed through the need for a better understanding of the behavior of materials at high strain rates. As strain rates change, the stress-strain properties of the material may also change. Bar impact methods such as the split-Hopkinson pressure bar, apply strain rates to materials from  $5 \times 10^1$  to  $10^4$  per second with loading rise times from approximately  $10^{-4}$  to  $10^{-6}$  seconds.

The split-Hopkinson pressure bar has evolved as a method to measure the stress-strain properties of materials at high strain rates. Only recently, the bar has been used in measuring dynamic properties of soils. Recently the device was used to measure strain rate properties of soils (Felice, 1986), while in this investigation and the investigation by Ross et al. (1988) have used the SHPB to measure the effects of propagating a single transient pulse through a soil sample.

## 1. The Hopkinson Bar

Hopkinson (1914) developed a laboratory apparatus for measuring the maximum pressure developed and loading duration for an explosive impact in the laboratory. Hopkinson's schematic of the device is shown in Figure 2.2. A compressive stress pulse was generated by firing a cylindrical explosive, marked "A" in the figure, at the end of a steel bar (marked "C" in the schematic). At the other end of the bar a "time piece" (shown as "B" in the figure) was magnetically attached. This time piece was a section of steel with the same diameter as the incident bar, but of variable length. When the compressive pulse passed through the time piece, the wave was reflected off the end, which created a tensile pulse in the opposite direction. When the tensile wave met the joint between the time piece and bar, the magnetic joint could not transmit the tensile wave causing the time piece to accelerate away from the bar into a ballistic pendulum, which is shown as "D" in the schematic. The pendulum was used to measure the momentum of the time piece. If the time piece was of a length such that the entire pulse was trapped within it, the incident bar would not move once the time piece separated. The duration of the pulse was then twice the length of the time piece multiplied by the wave velocity of the material.

From this apparatus, the maximum stress applied to the bar could be determined from the momentum trap, and the duration of the pulse (the wavelength) could be determined. Because of limitations in

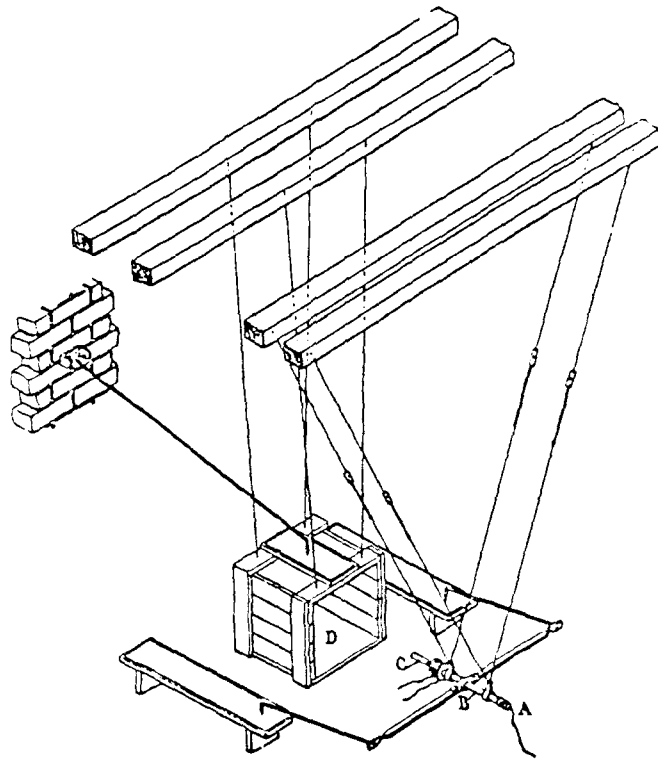


Figure 2.2 Apparatus Developed by Hopkinson (Hopkinson, 1914)

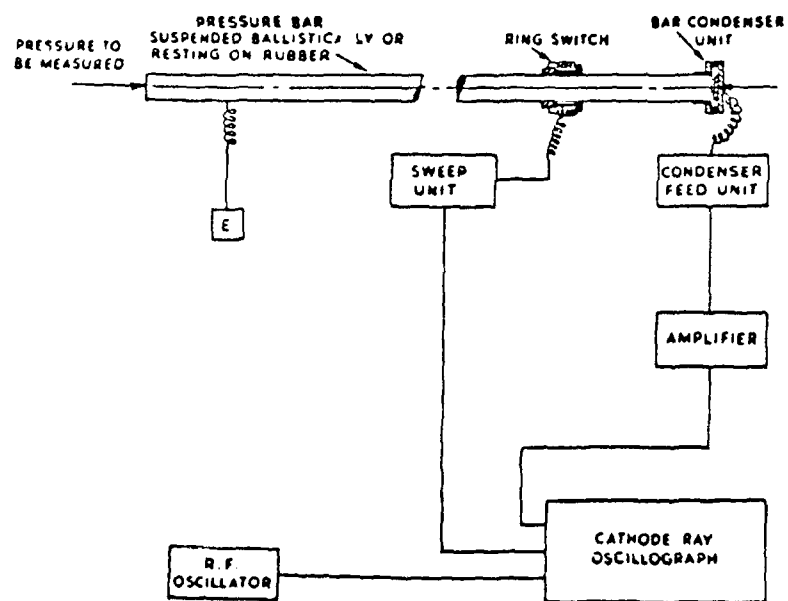


Figure 2.3 Apparatus Developed by Davies (Davies, 1948)

the equipment, the pressure-time history of the pulse as it travelled through the bar could not be determined.

## 2. The Davies Bar

R.M. Davies (1948) updated the Hopkinson apparatus by replacing the time piece with a bar condensor unit to measure displacements at the end of the bar. Figure 2.3 shows the bar condensor unit as it fit over the free end of the incident bar. This configuration allowed the incident bar to be one face of a parallel plate condensor, while the bar condensor was used as the other face.

Davies used the relationship between compressive stress and particle velocity to relate the displacement at the end of the bar to the stress-time history developed by the compressive wave. Stress is related to particle velocity by:

$$\sigma = \rho V_c \frac{du}{dt} \quad (2.8)$$

where the particle velocity is  $du/dt$ . As a compressive stress pulse travels down the bar to the free end, the particle velocity doubles giving:

$$\sigma = 1/2 \rho V_c \frac{du}{dt} \quad (2.9)$$

or

$$\frac{du}{dt} = \frac{2\sigma}{\rho V_c} \quad (2.10).$$

By utilizing the bar condensor unit, the Davies bar gave the displacement-time history of the pulse, which was then differentiated

and used in equation 2.10 to find the pressure time history of the pulse.

### 3. The Kolsky Device (Split-Hopkinson Pressure Bar)

Kolsky (1949) modified the Davies bar to allow for the determination of the dynamic stress-strain properties of materials. As shown in Figure 2.4, the modifications consisted of separating the bar into two pieces (the incident and transmitter bars) to allow for the placement of a thin specimen of metal, rubber, or other material between the bars. The apparatus utilized the same type of bar condensor unit at the end of the transmitter bar used by Davies to determine the displacement of the end of the bar, while using a cylindrical condensor to determine the radial displacement of the incident bar.

Kolsky (1948, 1963) has shown that the relationship between the incident and transmitter bar displacements can be used to determine the stress-strain relationship for the thin specimens. The thin specimens allow for multiple reflections to occur within the samples in order to create a uniform stress throughout the specimen.

Fletcher and Poorooshasb (1968) determined the stress-strain relationship for clay samples using a SHPB under saturated conditions. The magnitude of the stress through the soil were varied from zero to 830 kPa. Felice, Gaffney, Brown and Olsen (1987) utilized the SHPB to measure the stress-strain properties of compacted sands. In both of these investigations, thin specimens were used which had a length to diameter ratio of 0.1.

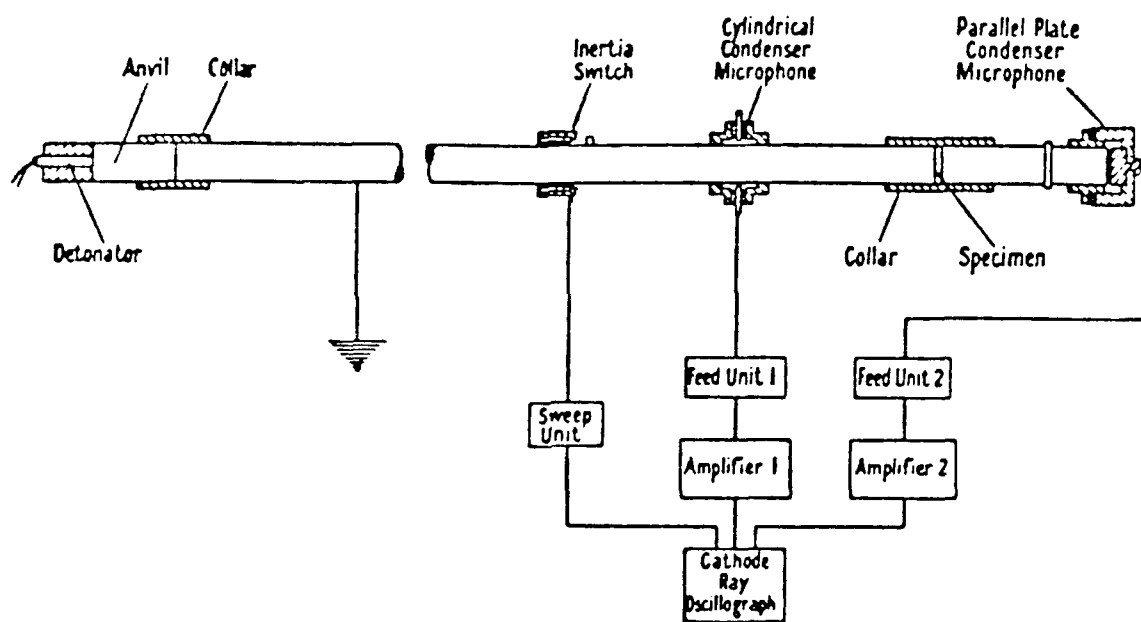


Figure 2.4 Kolsky Apparatus (Kolsky, 1963)

## C. CAPILLARITY AND UNSATURATED SOIL MECHANICS

### 1. Capillarity

Capillarity is a phenomena that occurs in soils due to the surface tension of water in contact with air. Figure 2.5 shows the relationship between capillary menisci and individual soil particles. Holtz and Kovacs (1981) explain that the surface tension of the water increases the intergranular stress between the two soil particles. Lambe and Whitman (1969) show that capillary forces cause sand grains to resist rearrangement at low water contents. This behavior is referred to as bulking and is shown in Figure 2.6.

McWhorter and Sunada (1977) show that the capillary pressure is a function of surface tension and pore size radius. This relationship is expressed by:

$$P_c = u_a - u_w = \frac{2T}{r_m} \quad (2.11)$$

where  $u_a$  is the pore air pressure,  $u_w$  is the pore water pressure,  $T$  is the surface tension and  $r_m$  is the radius of the air-water interface. The value  $r_w$  depends on soil type, grain size and shape, gradation, and packing.

Equation 2.11 shows that the capillary pressure and therefore, the use of water due to capillarity, are function sof the radius of the air-water interface. For the capillary rise to increase, the pore space that the water occupies must become increasingly smaller. As a

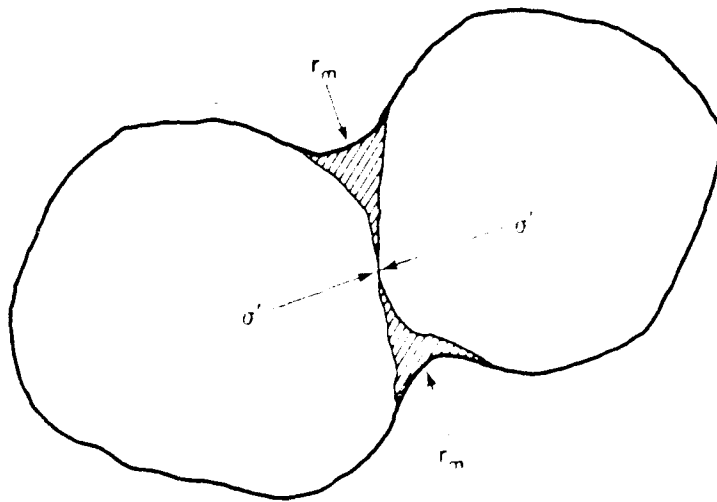


Figure 2.5 Sand Grains Held Together Due to Capillarity (Holtz and Kovacs, 1981)

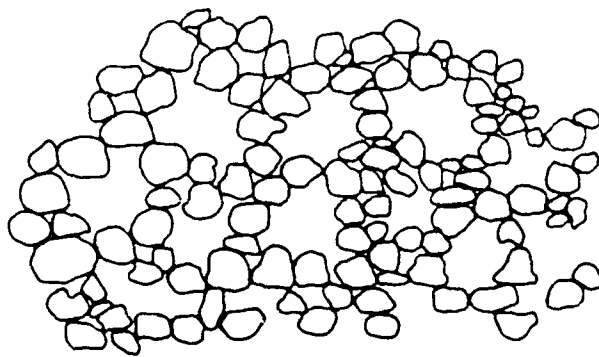


Figure 2.6 Bulking in Sand (Holtz and Kovacs, 1981)



result, a relationship exists between the capillary pressure and saturation level of the soil at a particular point above the groundwater table. This relationship can be expressed by a capillary pressure-desaturation curve as shown in Figure 2.7.

Corey (1986) states that the relationship between capillary pressure and saturation is not unique, but depends on the saturation history. The drainage curve in Figure 2.7 is obtained by starting with a water saturation of 100 percent, and increasing the capillary pressure to obtain the relationship as shown. The wetting curve is obtained by starting with a moist soil and allowing the soil to imbibe water. The two curves are different due to a hysteresis effect, and in general, soils in the field have capillary pressure-saturation distributions somewhere between the wetting and drying curves.

Corey (1986) states that the hysteresis may be due to several effects. One effect is due to wettability changes which depend on which phase (air or water) first comes in contact with the soil particles. A second effect is illustrated in Figure 2.8 which shows the results of drainage or imbibition on capillary tubes with irregular cross-sections. Because of the increase in pore radius, the imbibition capillary is unable to attain the same capillary pressure (or capillary rise) as the capillary which was initially saturated and allowed to drain and equilibrate.

The value of  $S_r$  shown in Figure 2.7 is referred to as the residual saturation. This minimum saturation only occurs due to drainage by gravity. Soils can reach a lower saturation level by evaporation, plant uptake of soil moisture, and variations in

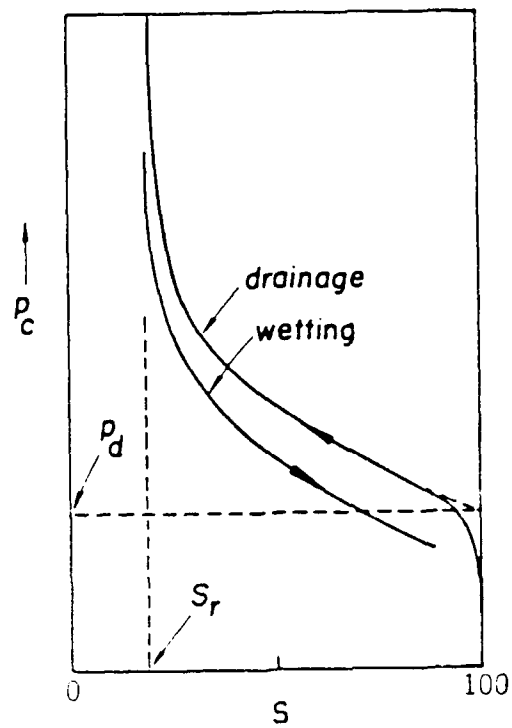


Figure 2.7 Capillary Pressure-Desaturation Curves (Corey, 1986)

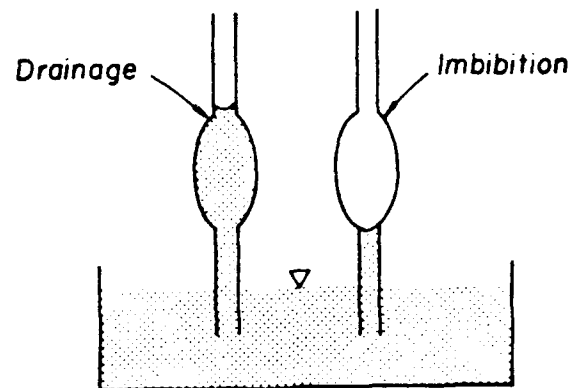


Figure 2.8 Drainage Versus Imbibition Schematic (Corey, 1986)

temperature. This saturation level is considered to be constant for large values of  $P_c$ . The value  $P_d$  shown in the same figure is called the displacement pressure of the soil. For values of  $P_c < P_d$ , the water is still saturated, which makes it within the zone of the "capillary fringe". Once the displacement pressure is reached, desaturation of the wetting cycle begins to occur.

The capillary pressure-desaturation curves can be determined by the use of a pressure plate apparatus (Klute, 1986). The apparatus applies positive air pressure to moist soil samples while the water within the samples remains at atmospheric pressure. The water within the samples is allowed to drain and come into equilibrium with the air pressure. The saturation level of the soil is then measured, and higher air pressures are applied to obtain points on the wetting curve as shown in Figure 2.7. Imbibition curves are generated by allowing water to flow into the soil samples which are initially under high air pressures. The air pressure is reduced successively for each point on the wetting curve.

As explained previously, under field conditions the pore air pressure is usually atmospheric, while the pore water pressure is negative (gage). With the pressure plate apparatus, the pore air pressure is positive while the pore water pressure remains atmospheric. In both cases, the capillary pressure ( $u_a - u_w$ ) is constant. Therefore, the pressure-saturation relationship is the same in the field and when using the pressure plate, which is independent of the individual values of  $u_a$  and  $u_w$ . Because of this relationship,

large capillary pressures can be applied to soil samples in the laboratory.

## 2. Unsaturated Soil Mechanics

Bishop et al. (1960) presented an equation for the determination of the effective stress in an unsaturated soil based on Terzaghi's theory of effective stress for saturated soils. The equation takes the form:

$$\sigma' = (\sigma - u_a) + \chi (u_a - u_w) \quad (2.12)$$

where  $\sigma'$  is the effective stress,  $\sigma$  the total stress,  $u_a$  the air pressure,  $u_w$  the water pressure.  $\chi$  is a parameter which is thought to depend mainly on saturation and to a lesser extent soil type, the cycle of wetting and drying, and stress change. For saturated conditions  $\chi = 1$ , while in dry conditions  $\chi = 0$ , which allows for transition to Terzaghi's effective stress equation.

Jennings and Burland (1962) have determined that the parameter  $\chi$  varies with changes in saturation for various soil types. In fact, it has been shown that  $\chi$  is unique for a specific soil, and that the value of  $\chi$  may vary, depending on the saturation level of the soil. This, in effect shows that the principle for effective stress for unsaturated soils presented by Bishop et al. is not sufficient for determining the volume change and shear strength characteristics of unsaturated soil.

Based on the results obtained by Jennings and Burland (1962), Bishop and Blight (1963) have modified the theory by showing that

volume change and shear strength relationships of soil are not only based upon the effective stress, but also on the stress paths of the two components  $(\sigma - u_a)$  and  $(u_a - u_w)$ .

Matyas and Radhakrishna (1968) have proposed that the relationship between soil properties (shear strength and volume change) may be related to the two stress parameters  $(\sigma - u_a)$  and  $(u_a - u_w)$  rather than trying to correlate them to a single value of effective stress.

Based on this proposal, Matyas and Radhakrishna have related void ratio and saturation directly to the two independent stress components  $(\sigma - u_a)$  and  $(u_a - u_w)$ . From this, predictions can be made for changes in void ratio and saturation under field conditions.

In all of the theories for unsaturated soil mechanics discussed up to this point the soil is considered to consist of three independent phases, solid, liquid and gas. Fredlund and Morgenstern (1977) have proposed a fourth independent phase which is the air-water interface, or contractile skin. They have shown that the contractile skin has unique properties that cause it to behave more as a solid than a liquid. Based on this theory, they have presented a four phase system for unsaturated soil mechanics in which two of the phases come into equilibrium under applied stress (soil particles and contractile skin) and two phases which flow under applied stress (air and water).

Due to the creation of a four phase system, force equilibrium equations were developed for each phase of the unsaturated soil based on multiphase continuum mechanics. From this, one of the following

three normal stress variable combinations can be used to define the stress state of the unsaturated soil. The stress variables are:

$$(\sigma - u_a) \text{ and } (u_a - u_w)$$

$$(\sigma - u_w) \text{ and } (u_a - u_w)$$

$$(\sigma - u_a) \text{ and } (\sigma - u_w).$$

Fredlund (1979) recommends that the first combination be used because the effects of changes in total stress and pore pressure can be separated.

The stress variables  $(\sigma - u_a)$  and  $(u_a - u_w)$  yield a smooth transition from unsaturated to saturated conditions. As saturation approaches 100 percent, the pore air pressure approaches the pore water pressure. The capillary pressure  $(u_a - u_w)$  then goes to zero and the pore air pressure term in the first variable becomes the pore water pressure.

Constitutive relationships for volume change and consolidation theory have been presented by Fredlund and Morgenstern (1976), Fredlund and Hasan (1979), Fredlund et al. (1980) and Fredlund (1986). Based on the constitutive relations for volume change presented by Fredlund and Morgenstern (1976), the constitutive equation for volumetric strain of the soil structure,  $\epsilon_v$ , can be written:

$$\epsilon_v = C_t d(\sigma - u_a) + C_w d(u_a - u_w) \quad (2.13)$$

where  $C_t$  is the compressibility of the soil structure with respect to a change in  $(\sigma - u_a)$ , and  $C_w$  is the compressibility of the soil structure with respect to a change in  $(u_a - u_w)$ . In Figure 2.9 this

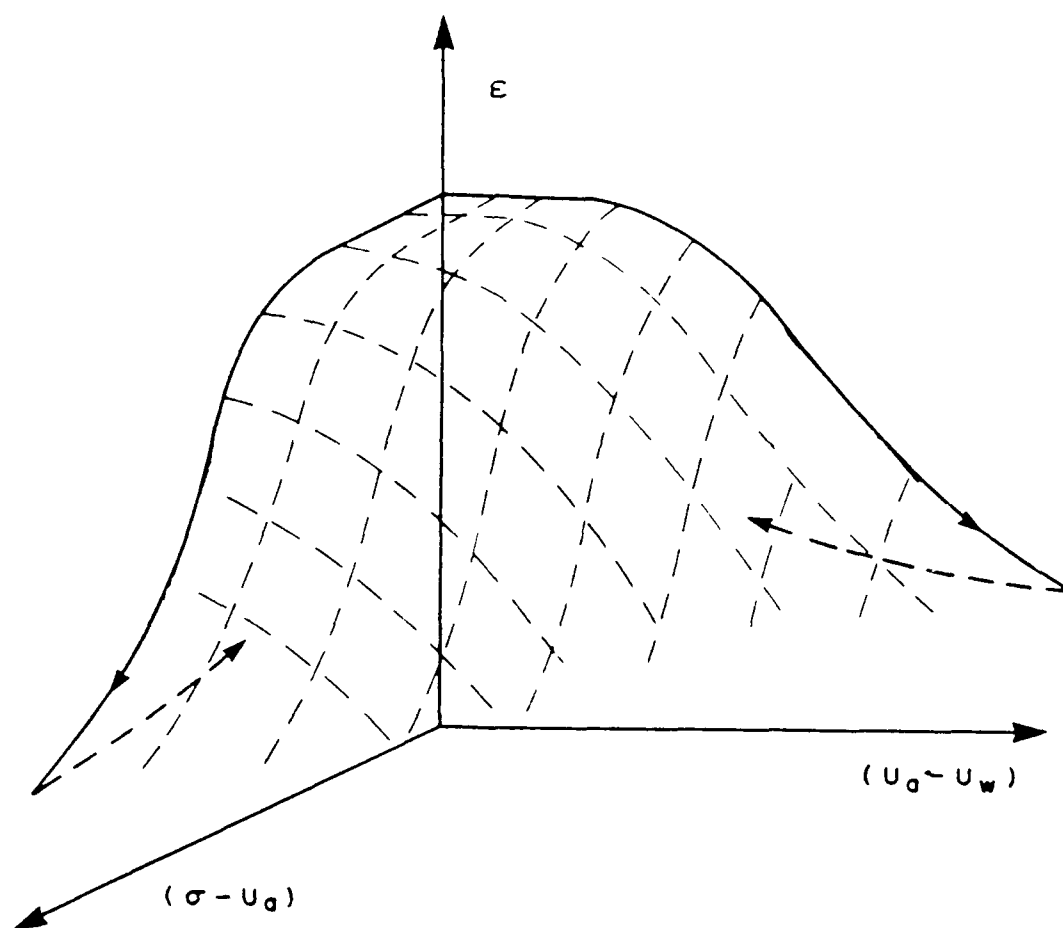


Figure 2.9 Stress State Variables Versus Strain (Fredlund, 1986)

relationship can be presented in a three dimensional plot of void ratio versus  $(\sigma - u_a)$  and  $(u_a - u_w)$ .

The soil structure constitutive relationship is not sufficient to completely describe the state of the unsaturated soil. The stress history of the soil, and air or water constitutive relationships must also be evaluated (see Fredlund and Morgenstern, 1977).

#### D. COMPACTION OF UNSATURATED COHESIONLESS SOILS

Comparing wave propagation velocities obtained in this investigation with previously published results, it will be shown that the method of sample compaction is of considerable importance. A sample compacted moist will often give different results than a sample compacted dry, then saturated and desaturated to the same moisture content and dry density. These differences may be attributed to variations in lateral stress and fabric developed during the compaction process.

For cohesionless materials compacted by a dynamic compaction technique, the relationship between dry density and moisture content takes the form of Figure 2.10. Foster (1962) states that this type of compaction curve will occur when the material is permeable enough to impede the development of positive pore pressures during compaction. Lambe and Whitman (1969) attribute the low densities at lower water contents to bulking; a phenomena which occurs when the capillary forces of the soil resist particle rearrangement.



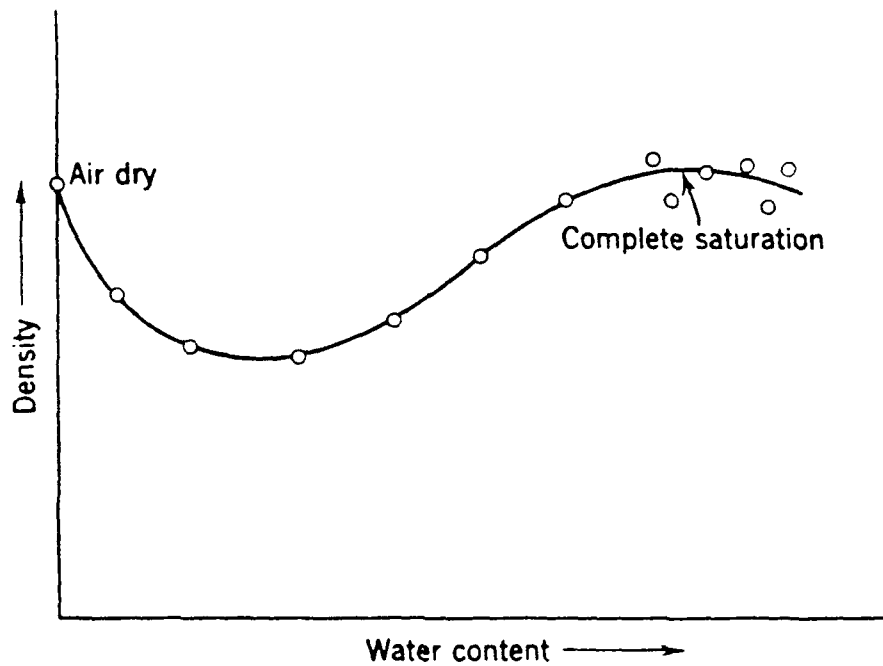


Figure 2.10 Compaction Curve for Cohesionless Soils (Foster, 1962)  
"Constant Energy"

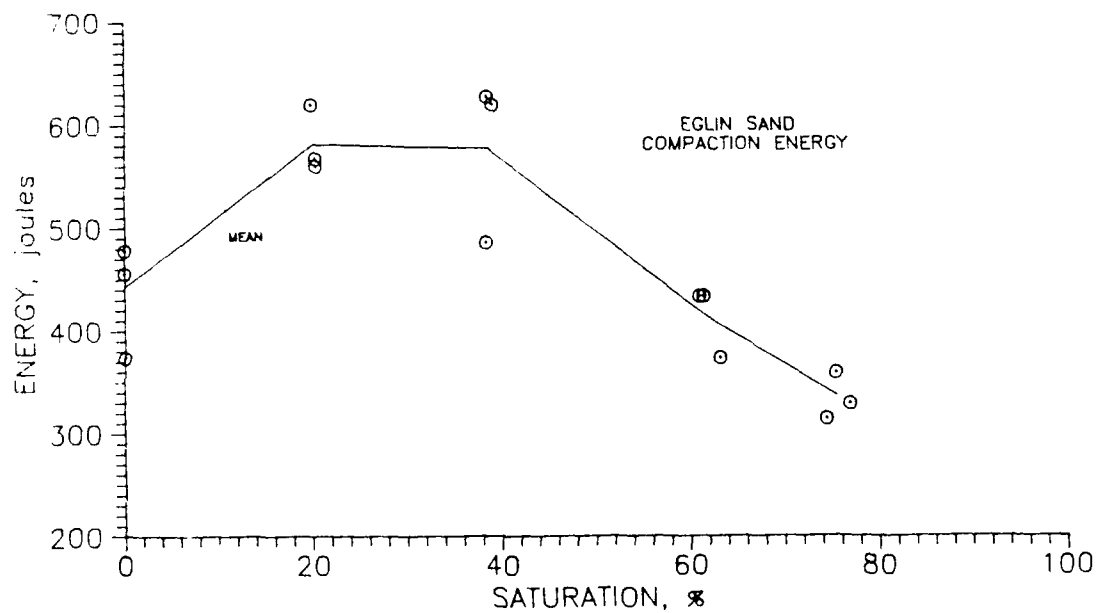


Figure 2.11 Compaction Energy Versus Saturation (Ross, 1989)  
"Constant Dry Density"

In order to determine the relationships between saturation and compaction energy, Ross (1989) developed a compaction energy apparatus. Eglin sand was mixed at a particular moisture content and loosely placed within a sample container which did not permit lateral deformation. A 24.5 N hammer was dropped on the sample from a height of 30.5 cm. The number of hammer drops required to compact the sample to a dry density of  $1760 \text{ kg/m}^3$  was recorded. Subsequent tests were performed on samples with different saturation levels. Figure 2.11 shows the relationship between saturation and the amount of energy required to compact Eglin sand to a constant dry density. The amount of energy required to compact the sand increases by approximately 22 percent, then decreases with any further increase in saturation. It appears that at intermediate saturation levels, the capillary stress between the sand particles increases the stiffness of the sand. As a result, more energy is required to break the capillary bonds and compact the sample.

Very little research has been performed in determining the influence of saturation on changes in lateral stress under conditions of cyclic loading. Such loading occurs in the dynamic compaction process. For dry sands, Lambe and Whitman (1969) have shown that under confined compression conditions, an increase in lateral stress occurs during cycles of loading and unloading. The vertical force applied to the soil causes the individual soil particles to compress and slide in the vertical direction. Upon unloading, the particles regain their original shape. This causes reverse sliding on the grain-grain contacts, causing the horizontal stress to increase. Youd

and Craven (1975) have shown that for dry 20-30 Ottawa sand, the amount of increase in lateral stress was greatest during the first cycle of loading and unloading, and diminished with each cycle thereafter. D'Appolonia et al. (1969) have shown that when a vibratory roller is used, the static horizontal stress was found to increase slightly with each roller pass. They also show that if two samples are prepared having the same dry density, but different values of  $K_0$  (the ratio of horizontal to vertical stress under static conditions), the sample with the higher  $K_0$  will be less compressible. They conclude that the compaction process is similar to preloading.

Drnevich et al. (1967) have shown that the effects of cyclic preloading on a dry 20-30 Ottawa sand specimen increases the shear modulus of the sample even if the sand density remains constant. Once the maximum increase in modulus occurs, any further prestraining begins to reduce the effects.

Hendron et al. (1969) measured the maximum horizontal and lateral stresses developed during their studies on the effects of saturation on soil compressability. For a sample of sandy silt compacted moist, the ratio of lateral stress to maximum axial stress ( $K_0$ ) increases up to a particular intermediate saturation level, then decreases with a further increase in saturation. The results are for static loading, but it may be assumed that the trend also exists once the vertical load is removed.

Various investigators have shown that differences in fabric or pore size distributions result from sands being compacted by different techniques and moisture contents. Specifically, Mulilis et al. (1977)

have shown that various compaction techniques and water contents will affect the liquefaction potential of sands. Based on their tests using eleven different compaction techniques on dry and moist sand, they conclude that the differences in liquefaction potential are due to differences in the orientation of contacts between sand grains and the uniformity of packing.

Ladd (1977) performed cyclic triaxial strength tests on sands compacted by various methods and with different moisture contents. It has been found that the method of compaction of the sand is of secondary importance to the moisture content of the soil when explaining the differences in cyclic behavior that was observed. Ladd has hypothesized that sand specimens compacted moist tend to have a more random fabric than those prepared by dry methods because the capillary stress tended to impede particle movement. As a result, sands with a random fabric tend to have a greater stiffness than sands with more oriented fabric.

Juang and Holtz (1986) studied the pore size distributions of sandy soils compacted to a constant dry density but at different moisture contents. They have determined that as the moisture content increases to the optimum amount, the pore size goes from a condition of two dominant pore sizes to one dominant pore size. As a result of increasing the moisture content, the larger pore mode tends to decrease for the same compactive effort. As a result, the permeability of the soil compacted dry is higher than that compacted moist. Similar results were obtained by Nimmo and Akstin (1988), who concluded that compaction primarily affects the large pore mode, while leaving the small pore mode relatively unchanged.

## E. COMPRESSIBILITY AND WAVE PROPAGATION THROUGH CONFINED SOILS

### 1. Compressibility

#### a. Dry Sands

From elasticity theory, a relationship was derived which links the propagation velocity of a wave to the stiffness of the soil. For a compressional wave the relationship is as follows:

$$v_c = \left\{ \frac{D}{\rho} \right\}^{0.5} \quad (2.3).$$

This equation, derived from elastic theory, is only true within the elastic limits of the material. For conditions where the stress applied is outside of the material's elastic range, equation 2.3 is only approximately correct. Whitman et al. (1960) state that one of the differences between the propagation of a wave through soils and through an ideal elastic medium is that the soil is an assemblage of discrete particles.

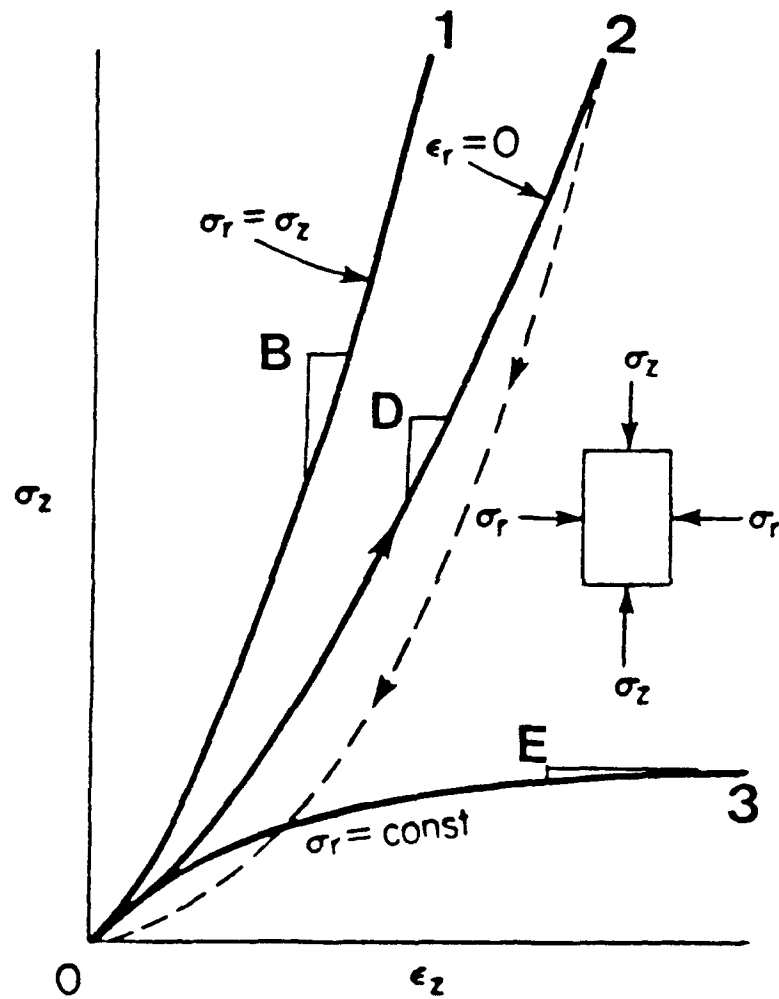
If the mineral skeleton is observed at a microscopic level it can be seen that when a soil is loaded, the stress is transmitted across the small particle contacts. Because these contacts gain their strength from cementation, friction or capillarity, they are weak in compression when compared to a material such as steel. As a result it takes very little energy to break these bonds and cause compression or strain. Whitman et al. (1960) states that the deformation of the soil mass is brought about largely by distortion of the points of contact between the particles. The resistance of a soil mass to deformation

is determined largely by the distortion resistance of these contact points.

Under all loading conditions, the soil will rearrange its structure elastically and plastically to come into equilibrium with the applied load. If the applied load is small, the majority of the structure will deform in an elastic manner. Once the load is removed only a small portion of the deformation will be irreversible (linear stress-strain behavior). Once the loading becomes larger than the elastic limit of the soil, the particles will permanently rearrange themselves in order to equilibrate with the applied load (nonlinear stress-strain behavior).

The shape of the stress-strain curve which exhibits nonlinear behavior is a function of the boundary conditions imposed on the soil. Richart et al. (1970) explain that curve 1 in Figure 2.12 is created when the lateral strain is equal to the vertical strain under hydrostatic loading. Curve 2 represents the behavior of "strain hardening" which occurs when the lateral strain is equal to zero. For the condition where there is no restriction on the amount of lateral strain, a curve such as 3 is developed.

Whitman et al. (1964) have hypothesized that under conditions of zero lateral strain (confined compression) the stress-strain curve is s-shaped. When the load is initially applied the grains undergo elastic deformations. As the stress is increased the contact points between particles slip, causing displacement of the grains. This results in a decrease in modulus. Slippage causes the grains to roll past one another into a more compact, dense condition. As the particles move into the more compact condition, the modulus increases.



1. Isotropic Compression
2. Confined Compression
3. Triaxial Compression ( $\sigma_2 = \sigma_2 = \sigma_r$ )

Figure 2.12 Theoretical Stress-Strain Curves for Different Lateral Confinement (Richart et al., 1970)

Once the stress is large enough to cause grain crushing, the modulus decreases until a more compact particle arrangement is formed.

Hendron (1963) performed one-dimensional compression tests on four different sands utilizing a high pressure one-dimensional compression apparatus. This compression device imposes stresses of up to 22,100 kPa to the soil samples. All tests were performed on dry sands under very low loading rates. The test results show that as the stress is increased, the shape of the stress-strain curves behave similarly to that found by Whitman et al (1964). He notes that significant grain crushing did not occur below stresses of 20,700 kPa. Hendron has also found that for the sands tested, the constrained modulus is proportional to the vertical applied stress to the one third power.

#### b. Unsaturated Sands

Under unsaturated conditions the behavior of the soil is much more complicated than the dry or fully saturated conditions. For small stress changes the compressibility of the soil is governed by the mineral skeleton. At larger values of stress, the strain will be large enough to cause the soil to saturate, which will reduce the soils compressibility considerably.

Hendron et al. (1969) performed high pressure (0 to 138,000 kPa) static, one-dimensional compression tests on samples of sandy silt. Samples were compacted moist to various dry densities in consolidation rings by use of a Harvard miniature type compactor. Figure 2.13 shows the results obtained. The figure indicates that at



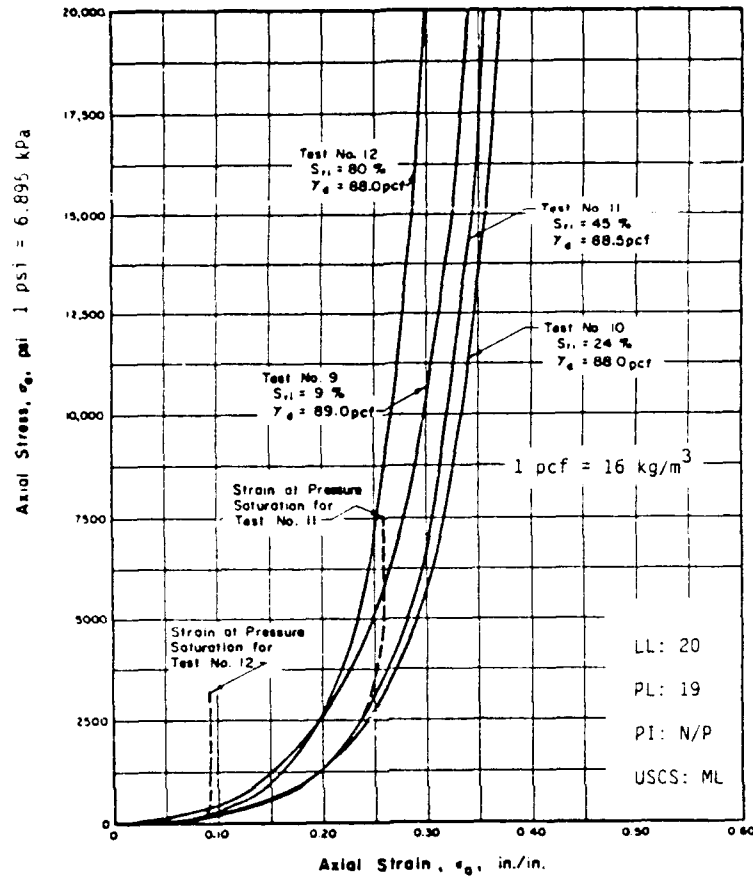


Figure 2.13 Stress-Strain Curves For Sandy Silty at Various Saturation Levels (Hendron, et al., 1969)

- Spheres  $\frac{1}{8} \pm 10 \times 10^{-6}$  in. diameter
- △ Spheres  $\frac{1}{8} \pm 50 \times 10^{-6}$  in. diameter

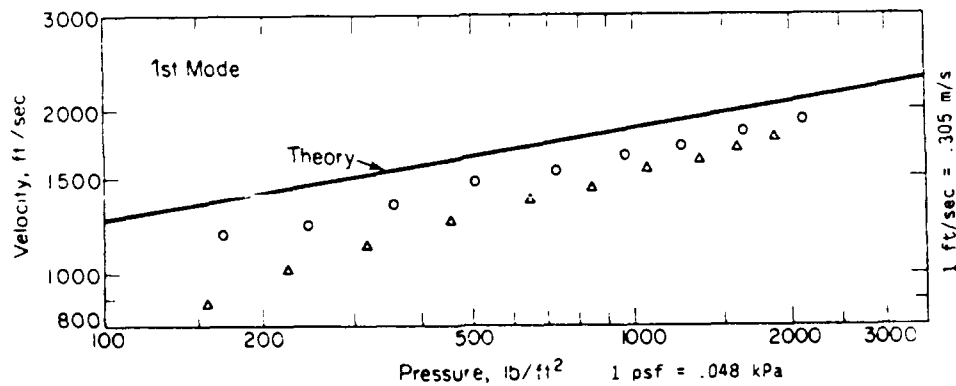


Figure 2.14 Variation of Compression Wave Velocity with Confining Stress for Steel Spheres (Duffy and Mindlin, 1957)

lower stress levels the more saturated samples are more compressible. As the stress level increases the wetter samples reach full saturation before dryer samples. As a result the increase in stiffness due to saturation occurs at lower stress levels for wetter samples. Based on the test results, it has been concluded by the authors that the most important variables governing one-dimensional stress-strain relations are void ratio and saturation level.

Based on their experimental results, Hendron et al. (1969) present an equation for the determination of the secant constrained modulus for stress levels above 21,000 kPa. The equation is valid for unsaturated soils which are either remolded or undisturbed, as the results of their analysis show that the modulus will be the same for stresses over 21,000 kPa.

Balakrishna Rao (1975) has attempted to develop a method for predicting stress-strain curves for a given soil under varying degrees of saturation. An oedometer was used for the testing which allowed for stresses ranging from zero to 4800 kPa, and loading rates from 3 to 30 milliseconds. Two sands were tested, a 20-30 Ottawa sand and concrete sand, which were compacted moist to a constant dry density of  $1680 \text{ kg/m}^3$  to obtain a particular saturation level. The method of compaction used was not given in the report. Balakrishna Rao has concluded that for saturation levels between zero and 60 percent, the water has little influence on the stress-strain relationships for either sand studied.

### c. Loading Rate Affects

Whitman (1970) concluded that time dependent effects on the value of constrained modulus can be ignored for dry granular soils subjected to loadings having millisecond or larger rise times. It is noted that time effects may become important when the duration of the stress pulse is below approximately one millisecond, but further research is required to verify the findings.

Jackson et al. (1980) performed tests on three dry sands under dynamic loadings. The loading rate does not effect the value of constrained modulus for rise times above 1 millisecond. For rise times between 0.1 and 1 millisecond, the constrained modulus increases by an order of magnitude. No theory has been developed to why this effect occurs.

## 2. Wave Propagation

Various studies have been performed to determine the relationship between stress wave propagation and soil parameters including void ratio, confining stress, soil type, grain shape, grain size distribution, saturation and soil type. Most of the research has been performed on dry or saturated soils, while little has been done in the area of compressive wave propagation through unsaturated soils.

#### a. Low Intensity Waves

Duffy and Mindlin (1957) proposed one of the earliest theories relating the stress wave velocity with stress-strain properties of a dry granular medium has been proposed by Duffy and Midlin (1957). Their theory is based on the elastic properties of a face-centered cubic array of spheres and the theory of elastic bodies in contact (including normal and tangential forces). From the theory of the elastic behavior of spheres in contact, the longitudinal (and bulk) modulus vary with confining stress to the one-third power. From the relationship between wave velocity and modulus (equation 2.1) they anticipated that the wave velocity would vary with confining stress to the one-sixth power.

A portion of the experimental results obtained are shown in Figure 2.14. Wave velocities predicted by the theory are higher than those resulting from experimentation, though the differences decrease as the confining stress is increased.

Whitman, Roberts and Mao (1960) analyzed soniscope tests (used for field esting of concrete by a pulsing technique) performed by Martin (1957) on Vicksburg loess to study the effects of moisture content on sonic propagation velocity. Figure 2.15 presents the results obtained by Martin for the relationship between dry density and compressional wave velocity, with water content for various compaction energies. Whitman et al. (1960) observed from Figure 2.15 that the wave velocity drops as the molding water content is increased above the optimum level. Since a soil can have the same dry density above and below the optimum moisture content, they conclude that other

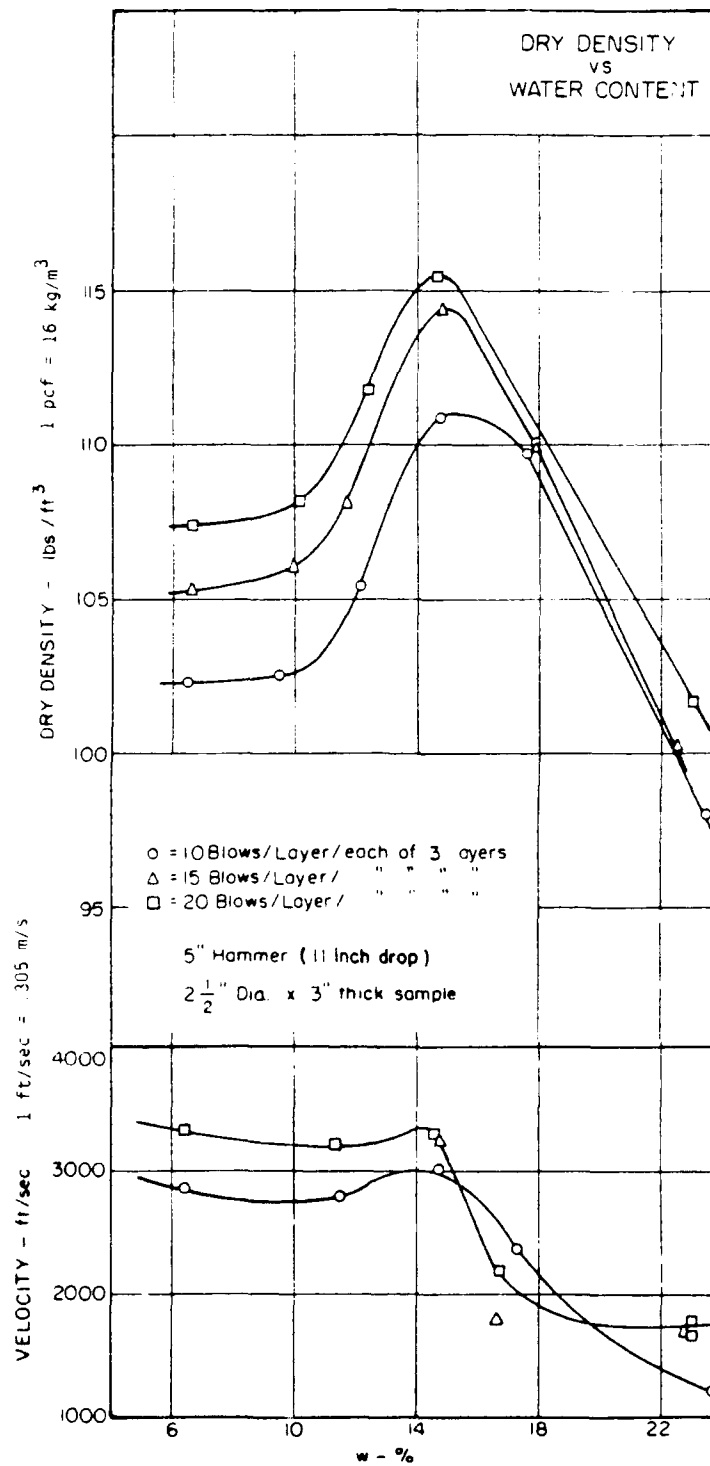


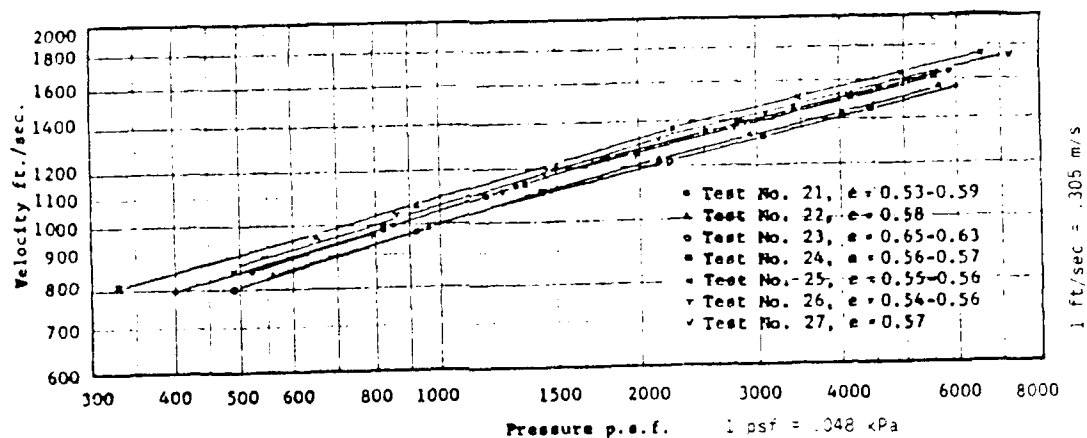
Figure 2.15 Variation of Dry Density with Compactive Effort and Moisture Content for Vicksburg Loess (Martin, 1957)

factors than dry density must affect the wave velocity. No explanation is given as to what the effect is.

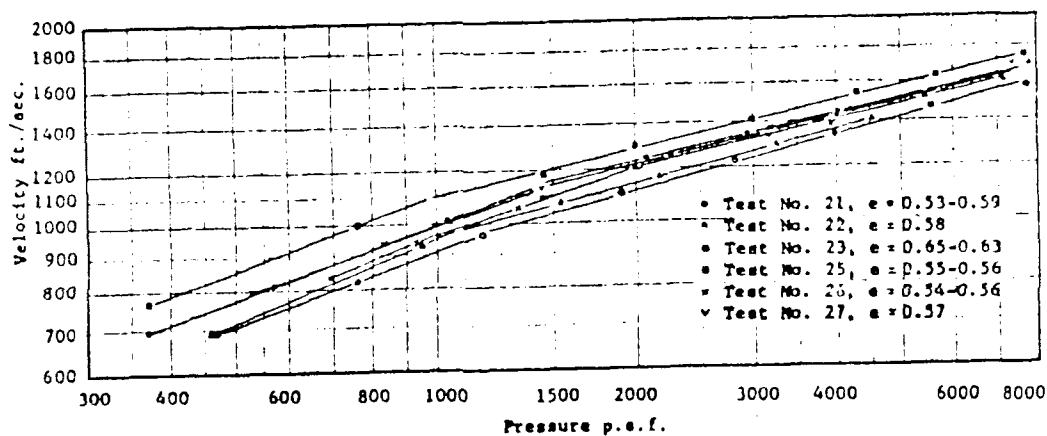
Hardin (1961) utilized an early resonant column device to determine the relationship between elastic compressional and shear wave velocities, with confining stress, void ratio and sand type for dry, saturated and drained samples. The drained samples had an average moisture content of 1.4 percent. Hardin has found that as the confining stress is increased, the wave velocity increases, and as the void ratio is increased, the wave velocity generally decreases. Some of the results for dry Ottawa sand are presented in Figure 2.16. The wave velocity through the saturated samples was generally less than either the drained or dry samples. He attributed this to the drag of the water in the pore spaces, though it should be noted that from equation 2.3, the increase in density of a saturated specimen will also reduce the wave velocity.

Based on all of the experimental results, Hardin concluded that for dry, saturated or drained specimens under a confining stress of between 13,800 and 55,200 kPa, an exponent of  $1/4$  should be applied to the confining stress when relating it to wave velocity. For a confining stress below 13,800 kPa, the exponent varies between  $1/2$  and  $1/4$  depending on moisture content and grain angularity.

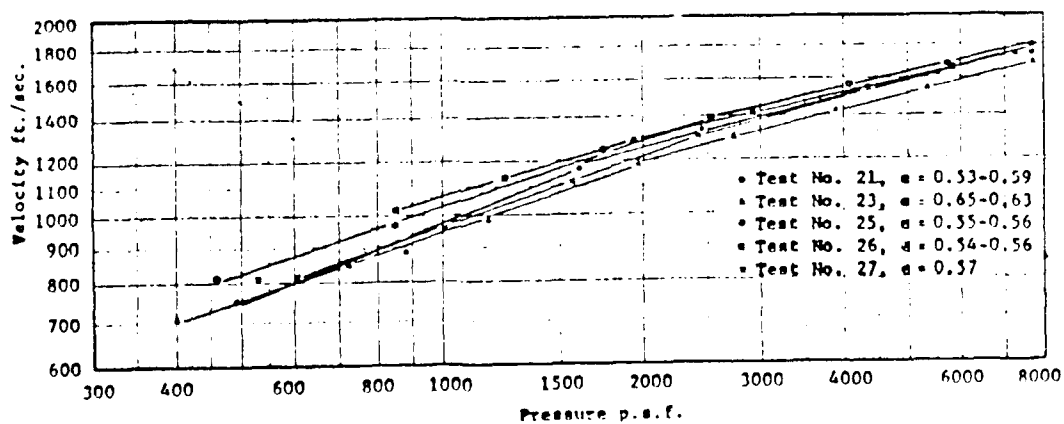
Whitman (1970) theorizes that at high saturation levels, the pore phase of a soil is much less compressible than the mineral skeleton. This allows the compression wave to travel primarily through the pore phase. At lower saturation levels, the mineral



a. Dry



b. Saturated



c. Moist

Figure 2.16 Variations of Wave Velocity with Confining Stress  
a. Dry, b. Saturated, c. Moist (Hardin, 1961)

skeleton is less compressible than the pore phase, allowing the majority of the wave to travel through the skeleton.

Whitman (1970) presents a mathematical model which relates saturation to wave velocity through the equation:

$$v_c = \left\{ \frac{\frac{u'_a}{n(1-S)} + D_s}{((1-n)G_s + S n)\rho_\omega} \right\}^{1/2} \quad (2.14)$$

where  $u'_a$  is the absolute air pressure,  $n$  is the porosity,  $S$  the saturation level,  $D_s$  the constrained modulus of the mineral skeleton and  $G_s$  the specific gravity. This relationship is based on a modified rule of mixtures. When the saturation approaches 100 percent, the wave velocity increases dramatically. Whitman states that on the basis of this model, the threshold value of saturation is unity. For any value of saturation less than 100 percent, the compressional wave velocity is controlled by the mineral skeleton.

A model has been presented by Anderson and Hampton (1980) for determining the sound velocity in a gassy sediment. The model is based on the accoustical properties of the gassy sediment and an equation for simple mixtures. The equation takes the form:

$$v_c = \left\{ \frac{K}{\rho} \right\}^{0.5} \quad (2.15).$$

$K$  is the aggregate bulk modulus which is based on a parallel spring assumption for the contributions of stiffness due to the soil solids, water and air. The soil density,  $\rho$ , is based on a modified rule of mixtures which is an extension of the equation presented by Wood (1930). Richart et al. (1970) presents a similar model for estimating the compression wave velocity in an unsaturated soil.



#### b. High Intensity Waves

Stoll and Ebeido (1965) have performed shock wave propagation tests on dry 20-30 Ottawa sand under conditions of limited radial strain. An input pressure pulse of 552 kPa and a rise time of 20 microseconds was used under a confining vacuum which varied from 5.8 to 95.8 kPa. The results obtained are shown in Figure 2.17. Also plotted are results obtained by Hardin (1961). The tests performed at high amplitudes and loading rates (Stoll and Ebeido) result in higher wave velocities than obtained under elastic conditions (Hardin, 1961). Because the samples were laterally confined in this analysis, the stress-strain curve is concave to the stress axis. As the applied stress increases, the modulus increases under this condition. As a result, equation 2.3 would predict that the wave velocities should be higher under this condition than when soils are tested under elastic conditions, or when there is no lateral confining stress. Stoll and Ebeido also show that as the rise time decreases, the wave velocity increases. This would indicate that the rate of loading changes the modulus.

Ross et al. (1988) have utilized a split-Hopkinson pressure bar to test the effects of varying moisture content on wave velocity and stress transmission for four different sands. All tests have been performed under confined compression conditions, with an incident stress of 177 kPa and a rise time of 15 microseconds. All sand samples were mixed with a particular amount of water, then compacted moist to a constant dry density. Figures 2.18 through 2.21 show the results obtained by Ross et al. for the 20-30 Ottawa and Eglin sands.

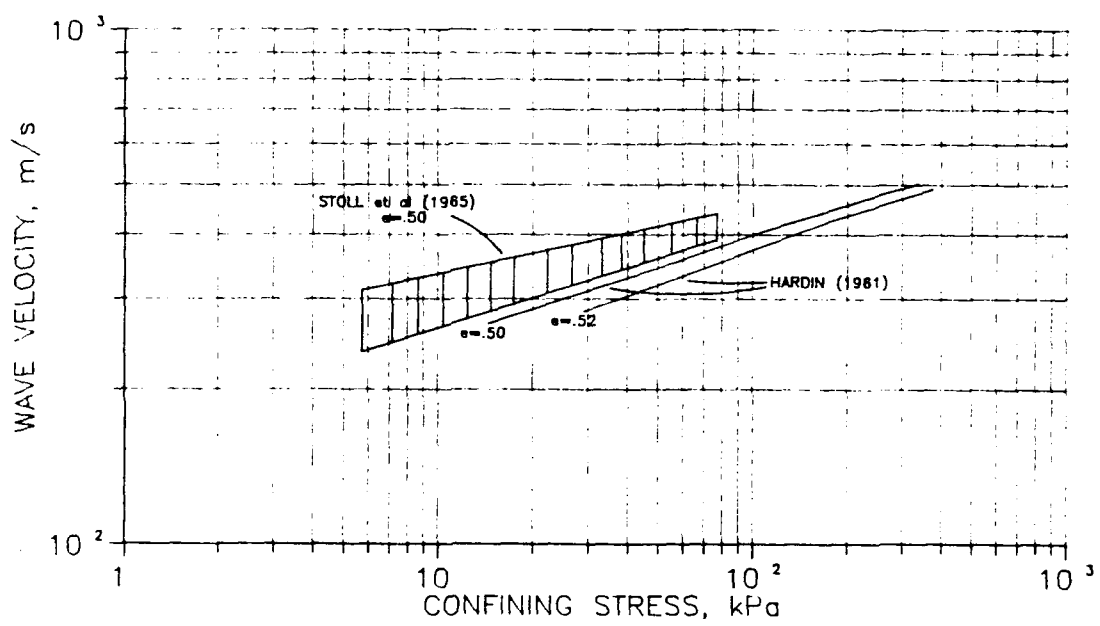


Figure 2.17 Variations of Wave Velocity with Confining Stress  
(Hardin, 1961; Stoll and Ebeido, 1965)

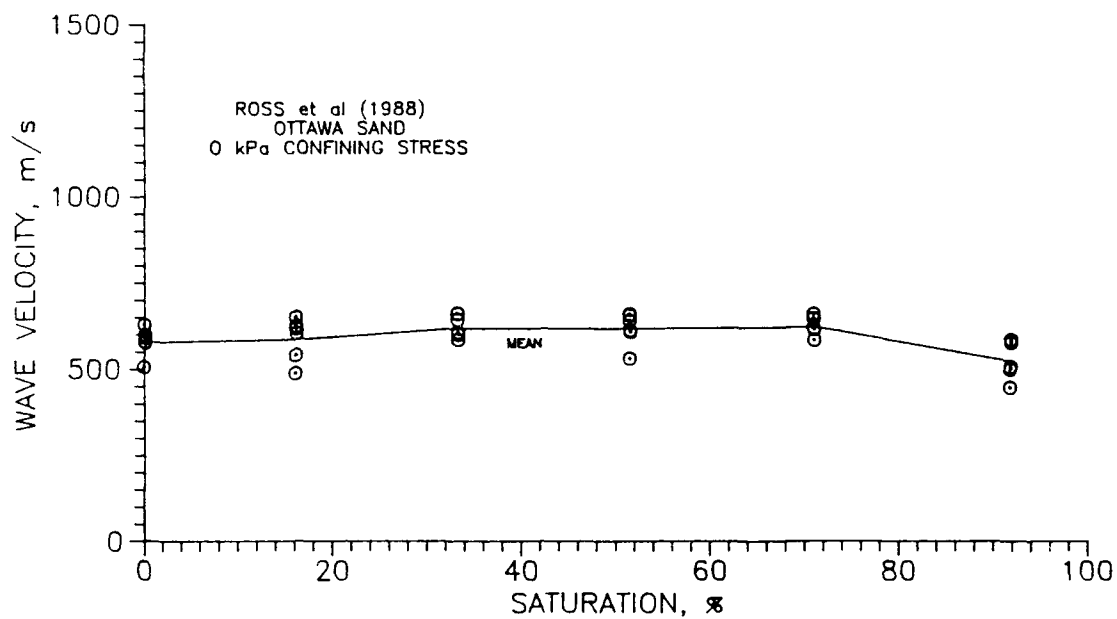


Figure 2.18 Wave Velocity Versus Saturation for 20-30 Ottawa Sand (Ross et al., 1988)

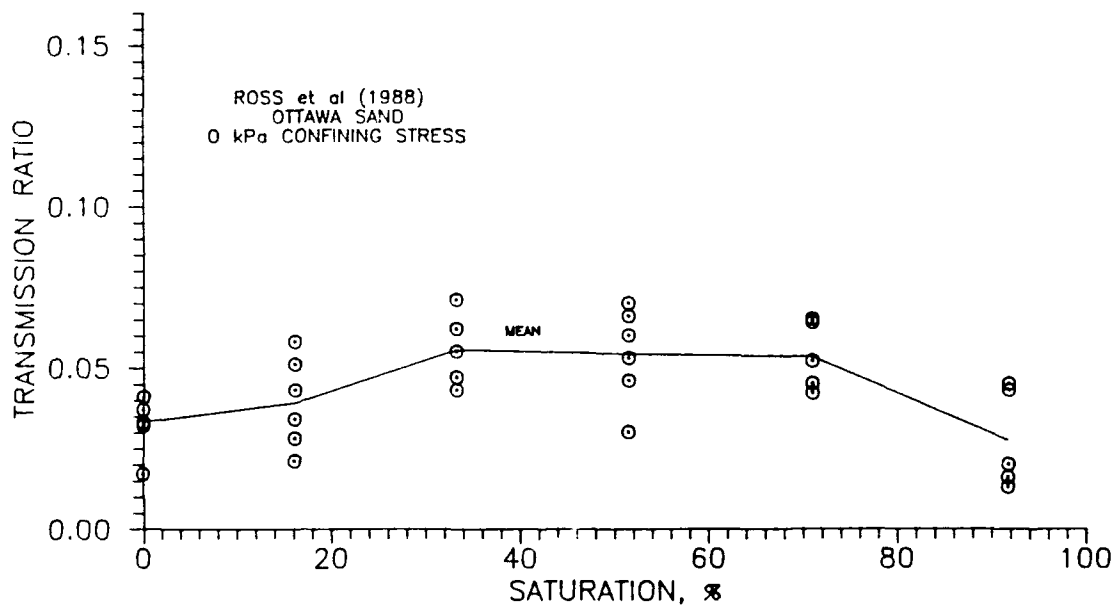


Figure 2.19 Transmission Ratio Versus Saturation for 20-30 Ottawa Sand (Ross et al., 1988)

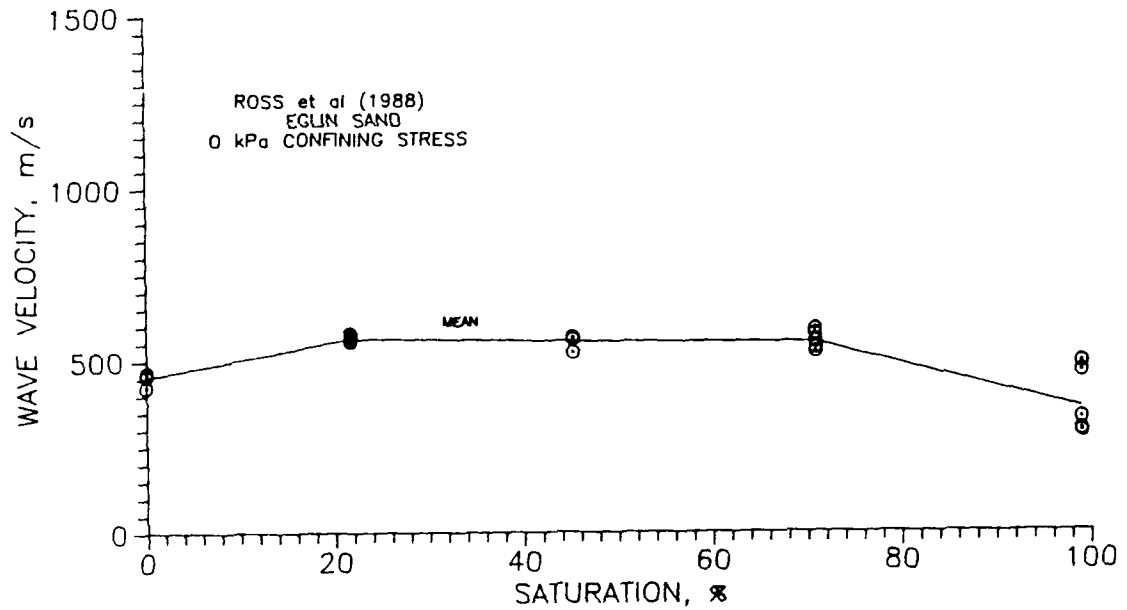


Figure 2.20 Wave Velocity Versus Saturation for Eglin Sand  
(Ross et al., 1988)

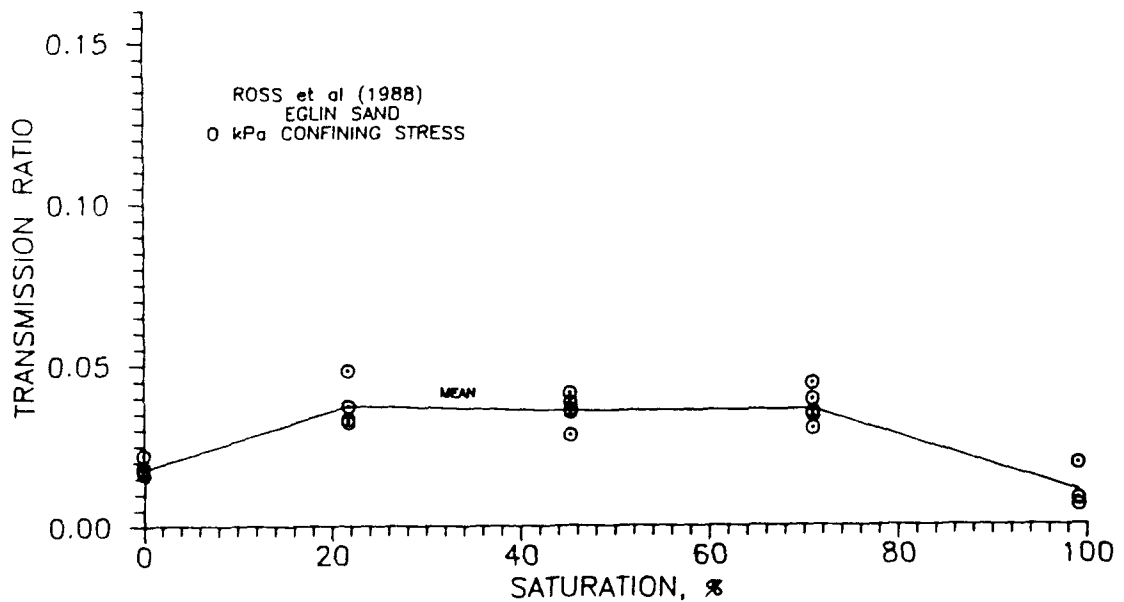


Figure 2.21 Transmission Ratio Versus Saturation for Eglin Sand  
(Ross et al., 1988)

The wave velocity and stress transmission values increase as the saturation level increases from 0 to approximately 40 percent, then decrease with any further increases in saturation. Quasi-static stiffness tests show similar results as shown in Figure 2.22.

The authors show that the trends obtained may be explained by the effects that saturation and capillary stress have on effective stress. In order to quantify this relationship, they utilize equation 2.12 and assume that the parameter  $\chi$  is equivalent to the saturation level of the sand. The increase in effective stress due to saturation is presented in Figures 2.23 and 2.24 for both the Eglin and Ottawa sands. These figures show similar trends to those for wave velocity, stress transmission and stiffness, though the magnitudes of the increase in effective stress due to capillarity are small.

Ross et al. (1988) concluded that the increase in effective stress can be attributed to the effects of capillarity. But, the increase in stress transmission ratio at intermediate saturations is approximately two to three times the dry or near saturated values, while the increase in effective stress due to capillarity is very small. As a result of the small increase in effective stress due to capillarity, the effective stress equation by Bishop et al. (1960) may not be adequate to explain the trends observed. They also state that the energy required to compact the specimens may affect the results.

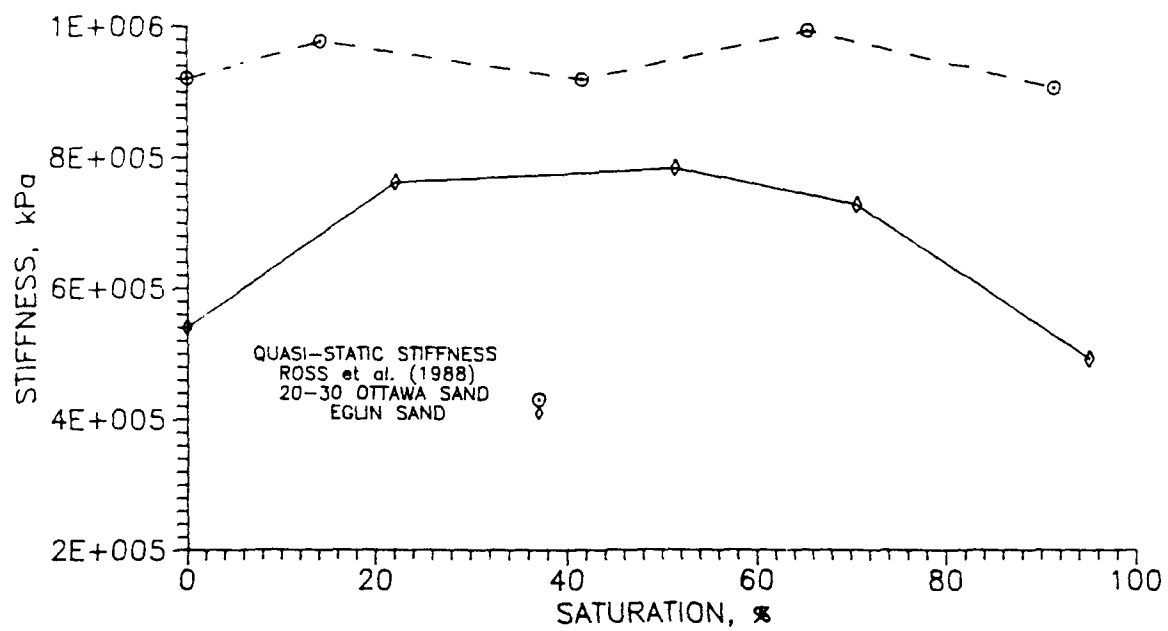


Figure 2.22 Quasi-Static Stiffness Results for 20-30 Ottawa and Eglin Sands (Ross et al., 1988)

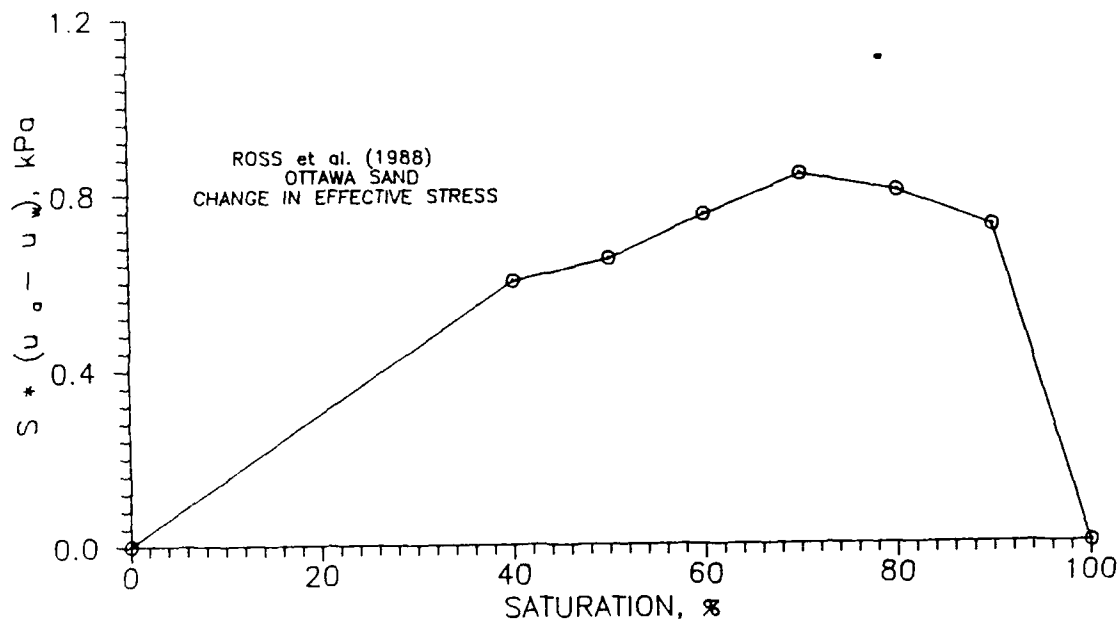


Figure 2.23 Increase in Effective Stress Due To Capillarity  
for 20-30 Ottawa sand (Ross et al., 1988)

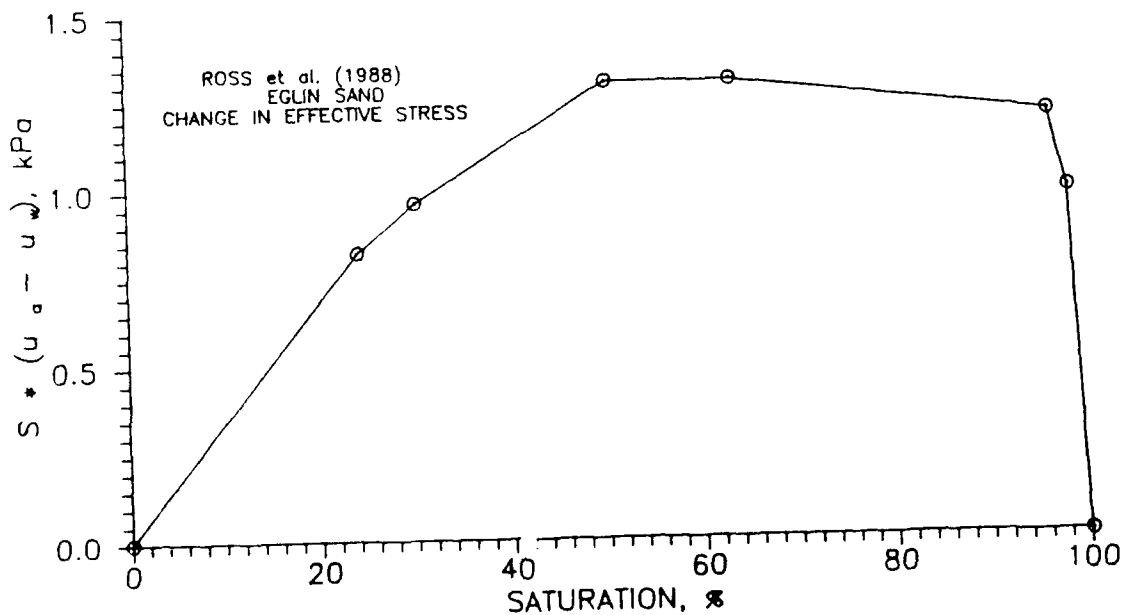


Figure 2.24 Increase in Effective Stress Due to Capillarity  
for Eglin Sand (Ross et al., 1988)

### 3. Comparisons between Compressibility and Wave Velocity

Moore (1963) performed static and dynamic one-dimensional compression tests and compressive wave propagation tests on dry Monterey sand to determine the relationship between the experimental constrained modulus and that determined from the wave propagation velocity through equation 2.3. A resonant column device which has the ability to confine the specimens laterally was used to determine the wave velocities. The confining stress magnitudes were varied between 103 and 2069 kPa, and the soil was compacted to a dry density of 1600 kg/m<sup>3</sup>. Dynamic compression tests were performed utilizing several different devices.

An example of the results obtained are shown in Figure 2.25. The wave propagation velocity values have been corrected for dispersion that was shown to occur during testing. Moore has concluded that in general the static and dynamic moduli are the same as the modulus based on wave velocity at low and high stress levels, while they diverge at intermediate levels. A considerable amount of scatter occurred in the data which could be a result of stress history effects or experimental error.

Calhoun and Kraft (1966) performed high stress (5,500 kPa) laterally confined compression tests on unsaturated silt in order to develop a mathematical model to determine the compressive wave velocity and attenuation based on the stress-strain relationships determined at high stresses. The model developed is based on a model by Weidlinger and Matthews (1964) which defines one-dimensional shock



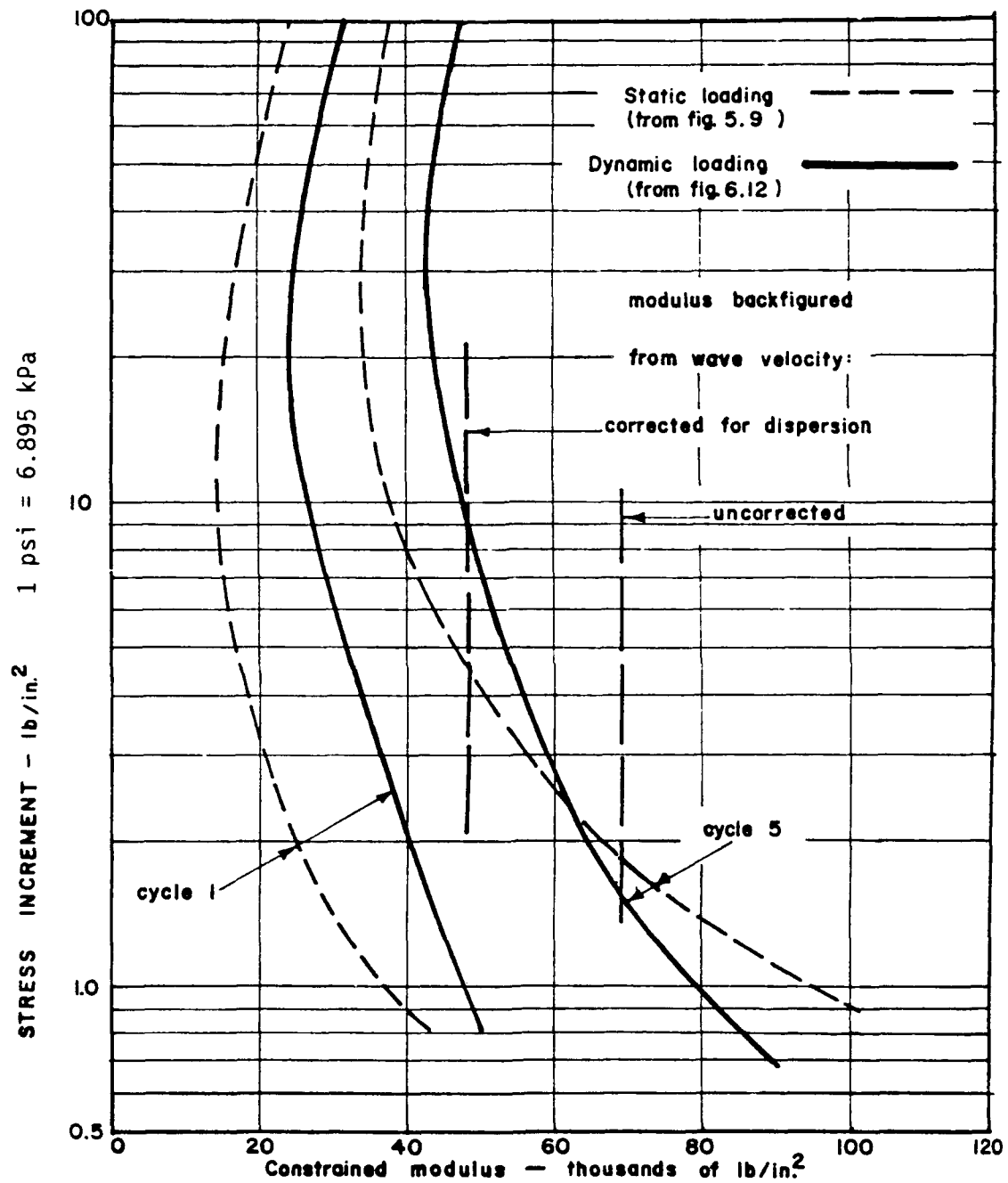


Figure 2.25 Variations of Wave Velocity with Confining Stress for Monterey Sand Due to Static, Dynamic and Wave Propagation Methods (Moore, 1963)

wave phenomena in a nonlinear, locking medium. Combining this model with the equation for momentum and a governing shock equation, equations for predicting stress wave propagation and attenuation with depth have been developed. From these equations, Calhoun and Kraft found that wave propagation and attenuation are functions of only the initial static surcharge (confining stress) when the soil saturation is below 90 percent. Above 90 percent, the increase in modulus due to water becomes important. The results are based on silt samples which were compacted moist by use of a Harvard miniature compactor prior to confined compression testing.

#### F. ADDITIONAL USEFUL UNSATURATED SOIL RESEARCH

Wu et al. (1984) have performed resonant column tests on fine grained cohesionless soils to determine the influence of saturation on shear modulus. The relationship between wave velocity and shear modulus is similar to equations 2.1 through 2.3. Samples were compacted moist in a standard mold (3.6 cm in diameter and 8 cm high), and confining stresses were varied from 25 to 98 kPa.

The gradations of the soils tested are shown in Figure 2.26, and an example of the variation in shear modulus with saturation and confining stress is shown in Figure 2.27. A trend is developed with changes in saturation which is similar to that obtained by Ross et al. (1988). The maximum values of shear modulus for each soil type and confining stress used are shown in Table 2.1. It should also be noted that as the confining stress is increased, the wave velocity

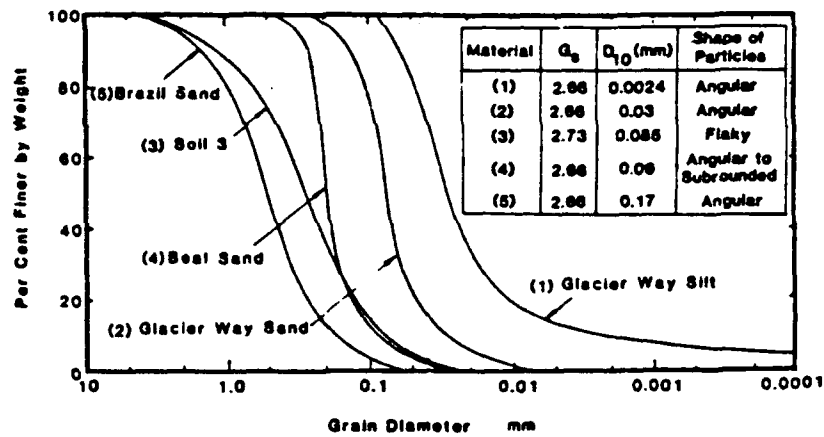


Figure 2.26 Gradations for Soil Types Used by Wu et al., (1984)

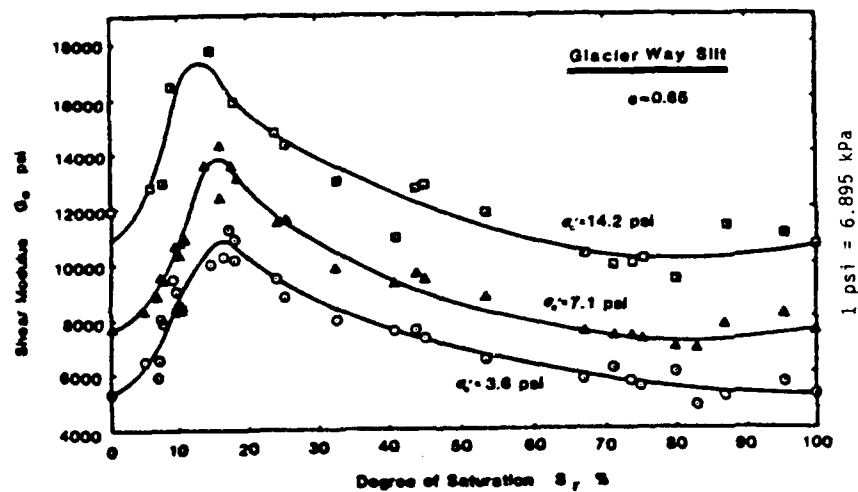


Figure 2.27 Variations of Shear Modulus with Saturation Under Several Confining Stresses for Glacier Way Silt (Wu et al., 1984)

Table 2.1 Maximum Variation in Shear Modulus with Changes in Saturation and Confining Stress (Wu et al., 1984)

Material tested (1)	$G_o$ ( $G_o$ in the moist condition)*			$(S_r)_{opt.}$ , as a percentage (5)
	$G_{o(dry)}$ ( $G_o$ in the dry condition)			
	$\sigma'_o = 3.6$ psi (2)	$\sigma'_o = 7.1$ psi (3)	$\sigma'_o = 14.1$ psi (4)	
Glacier Way Silt	2.05	1.78	1.66	17.5
Glacier Way Sand	1.62	1.44	1.37	10.0
Soil 3	1.84	1.65	1.56	9.0
Beal Sand	1.54	1.38	1.34	7.5
Brazil Sand	1.27	1.13	—	5.0

\*Herein the ratio of  $G_o/G_{o(dry)}$  is specifically denoted as the *maximum* value of the ratio and  $(S_r)_{opt.}$  is the optimum degree of saturation corresponding to this maximum value.

increases, but the trend obtained for the variations in shear modulus with saturation becomes less distinct.

In order to assess the influence of capillarity on the shear modulus, the effective stress equation 2.12 has been utilized by Wu et al. The results obtained are similar to those presented by Ross et al. (1988). Wu et al. found that the capillary influence is greatest in soils having a small effective grain diameter,  $d_{10}$ , and a low confining stress. An empirical relationship has also been presented relating shear modulus at any moisture content to the saturation level and dry shear modulus.

Hryciw and Dowding (1987) completed a laboratory study of the effects of saturation on cone penetration resistance. Samples were prepared at different saturation levels through a unique procedure. Samples were saturated, then vibrated to a particular relative density. Under pressure, carbon dioxide was then allowed to enter the

system. Once completed, the pressure was slowly reduced to allow the dissolved carbon dioxide to come out of solution. The amount of displaced water could then be measured to determine the degree of saturation. The results obtained are very similar to those presented by Wu et al. (1984) and Ross et al. (1988).

#### G. SUMMARY OF PREVIOUS RESEARCH

Literature pertinent to this investigation has been reviewed in this chapter. The sections on capillarity, unsaturated soil mechanics, compressibility, and wave propagation properties of unsaturated sands have shown that there has been little research performed in determining high intensity stress wave propagation parameters for unsaturated soils. The section on the effects of compaction procedures has shown that while there are documented cases of compaction effects on values of liquefaction potential, cyclic strength and permeability, little theory or experimental data has been developed to determine how and why it occurs.

Currently, there are no theoretical models to explain the results obtained by Martin (1957), Wu et al. (1984) and Ross et al. (1989). The theory of effective stress for unsaturated soils proposed by Bishop et al. (1960) may help in understanding how capillarity affects stress wave parameters. The theories presented by Fredlund (1986) have yet to be used in dynamic soil problems. Neither of the two models proposed for predicting the wave velocity in an unsaturated soil (Whitman, 1970; Anderson and Hampton, 1980) produce trends which are similar to those obtained for soils compacted moist.

There have been no detailed studies performed to determine if and how moisture in the compaction process effects the stiffness of sands under static and dynamic loading conditions. The trends obtained by Ross et al. (1988) do not behave in a manner predicted by any of the conventional unsaturated soil mechanics theories because the method of compaction could control the stiffness of the soil. Currently, there has not been enough research performed in the area of high intensity stress wave propagation to conclude whether the compaction technique is an important factor to consider.

### III. EXPERIMENTAL PROCEDURES

#### A. EQUIPMENT UTILIZED

##### 1. Description of Split-Hopkinson Pressure Bar

The apparatus which was used to measure the propagation of compression waves through unsaturated sand specimens is the split-Hopkinson pressure bar (SHPB) located at the Engineering and Services Center, Tyndall Air Force Base, Florida. The apparatus is the same as that used by Ross et al. (1986, 1988). This device has been designed to accommodate long specimen samples which have an aspect ratio (length / diameter of specimen) greater than one. This particular SHPB has been used in testing high strain properties of soil, concrete and mortar. The SHPB and electronic equipment are briefly discussed here. For a more complete discussion of the SHPB design, refer to Ross et al. (1986).

A schematic of the SHPB used is shown in Figure 3.1. A gas gun located at the left end of the I-beam is used to accelerate a striker bar through the barrel and impact the incident bar. This impact produces a stress pulse which travels down the incident bar. A portion of the wave will be transmitted through the sand sample, and into the transmitter bar according to the wave propagation theory presented in Chapter 2.

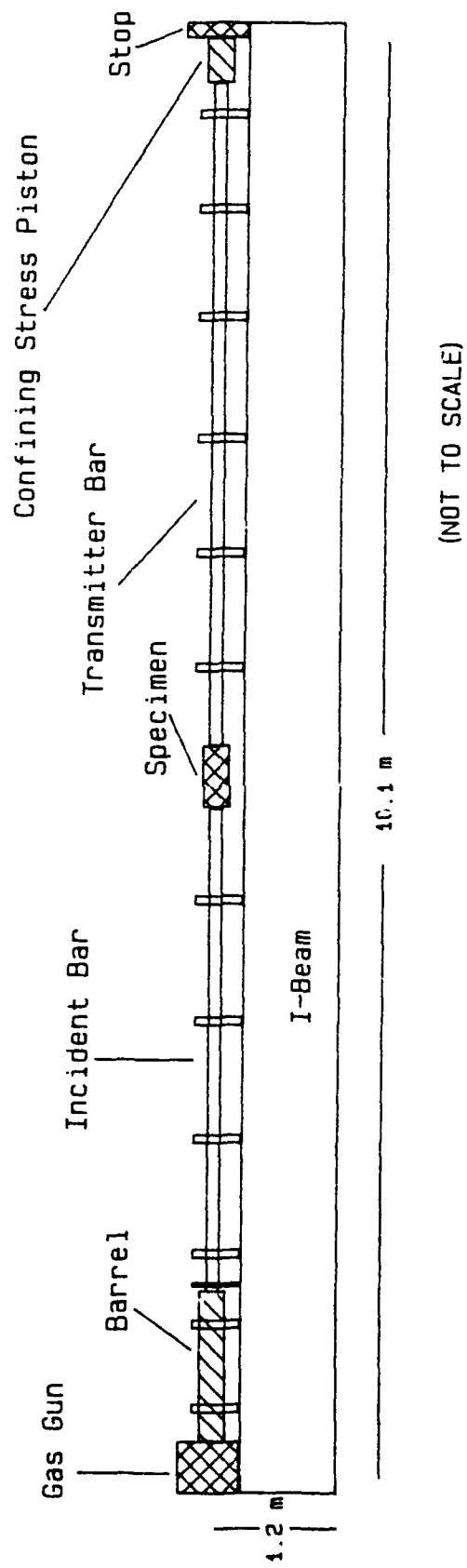


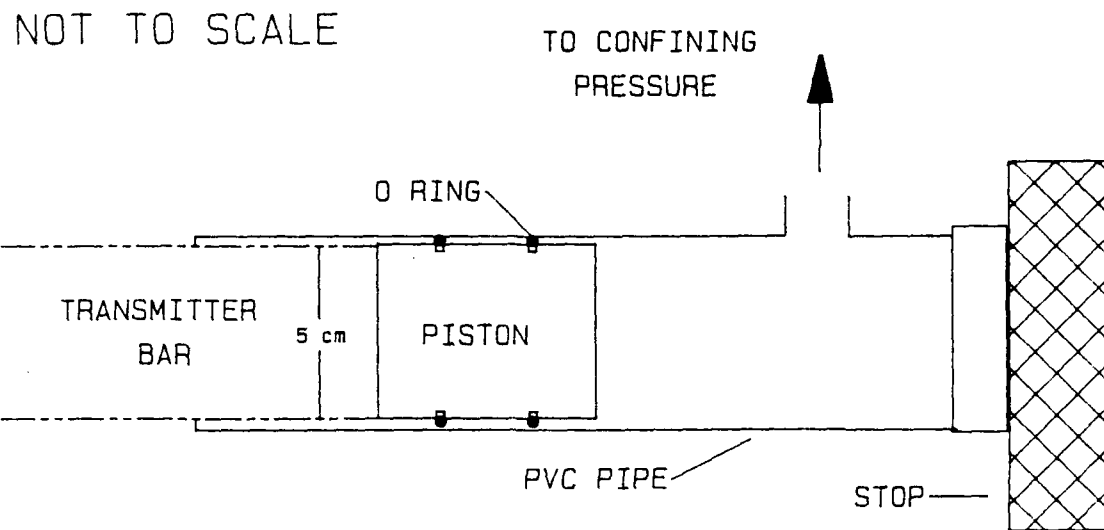
Figure 3.1 Schematic of Split-Hopkinson Pressure Bar



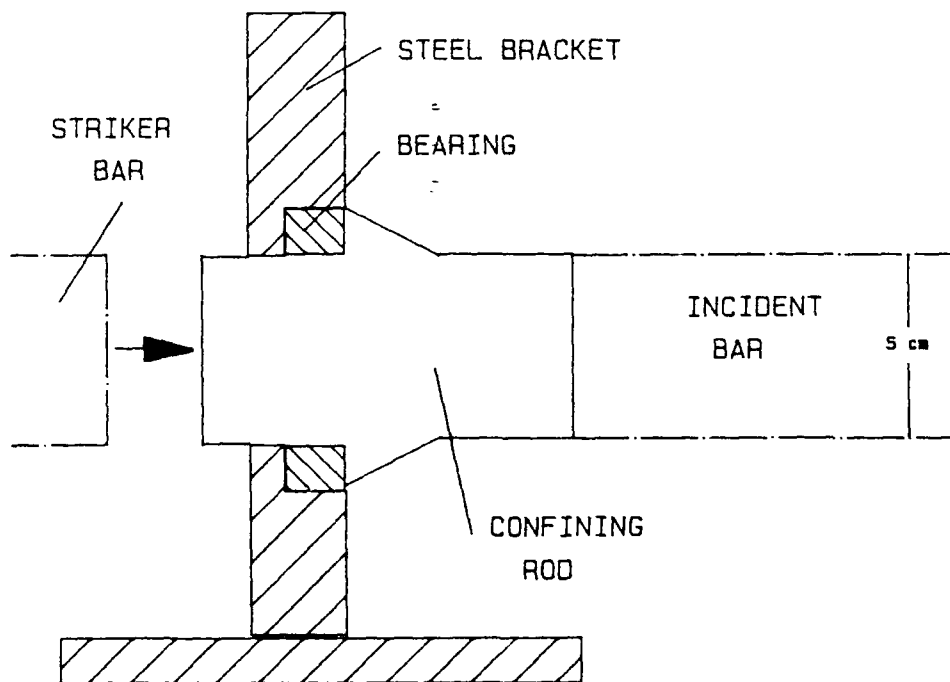
The gas gun launcher consists of two chambers and utilizes compressed nitrogen with a fast acting pressure relief piston. In this investigation a constant striker bar length of 20.32 cm was used, while the pressure within the outer chamber of the gas gun was kept at 172 kPa. This resulted in a striker bar velocity of approximately 13 meters per second for all tests performed. The impact of a steel striker bar of this length and velocity against a steel bar of the same diameter results in a stress pulse with a rise time of 15 microseconds, a pulse length of 80 microseconds, and a magnitude of approximately 290,000 kPa traveling through the incident bar.

The pressure bars used in the SHPB are composed of 5.08 cm diameter PH 13-8 Mo stainless steel rods. The incident bar was 3.66 m long, the transmitter bar 3.35 m long and the striker bar was 20.32 cm long. The pressure bars are held in place by Dodge Journal bearings spaced approximately 0.9 meters apart on top of the I-beam.

In order to create triaxial confining stress, confining pressure was required along the incident and transmitter bars. In order to accomplish this, axial confining pressure was applied through the pressure bars from a confining stress piston placed on the "free" end of the transmitter bar. Figure 3.2a is a schematic of the piston. In order to prevent the pressure bars and sample container from moving into the gas gun barrel upon application of the axial confining stress, a bracket was designed and placed between the incident bar-striker bar interface. As shown in Figure 3.2b a 10.2 cm long piece of stainless steel was machined to allow for the incident pulse to be transmitted from the striker bar to the incident bar while containing



(a)



(b)

Figure 3.2 Schematic of Axial Confining Stress Components  
a. Confining Piston, b. Confining Bracket

the axial confining stress. A bearing was placed within the bracket to allow for some movement of the confining rod during wave propagation.

The source of confining pressure for the lateral and axial confinement was a 830 kPa air compressor. In order to have the same pressure in the sample container and along the pressure bars, a single line of confining pressure connected to both the sample container and the confining piston was built as shown in Figure 3.3. Since the chosen confining fluid for the sample container was water, an air-water interface was placed between the air compressor and sample container.

## 2. Specimen Container

A schematic of the sample container used in this investigation is shown in Figure 3.4. The container was designed to allow for the application of variable confining stress around the sample, while preventing any lateral strain from developing while the compressive wave propagated through the specimen. The outer cylinder of the container is composed of 0.635 cm thick stainless steel. The cylinder has an inside diameter of 5.40 cm and a length of 15.24 cm.

In order to apply a confining pressure to the sand sample, a 1 mm thick membrane was used to line the inside of the steel cylinder. Two valves were connected to the cylinder to allow for the application of confining stress and vacuum between the steel cylinder and membrane

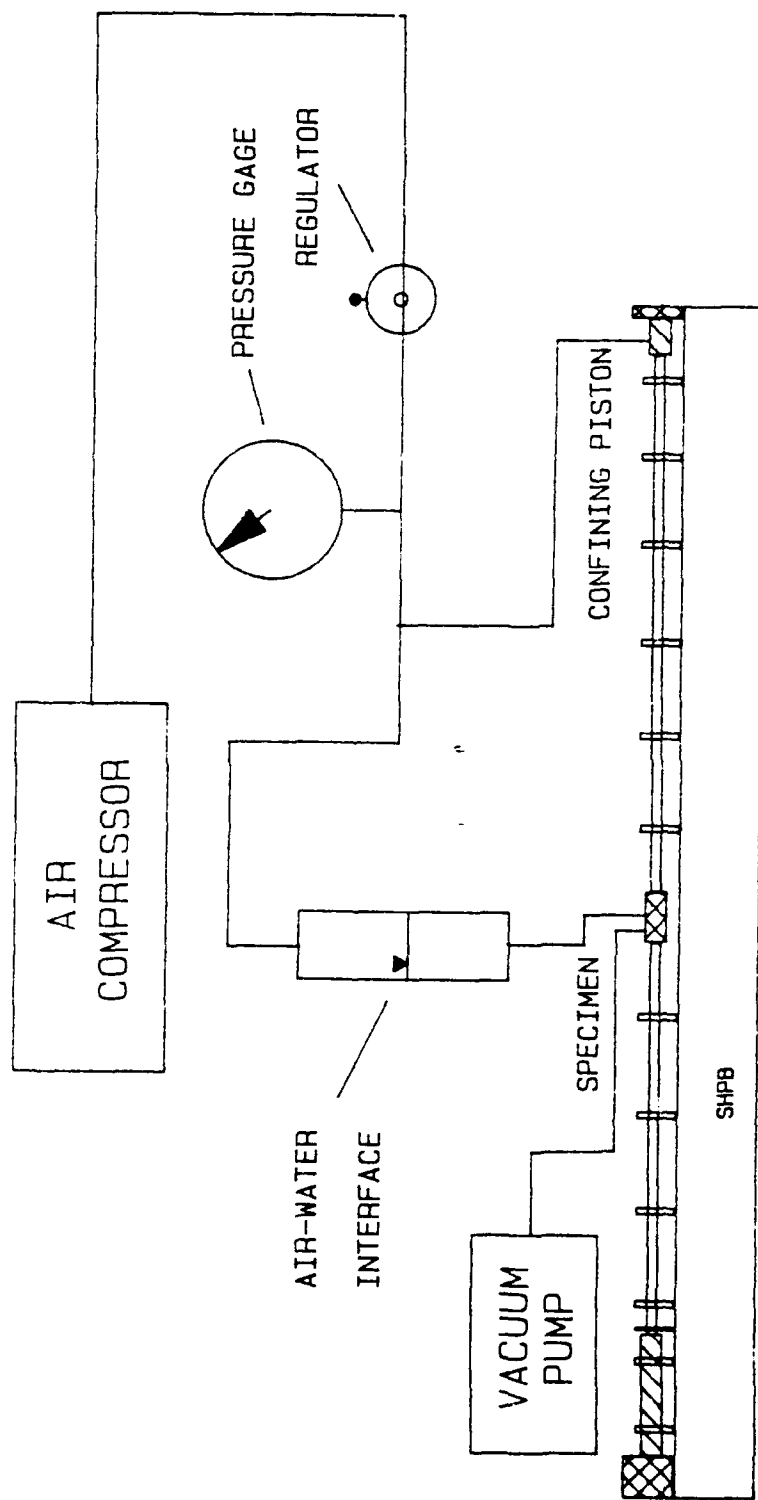


Figure 3.3 Schematic of Confining Pressure Apparatus

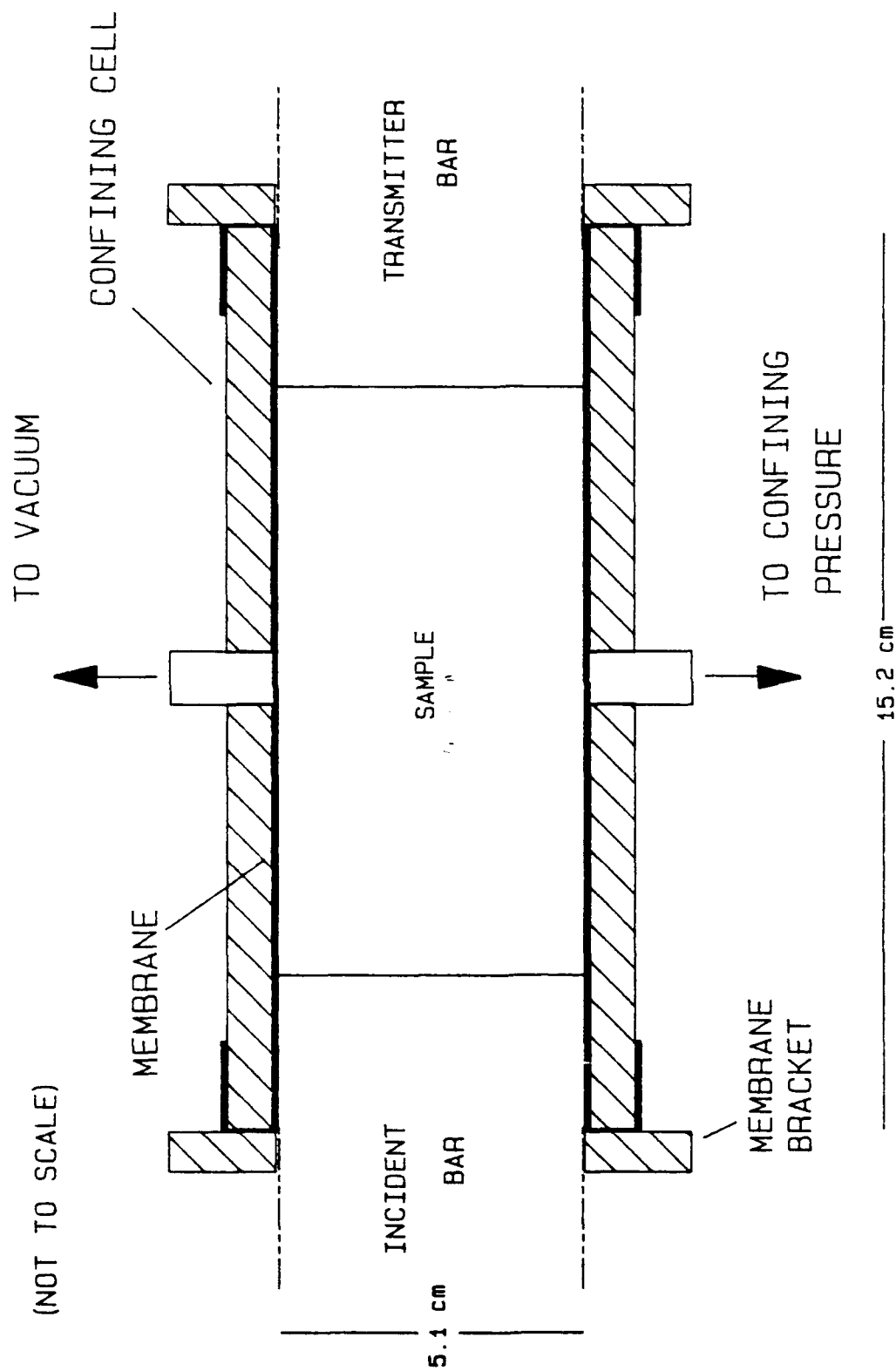


Figure 3.4 Schematic of Sample Container

membrane. Water was chosen as the confining fluid because its stiffness is sufficient to resist lateral expansion of the sand specimen.

### 3. Data Recording System

A schematic of the data acquisition system used in conjunction with the SHPB is shown in Figure 3.5. In order to measure the velocity of the striker bar before impact into the incident bar, an infrared emitter and sensor circuit was placed at the end of the barrel. The distance between the ends of the circuit was fixed, and a counter-timer unit was connected to the circuit allowing for the striker bar velocity to be calculated.

Two diametrically opposed strain gages were placed on both of the pressure bars to measure the properties of the propagating wave. Both sets of gages were located an equal distance from the specimen container. When the gages were triggered, the information received in each gage was sent through an amplifier to a two channel digital oscilloscope. The results obtained from the oscilloscope were digitized and stored on a floppy disk. The results could then be analysed on a personal computer. Figure 3.6 is a photograph of the oscilloscope and amplifiers used.

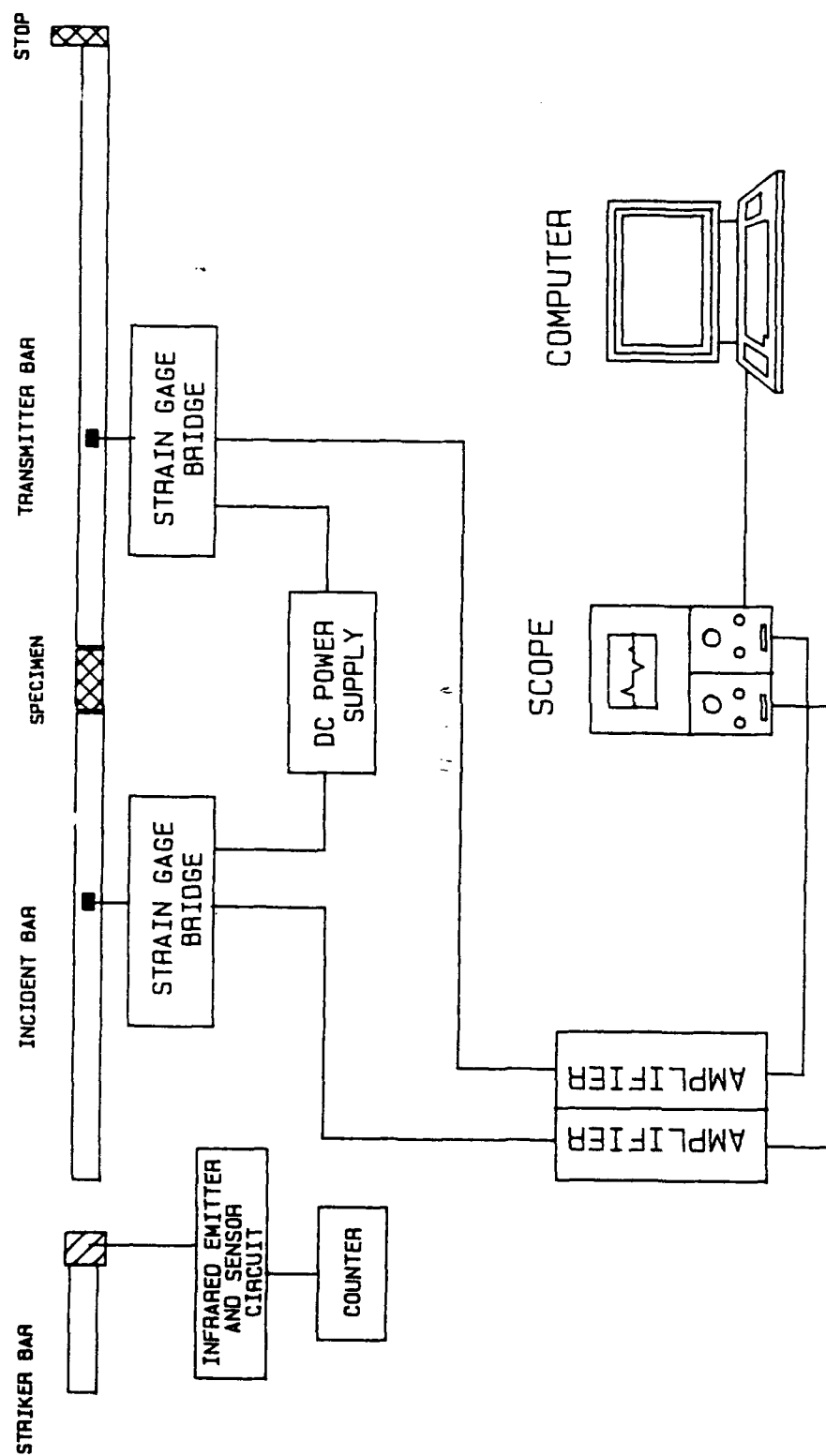


Figure 3.5 Schematic of SHPB Data Recording System

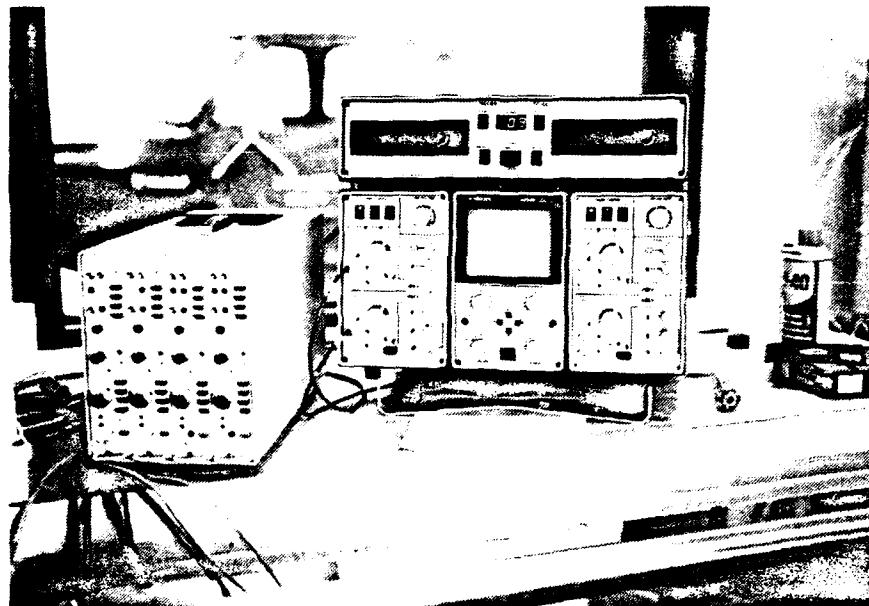


Figure 3.6 Oscilloscope and Amplifiers Used in Conjunction with SHPB Data Recording System

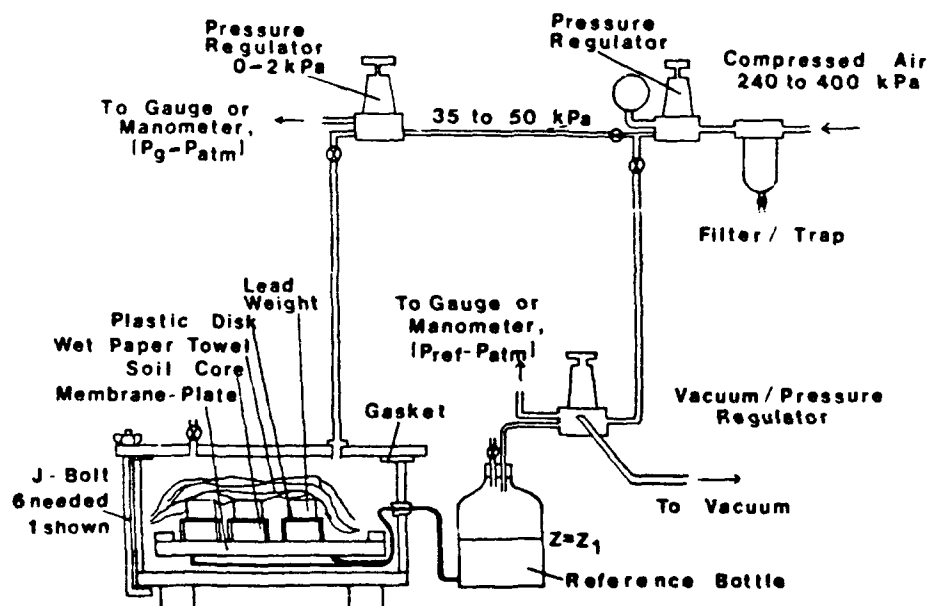


Figure 3.7 Standard Pressure Plate Apparatus



#### 4. Soil Saturation - Desaturation Equipment

For the samples compacted dry in this investigation, they were brought to the required saturation level by saturating the samples, then desaturating them by use of a pressure plate apparatus. All samples were compacted within the sample container described previously to a constant dry density of  $1760 \text{ kg/m}^3$ .

Once the samples were compacted they were placed in a saturation chamber. Vacuum was applied to the chamber to remove all of the air from the specimens, then water was allowed to slowly enter the system until the samples were saturated. Specimens were then transferred to a pressure plate apparatus for desaturation to a particular saturation level.

The pressure plate apparatus consists of a pressure chamber and saturated porous ceramic plate. A complete description of the pressure plate apparatus is given by Klute (1986). Figure 3.7 is a schematic of a standard pressure plate apparatus. The procedures used in this investigation generally followed the procedures outlined in ASTM D2325.

#### 5. Quasi-Static Confined Compression Apparatus

Quasi-static confined compression tests were performed to determine the relationship between saturation and constrained modulus under small strain rates. Samples were tested in the same specimen containers as used in the SHPB tests.

Figure 3.8a shows the specimen and loading apparatus utilized. Figure 3.8b is a photograph of the strip-chart recorder used to record the load-time curves of the specimens under one-dimensional compression and strain at a strain rate of  $10^{-1}$  per second.

## B. PROCEDURES

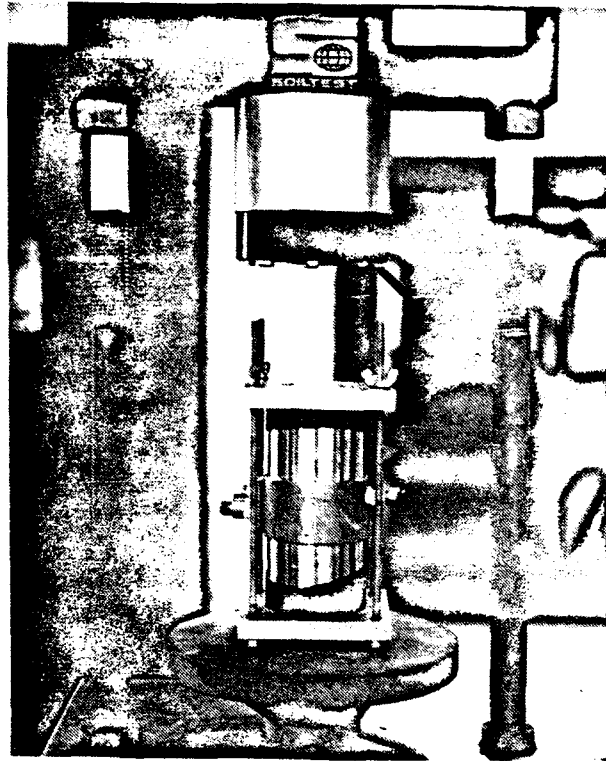
### 1. Sample Preparation

Both the Ottawa and Eglin sands were compacted in the same manner to a void ratio of 0.51. In order to obtain consistency, three samples were prepared simultaneously in three separate sample containers. Two of the samples were used in SHPB testing, while one sample was prepared for quasi-static compression testing.

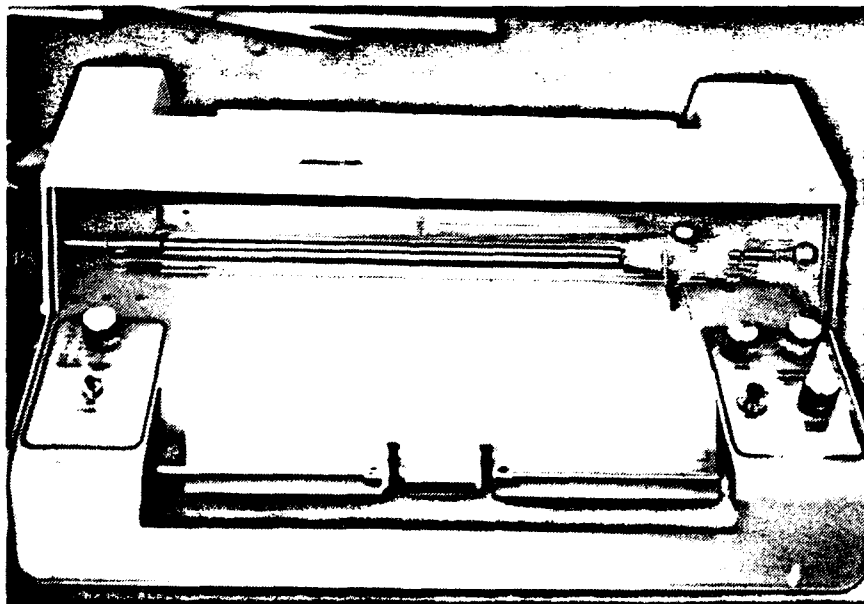
Each sample was compacted dry in four 2.54 cm lifts. One fourth of the sand by weight was poured into the container, then a 5.1 cm diameter steel rod was placed on top of the soil. The soil lift was then compacted dynamically by striking the top of the steel rod with a rubber mallet. Once the sand sample was compacted to a height of 2.54 cm, the next portion of the sand was added. The process was continued until the sample was compacted to a height of 10.16 cm.

### 2. Sample Saturation and Desaturation

Once the three duplicate samples were compacted, they were fully saturated by use of a saturation chamber, then desaturated to a particular level by use of the pressure plate apparatus. Due to the



a.



b.

Figure 3.8 Quasi-Static Confined Compression Apparatus, a. Load Cell and Sample Container, b. Strip-Chart Recorder

large sample height, equilibration would usually take eight hours or more. For higher pressures the samples were allowed to equilibrate for twelve or more hours. Once the specimens equilibrated, the pressure was reduced and the samples were removed and prepared for testing.

### 3. Split-Hopkinson Pressure Bar Tests

For triaxially confined tests, the confining stress piston was placed at the end of the transmitter bar prior to testing. If tests were to be run with zero confining stress, the piston was removed and the transmitter bar was placed directly against the stop.

The samples were removed from the pressure plate as needed for testing. Vacuum was then applied to the sample container in order to make it easier to place the sample between the pressure bars. Vacuum was also applied to remove any air from between the membrane and steel cylinder in preparation for applying the confining pressure. The sample container was then put in place between the pressure bars and a line for the confining stress was attached to the other valve on the sample container. The pressure bars were then pushed against the sample, and calipers were used to measure the position of the bars in relation to the sample. The vacuum was then turned off and water was pushed into the specimen container interface under slightly positive pressure. The valve to the vacuum was opened periodically to allow any trapped air to flow out of the interface. Figure 3.9 shows a specimen container in place between the pressure bars.

The specimen was now in position for testing. A confining stress of zero or 310.5 kPa was applied to the sample, and the amplifiers and digital oscilloscope were reset. A sampling rate of 0.5 microseconds was used for all SHPB tests. Once the test was performed, the data was immediately transferred to a floppy disk, and the sample was removed and its moisture content was determined according to ASTM D2216.

#### 4. Quasi-Static Compression Tests

The specimens for quasi-static testing were prepared in the same manner as those for SHPB testing. No confining stress was applied to any of the samples that were tested quasi-statically. Prior to placement on the load machine, a 5.08 cm steel bar was placed on both ends of the sample to allow for the application of the load. The sample container was then oriented vertically in the load machine. The test was performed and the load-time history was recorded using the strip-chart recorder. Once the test was complete, the moisture content was determined using the procedures of ASTM D2216.

#### 5. Capillary Pressure-Desaturation Curves

Capillary pressure-desaturation curves were generated for both sand types following the procedures described in ASTM D2325. Small sample containers were used to contain the samples on the pressure plate, and a piece of cheesecloth was placed over the bottom of each sample to hold the sand in place and allow sufficient contact between

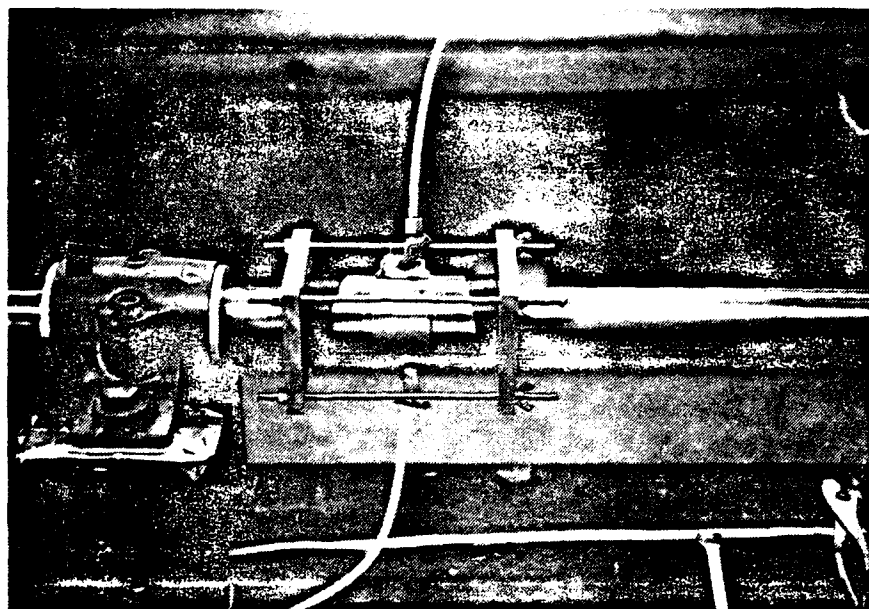


Figure 3.9 Specimen Container in Place Between Pressure Bars

the sand and the ceramic plate during desaturation. The sands were compacted to a void ratio of 0.51, the same as in all other testing.

For each saturation level, three samples of each sand type were desaturated. Once equilibrium was attained, the samples were removed, weighed, and then replaced for the next pressure increment. After the samples equilibrated under the largest pressure applied, the samples were removed, weighed, and then oven dried for moisture content determination. Pressures were applied from zero to approximately 82.7 kPa. For each pressure an average saturation level was obtained for each soil type and used for the capillary pressure-desaturation curves.

#### IV. EXPERIMENTAL RESULTS

##### A. PHYSICAL PROPERTIES OF SOILS

Two different sands were used in this research. A .22 kN bag of 20-30 Ottawa sand (ASTM C190) was obtained from the U. S. Silica Company, Ottawa, Illinois. A 300 N bag of the second sand, designated Eglin sand, was collected from Eglin Air Force Base, Florida. Both sands were thoroughly mixed with a sample splitter and the organics removed prior to use. The sands were then stored in covered containers, and samples were removed in a random fashion as needed.

A summary of the physical properties pertinent to this investigation are shown in Tables 4.1 and 4.2. Basic physical properties of each sand were evaluated according to standard laboratory procedures presented by the American Society of Testing and Materials. The test results given in this section are for the 20-30 Ottawa and Eglin sands which were compacted dry to  $1760 \text{ kg/m}^3$ , saturated, then desaturated to the required saturation by use of a pressure plate apparatus.

Grain size distributions for the 20-30 Ottawa and Eglin sands are shown in Figure 4.1. Based on the grain size distributions, the 20-30 Ottawa sand is classified as SP, while the Eglin sand is



Table 4.1 Physical Properties of 20-30 Ottawa Sand

Unified Soil Classification	SP
Specific Gravity	2.65
Particle Size Data:	
$d_{10}$	0.61 mm
$d_{30}$	0.67 mm
$d_{50}$	0.70 mm
$d_{60}$	0.71 mm
% passing #200 sieve	0%
$\rho_d$ maximum	1,566 kg/m <sup>3</sup>
$\rho_d$ minimum	1,532 kg/m <sup>3</sup>
(Kolbuszewki, 1948)	
Description of Soil	Poorly graded sand. Individual particles are subrounded to rounded in shape.

Table 4.2 Physical Properties of Eglin Sand

Unified Soil Classification	SP-SM
Specific Gravity	2.65
Particle Size Data:	
$d_{10}$	0.09 mm
$d_{30}$	0.19 mm
$d_{50}$	0.26 mm
$d_{60}$	0.31 mm
% passing #200 sieve	7.3%
$\rho_d$ maximum	1,626 kg/m <sup>3</sup>
$\rho_d$ minimum	1,558 kg/m <sup>3</sup>
(Kolbuszewki, 1948)	
Description of Soil	Poorly graded sand with silt. Individual particles are subangular to subrounded in shape.

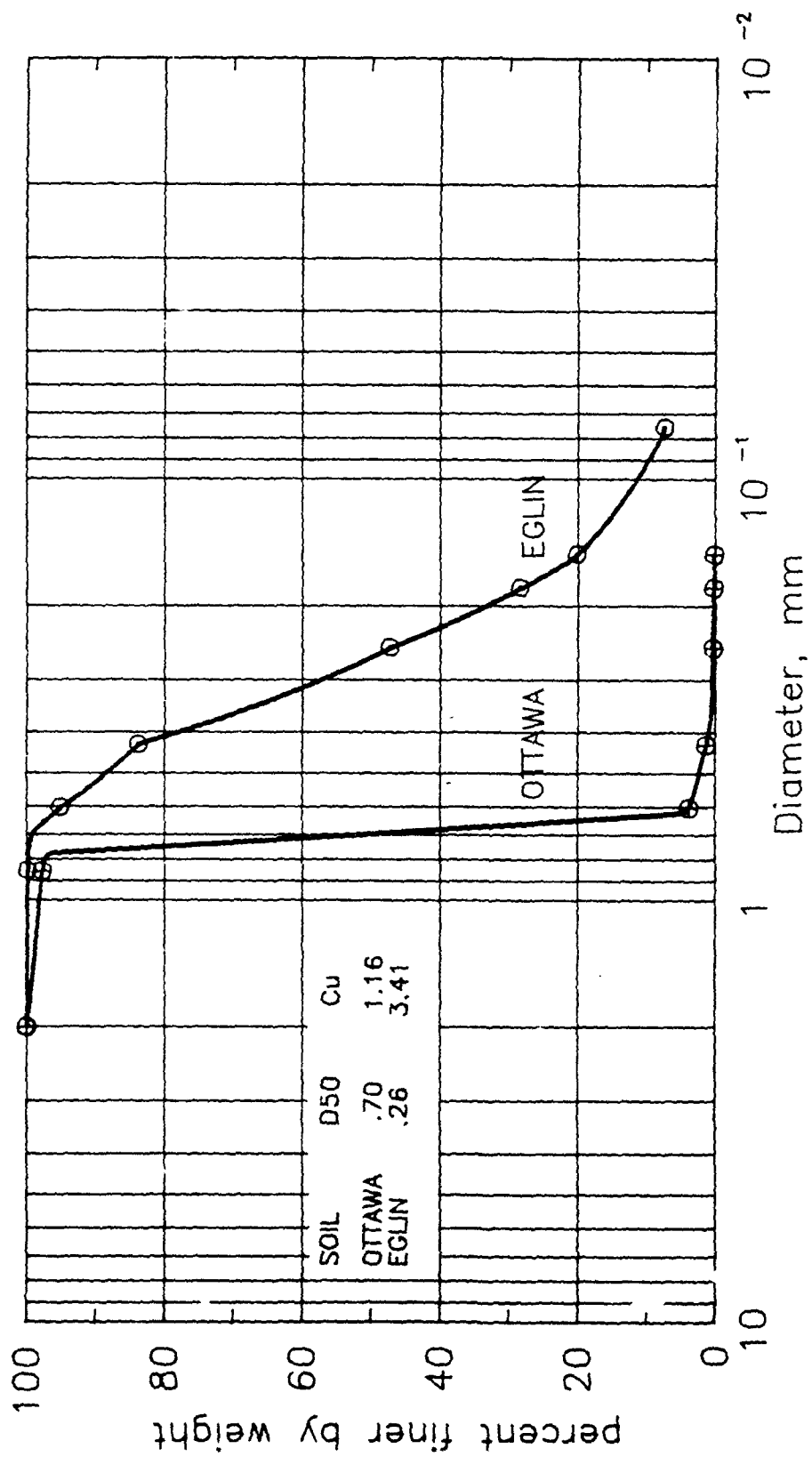


Figure 4.1 Grain Size Distributions for 20-30 Ottawa and Eglin Sands

classified as SP-SM according to the Unified Soil Classification System.

#### B. SPLIT-HOPKINSON PRESSURE BAR TEST RESULTS

High strain wave propagation tests were performed on both sands to determine the relationship between wave velocity and stress transmission with variations in saturation level and confining stress. A typical oscilloscope trace is shown in Figure 4.2. The signal obtained from the strain gage mounted on the incident bar is represented as a solid line, while the dashed line shows the signal obtained from the transmitter bar strain gage. For this figure, compressive waves are considered negative, while tensile waves are positive.

Figure 4.2 shows that the magnitude of the incident pulse ( $-2.9 \times 10^5$  kPa) is much greater than that of the transmitted pulse ( $-1.8 \times 10^4$  kPa). This is due to the difference in acoustic impedance of the steel pressure bars and the sand specimen. The difference is so large that the transmitted pulse was multiplied by ten in the figure for the purpose of presentation.

Based on wave propagation theory, a compressive wave traveling in a material of high acoustical impedance (steel bars) will transmit a portion of the compressive wave into a material of lower impedance (sand), while a portion of the pulse will be reflected back along the incident material in the form of a tensile wave. Figure 4.2 shows this relationship. It should be noted from equations 2.4 through 2.7

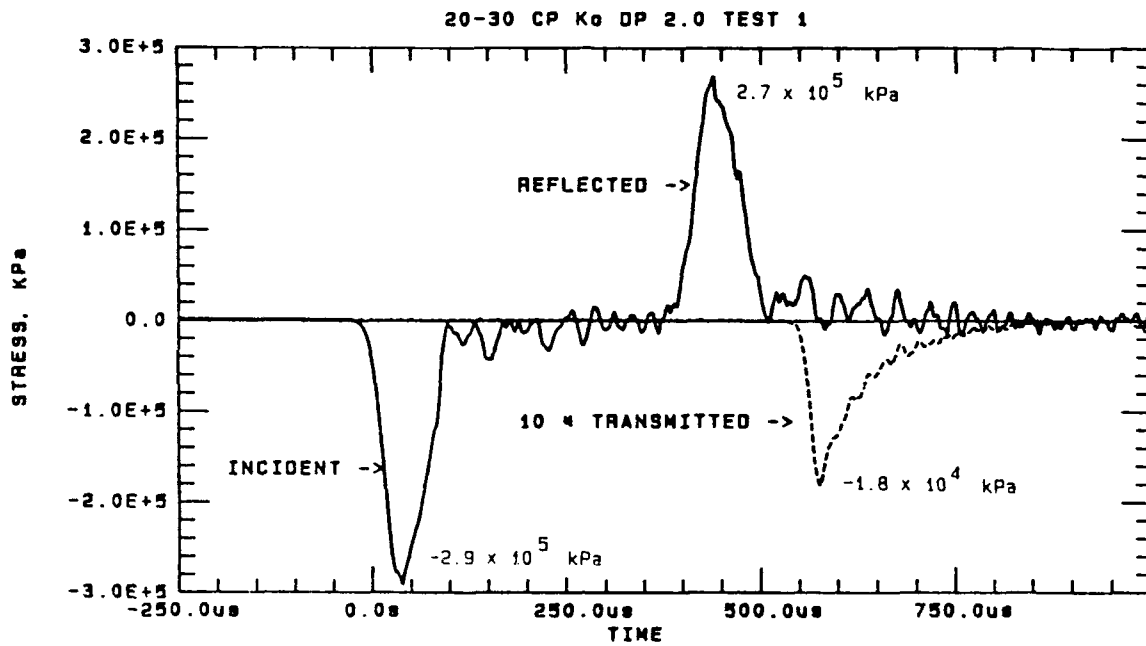


Figure 4.2 Typical Oscilloscope Trace of Compression Wave as Recorded by Pressure Bar Strain Gages

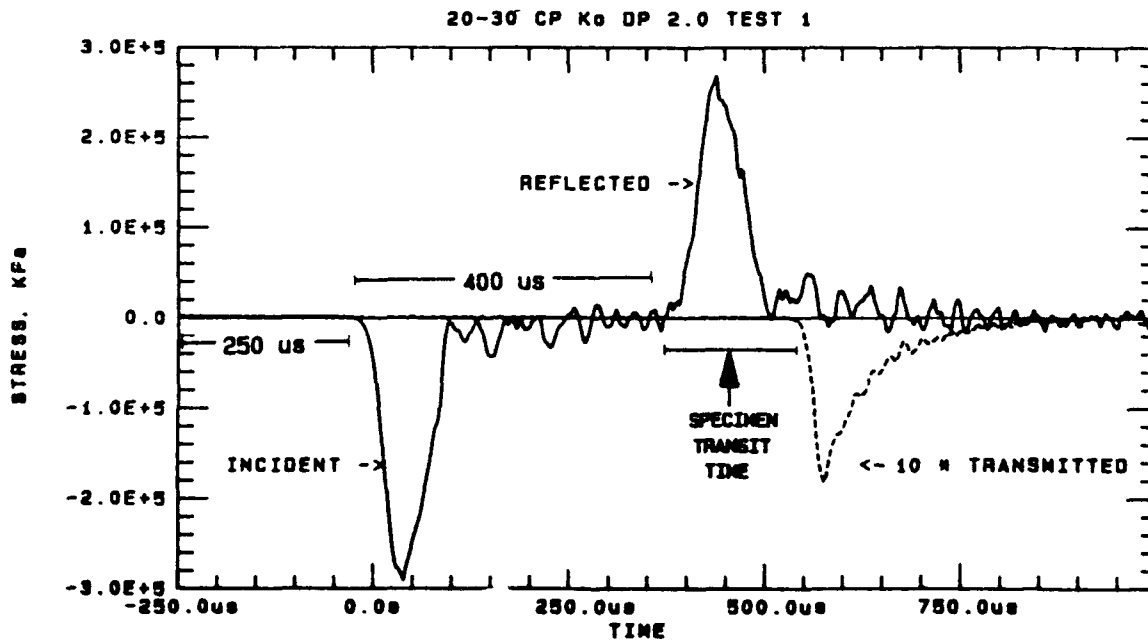


Figure 4.3 Typical Oscilloscope Trace with Wave Transit Times

that the maximum stress within the soil sample is approximately half the value in the transmitter bar.

The average wave velocity through the sample was determined by measuring the time required for the wave to travel between the incident and transmitter bar strain gages. For this particular SHPB a compressive wave travels at a rate of 1.97 microseconds per centimeter. Since the incident and transmitter bar strain gages are each 101.6 cm away from the end of each bar, a compressive wave would take 400 microseconds to travel from the incident strain gage to the transmitter strain gage if the pressure bars were in contact. To find the transit time across the specimen, 400 microseconds was subtracted from the time measured for the wave to travel between the pressure bar strain gages. The length of the specimen was known, allowing for the determination of the wave velocity. Figure 4.3 shows the specimen transit time determination on an oscilloscope plot. It should be noted that the velocity determined is an average velocity. No corrections were made to account for the attenuation of the wave due to damping as it passed through the sand specimen.

The maximum incident and transmitted stress was determined to be the peak stresses recorded on the oscilloscope by the incident and transmitter bar strain gages. Though the gages were mounted 101.6 cm away from the sample, no significant attenuation of the wave occurs in the steel bars between the strain gages and sample.

The data obtained for each test is shown in Tables 4.3 through 4.6. Values for peak incident, reflected and transmitted stresses, and wave velocities are given. The ratio of the incident to the transmitted

Table 4.3 SHPB Test Results for 20-30 Ottawa Sand Under Zero Confining Stress

SAMPLE NUMBER	SATURATION (%)	SAMPLE LENGTH (cm)	VOID RATIO	INCIDENT PEAK STRESS (kPa)	REFLECTED PEAK STRESS (kPa)	TRANSMITTED PEAK STRESS (kPa)	STRESS TRANSMISSION RATIO	WAVE SPEED (m/s)
Ko-0-1	0.0	10.16	0.51	-292596	267054	-18163	0.0621	574.0
Ko-0-2	0.0	10.24	0.53	-292596	263081	-3689	0.0126	564.2
Ko-0-3	0.0	10.24	0.53	-296285	266770	-9238	0.0312	550.5
Ko-0-4	0.0	10.16	0.51	-293731	264784	-19383	0.0660	612.0
Ko-0-5	0.0	10.16	0.51	-288623	256554	-17752	0.0615	601.2
Ko-0-6	0.0	10.16	0.51	-285501	265919	-22732	0.0796	637.0
Ko-1.5-1	5.3	10.16	0.51	-303380	265068	-11423	0.0377	547.7
Ko-1-1	5.4	10.16	0.51	-302813	261946	-15112	0.0499	572.4
Ko-1-2	7.3	10.16	0.51	-286069	263932	-13140	0.0459	561.3
Ko-1.5-2	8.4	10.16	0.51	-304799	268757	-13055	0.0428	572.4
Ko-2.0-1	12.8	10.16	0.51	-291745	269041	-18191	0.0624	625.2
Ko-2.0-2	16.1	10.16	0.51	-304232	263081	-5974	0.0196	546.2
Ko-4.5-1	16.4	10.08	0.50	-294583	253148	-12147	0.0412	580.6
Ko-4.5-2	25.4	10.16	0.51	-290326	251729	-8117	0.0280	564.5
Ko-4-2	29.8	10.16	0.51	-278974	252580	-16290	0.0584	603.0
Ko-3.7-2	33.0	10.16	0.51	-291461	255986	-8471	0.0291	566.0
Ko-2.5-1	33.3	10.16	0.51	-291745	267054	-7223	0.0248	570.8
Ko-3.7-1	34.3	10.08	0.50	-291745	258256	-15538	0.0533	626.1
Ko-2.5-2	37.3	10.16	0.51	-297704	263081	-14318	0.0481	585.6
Ko-2.9-3	39.9	10.16	0.51	-315016	274433	-6854	0.0218	541.8
Ko-2.9-2	42.9	10.16	0.51	-290893	264500	-13197	0.0454	580.6
Ko-2.9-4	44.5	10.16	0.51	-294583	257973	-10827	0.0368	552.2
Ko-2.9-1	61.9	10.16	0.51	-309340	284366	-3689	0.0119	523.7
Ko-3.0-2	70.7	10.31	0.54	-294866	262797	-8145	0.0276	522.5
Ko-3.0-1	81.5	10.31	0.54	-293447	264216	-9521	0.0324	570.1
MEAN		10.172	0.513	-295082				
ST. DEV.		0.051	0.010	7731				

Table 4.4 SHPB Test Results for 20-30 Ottawa Sand Under 310 kPa Confining Stress

SAMPLE NUMBER	SATURATION (%)	SAMPLE LENGTH (cm)	VOID RATIO	INCIDENT PEAK STRESS (kPa)	REFLECTED PEAK STRESS (kPa)	TRANSMITTED PEAK STRESS (kPa)	STRESS TRANSMISSION RATIO	WAVE SPEED (m/s)
45-0-1	0.0	10.24	0.53	-311610	273298	-28323	0.0909	682.6
45-0-2	0.0	10.16	0.52	-305083	255986	-27387	0.0898	666.2
45-4.4-1	4.8	10.16	0.51	-315867	274433	-25826	0.0818	659.7
45-4.4-2	5.2	10.16	0.51	-293164	268473	-27216	0.0928	691.2
45-1.5-4	7.4	10.24	0.53	-302245	268757	-31360	0.1038	689.5
45-1.5-5	7.5	10.16	0.51	-318138	265919	-30111	0.0946	686.5
45-3-3	13.6	10.16	0.51	-285501	260527	-23995	0.0840	686.5
45-3-4	20.2	10.16	0.51	-280393	267906	-23470	0.0837	651.3
45-2.9-3	31.1	10.16	0.51	-307070	273865	-29174	0.0950	710.5
45-3-2	41.0	10.16	0.51	-300542	269041	-28011	0.0932	659.7
45-2.9-1	44.7	10.31	0.54	-304799	285785	-16687	0.0547	631.1
45-1.5-3	51.5	10.31	0.54	-301110	280109	-19696	0.0654	614.2
45-1.5-2	54.8	10.31	0.54	-300826	286069	-23612	0.0785	637.0
45-3-1	61.3	10.16	0.51	-294015	260243	-30310	0.1031	679.6
45-2.9-2	64.5	10.39	0.55	-299975	275852	-27273	0.0909	700.2
45-2.9-4	73.6	10.16	0.51	-316151	260243	-27330	0.0864	651.3
45-1.5-1	78.3	10.31	0.54	-307353	282095	-21597	0.0703	653.4
45-2.9-5	81.3	10.16	0.51	-309056	270743	-21285	0.0689	668.4
45-0-1 (sat)	100.0	10.16	0.51	-300258	255702	-46330	0.1543	1421.0
MEAN		10.212	0.521	-302798				
ST. DEV.		0.074	0.014	9589				

Table 4.5 SHPB Test Results for Eglin Sand Under Zero Confining Stress

SAMPLE NUMBER	SATURATION (%)	SAMPLE LENGTH (cm)	VOID RATIO	INCIDENT PEAK STRESS (kPa)	REFLECTED PEAK STRESS (kPa)	TRANSMITTED PEAK STRESS (kPa)	STRESS TRANSMISSION RATIO	WAVE SPEED (m/s)
Ko-0-1	0.0	10.16	0.51	-283231	270176	-8627	0.0305	506.7
Ko-0-2	0.0	10.16	0.51	-286920	281244	-5747	0.0200	452.6
Ko-0-3	0.0	10.16	0.51	-282947	285217	-7762	0.0274	511.9
Ko-8.8-1	23.4	10.16	0.51	-290609	269041	-4285	0.0147	444.6
Ko-8.8-2	23.5	10.16	0.51	-277838	272446	-3888	0.0140	427.8
Ko-5.9-1	24.8	10.16	0.51	-290326	277555	-5491	0.0189	453.6
Ko-5.9-2	25.1	10.16	0.51	-293447	271595	-3916	0.0133	404.0
Ko-4.4-1	25.6	10.16	0.51	-287204	276419	-4285	0.0149	429.6
Ko-4.4-2	28.7	10.16	0.51	-290326	275000	-3377	0.0116	416.4
Ko-3.7-2	29.6	10.16	0.51	-285217	276987	-2341	0.0082	392.3
Ko-3.7-1	32.6	10.16	0.51	-288623	263365	-6357	0.0220	454.6
Ko-2.2-2	45.2	10.16	0.51	-286069	270176	-3136	0.0110	415.5
Ko-2.9-2	45.6	10.16	0.51	-287771	264784	-3732	0.0130	397.6
Ko-2.2-1	47.0	10.16	0.51	-282947	267338	-5506	0.0195	457.7
Ko-2.9-1	54.4	10.16	0.51	-349923	302529	-2824	0.0081	404.0
Ko-1.5-2	79.7	10.16	0.51	-301394	275852	-4285	0.0142	456.5
Ko-1.5-1	81.8	10.16	0.51	-297137	269608	-4498	0.0151	483.8
MEAN		10.16	0.51	-291878				
ST. DEV.		0.000	0.000	15491				

Table 4.6 SHPB Test Results for Eglin Sand Under 310 Confining Stress

SAMPLE NUMBER	SATURATION (%)	SAMPLE LENGTH (cm)	VOID RATIO	INCIDENT PEAK STRESS (kPa)	REFLECTED PEAK STRESS (kPa)	TRANSMITTED PEAK STRESS (kPa)	STRESS TRANSMISSION RATIO	WAVE SPEED (m/s)
45-0-1	0.0	10.16	0.51	-284082	271027	-11196	0.0394	546.2
45-0-2	0.0	10.16	0.51	-286069	269608	-10997	0.0384	537.6
45-2.9-1	25.5	10.16	0.51	-282663	260243	-9748	0.0345	549.3
45-2.9-2	27.2	10.16	0.51	-282663	276419	-9692	0.0343	587.3
45-4.4-1	28.5	10.16	0.51	-285217	268189	-10884	0.0382	539.0
45-4.4-2	32.0	10.16	0.51	-284650	269041	-6343	0.0223	485.0
45-3.7-1	35.9	10.16	0.51	-300542	284933	-8230	0.0274	536.1
45-2.2-2	41.1	10.16	0.51	-296002	267054	-8571	0.0290	521.0
45-2.2-1	41.4	10.16	0.51	-283514	273014	-5988	0.0211	486.1
45-1.5-1	72.9	10.08	0.50	-289474	276987	-8443	0.0292	529.2
45-1.5-2	79.0	10.16	0.51	-286920	274717	-9053	0.0316	499.3
MEAN		10.15	0.5090	-287435				
ST. DEV.		0.021	0.0028	5529.4				

peak stress has also been calculated for each test and is included in the tables.

The relationship between saturation and wave velocity under the two confining pressures is given in Figures 4.4 through 4.7 for the 20-30 Ottawa and Eglin sands. Transmission ratio versus saturation is presented in Figures 4.8 through 4.11 for both sand types and confining stresses.

In order to show that the differences in trends obtained by Ross et al. on the same sands compacted moist to the same void ratio was not due to the use of different sample containers, several samples were compacted moist in the sample container used in this investigation, and tested on the SHPB. Figure 4.12 shows wave velocity and stress transmission results for the Eglin sand obtained by Ross et al. and in the current investigation.

In an attempt to determine the role of the moisture during the compaction process, several samples of Eglin sand were compacted moist in the sample container used by Ross et al. (1988). The specimen and container was then placed in an oven for a period of 24 hours to remove all moisture in the sample, then the sample was then tested dynamically on the SHPB. Figure 4.13 shows the results obtained.

### C. QUASI-STATIC STIFFNESS TESTS

Quasi-static stiffness tests were performed to determine the relationship between stiffness and saturation level under quasi-static loading rate conditions. The results obtained were used to predict the wave velocity using equation 2.3 based on the quasi-static



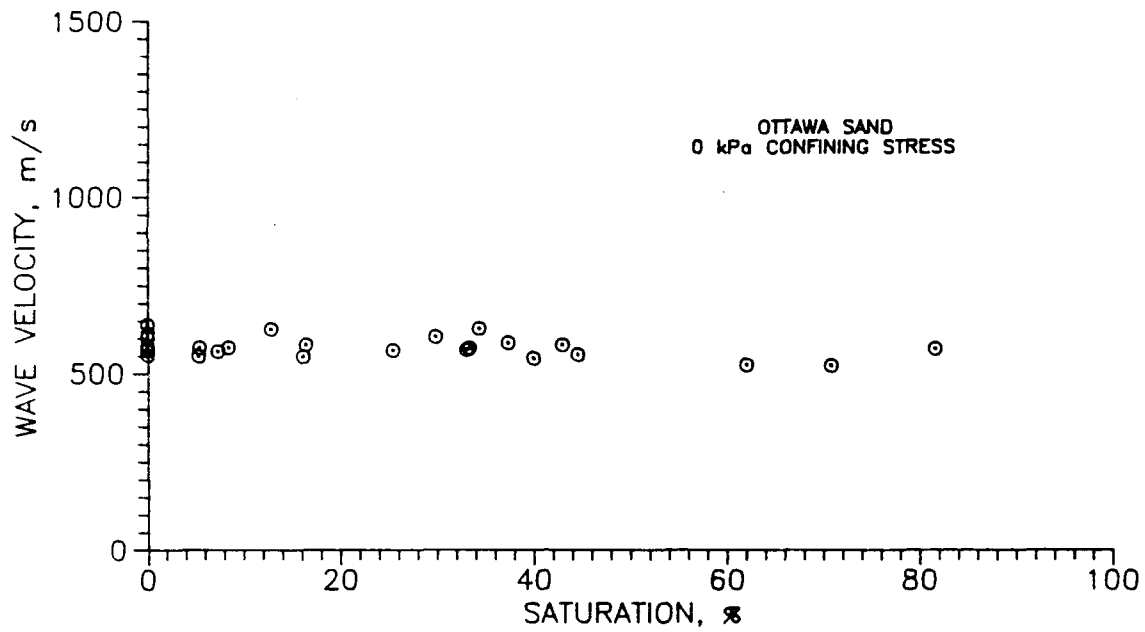


Figure 4.4 Wave Velocity Versus Saturation for 20-30 Ottawa Sand Under Zero Confining Stress

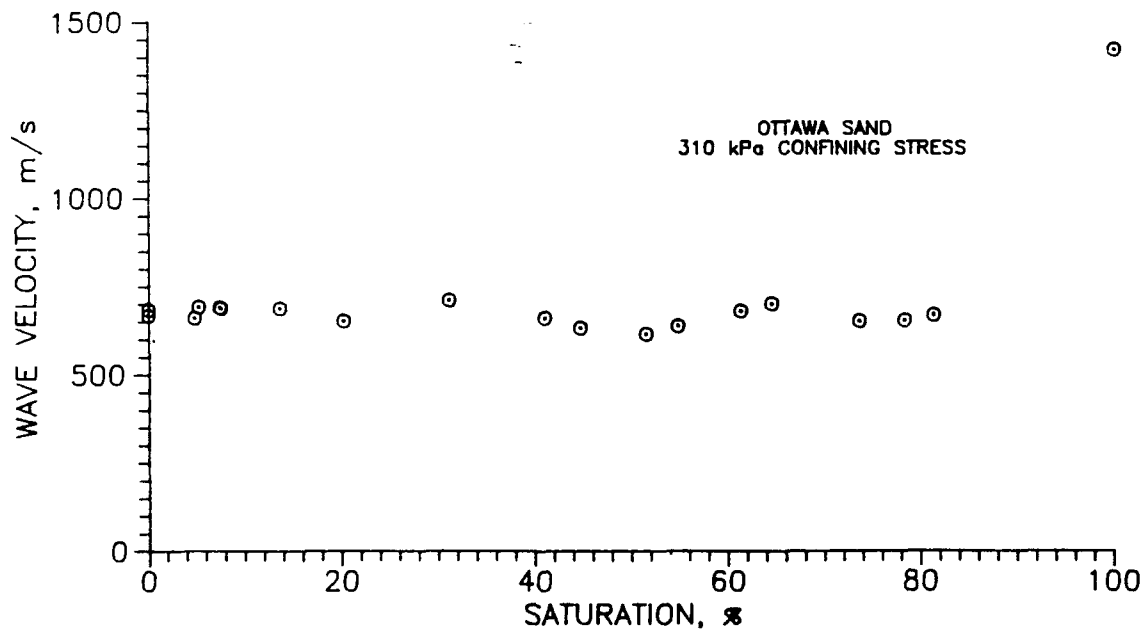


Figure 4.5 Wave Velocity Versus Saturation for 20-30 Ottawa Sand Under 310 kPa Confining Stress

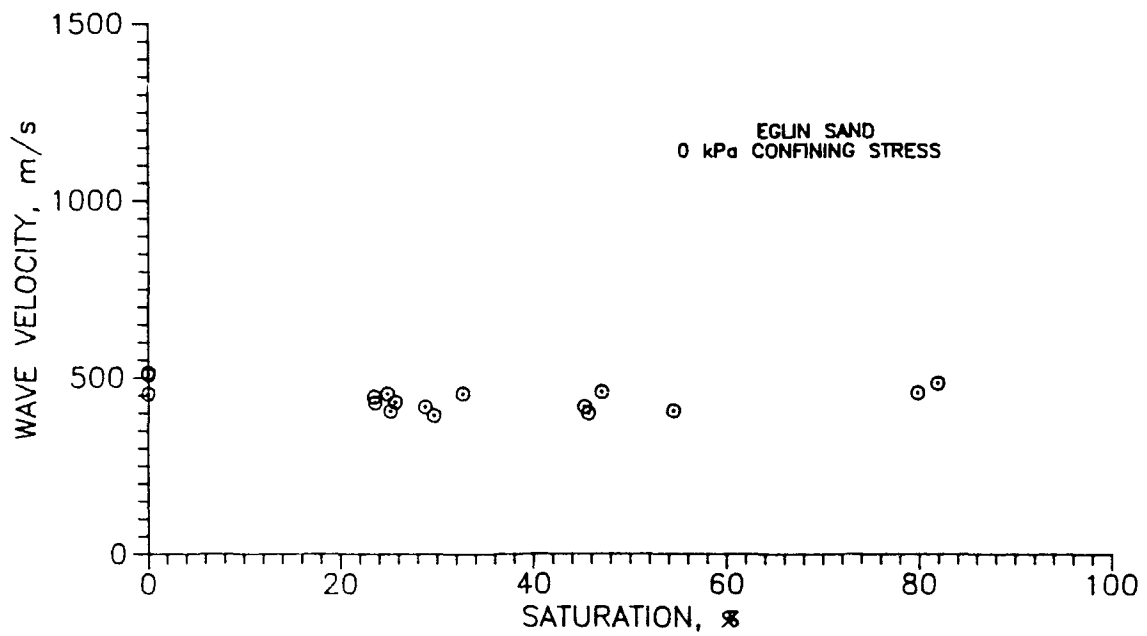


Figure 4.6 Wave Velocity Versus Saturation for Eglin Sand Under Zero Confining Stress

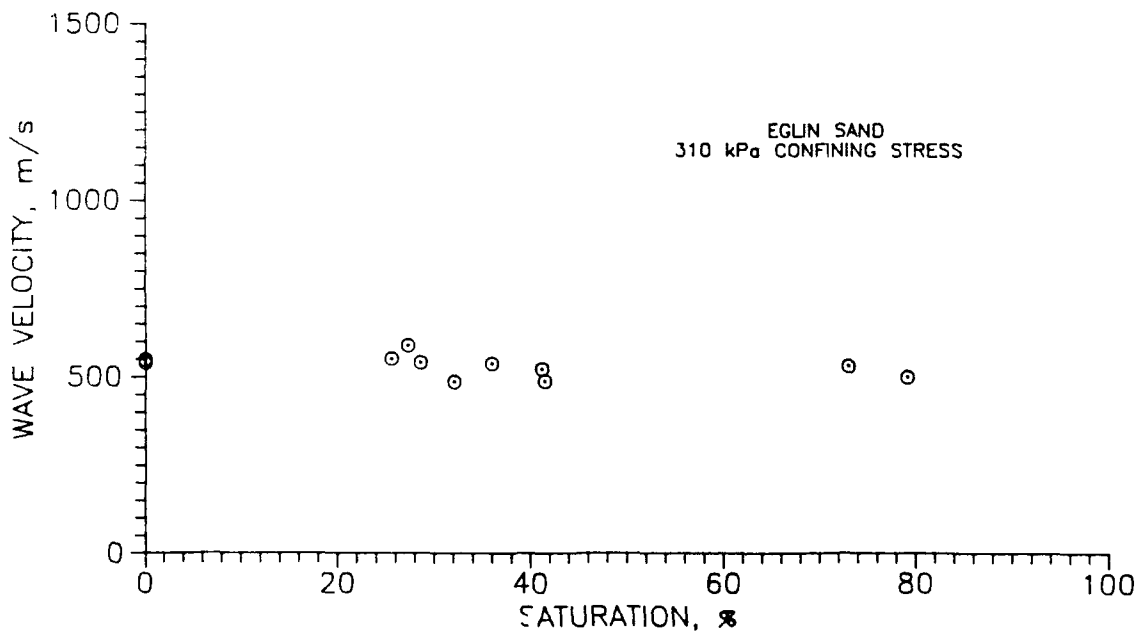


Figure 4.7 Wave Velocity Versus Saturation for Eglin Sand Under 310 kPa Confining Stress

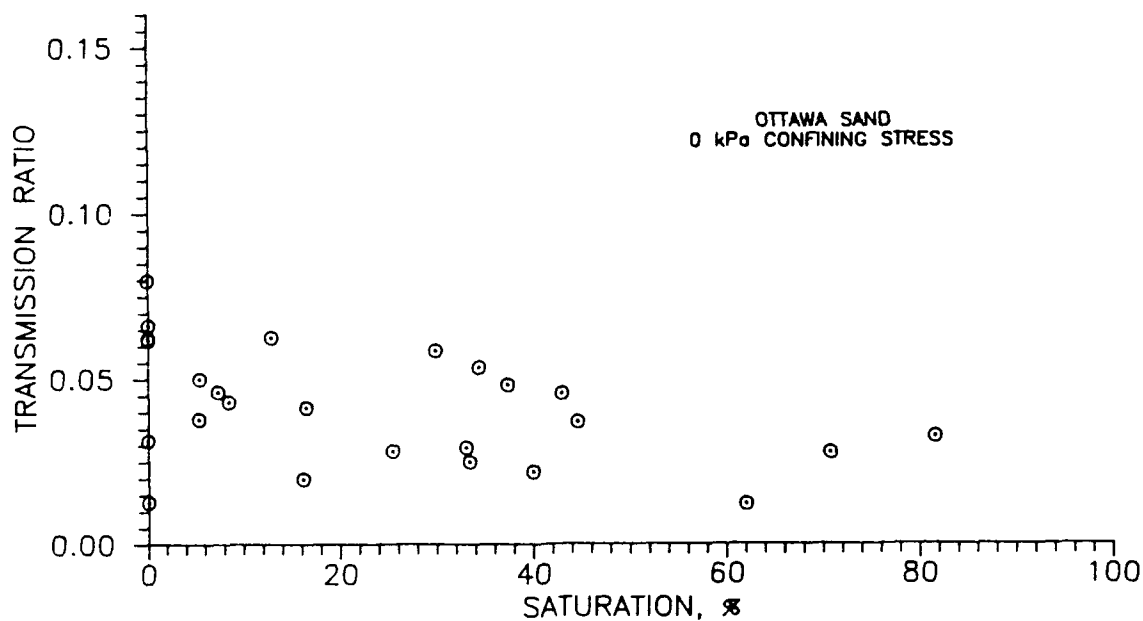


Figure 4.8 Transmission Ratio Versus Saturation for 20-30  
Ottawa Sand Under Zero Confining Stress

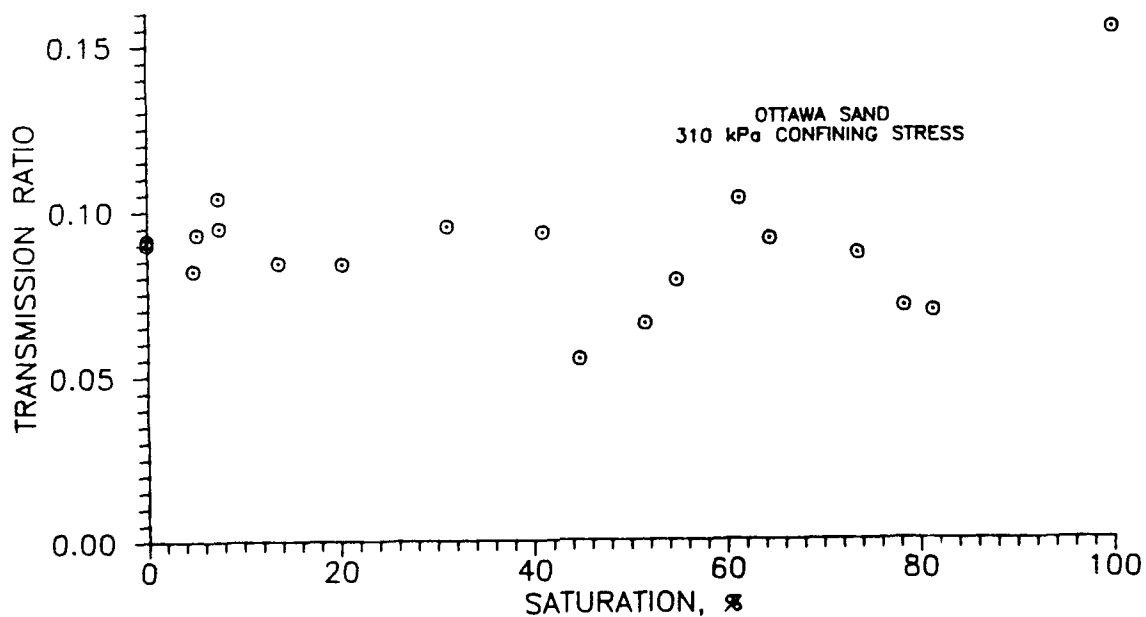


Figure 4.9 Transmission Ratio Versus Saturation for 20-30  
Ottawa Sand Under 310 kPa Confining Stress

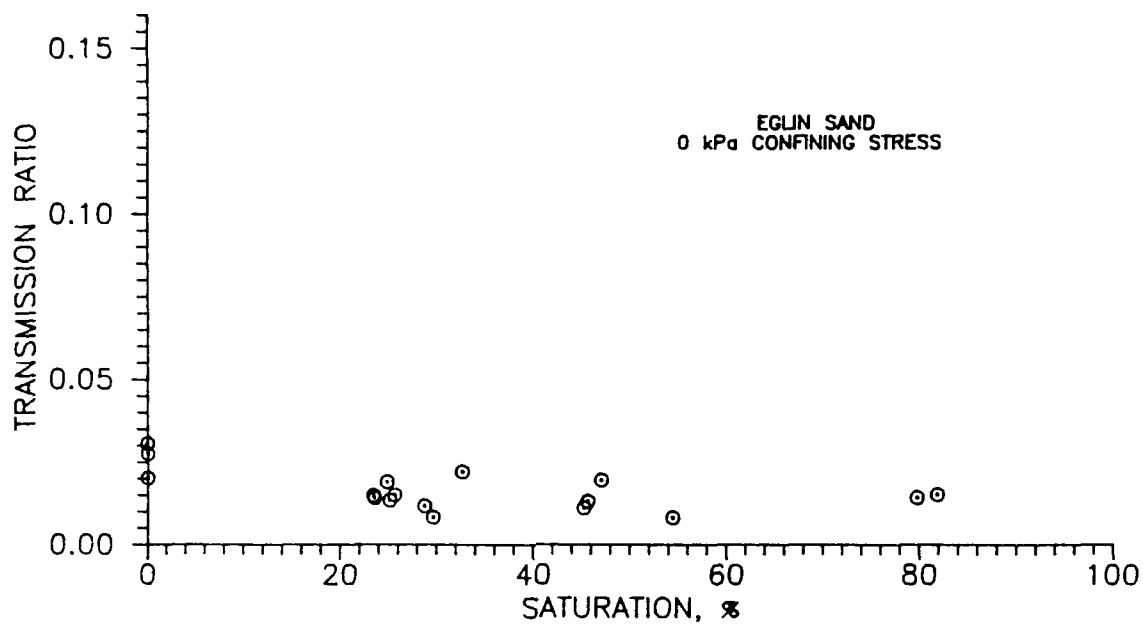


Figure 4.10 Transmission Ratio Versus Saturation for Eglin Sand Under Zero Confining Stress

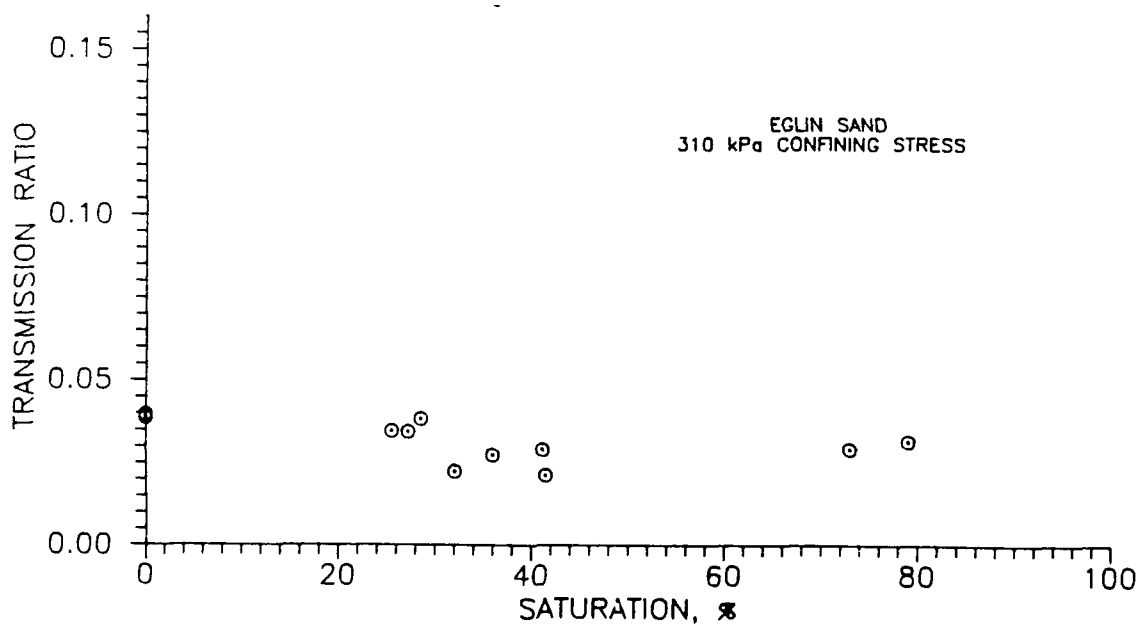
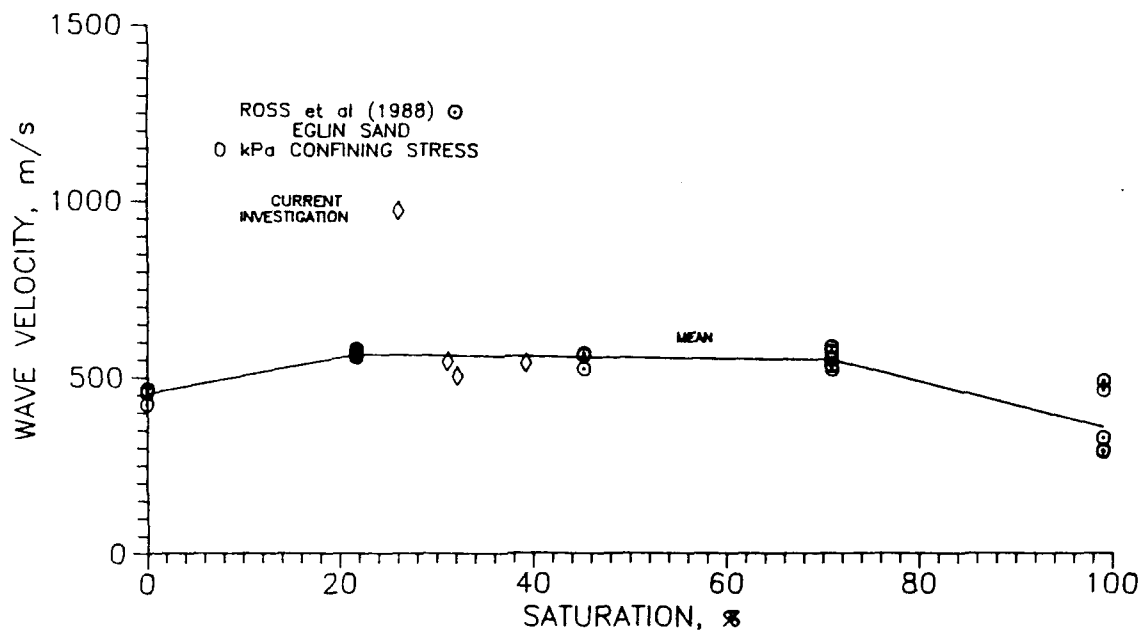
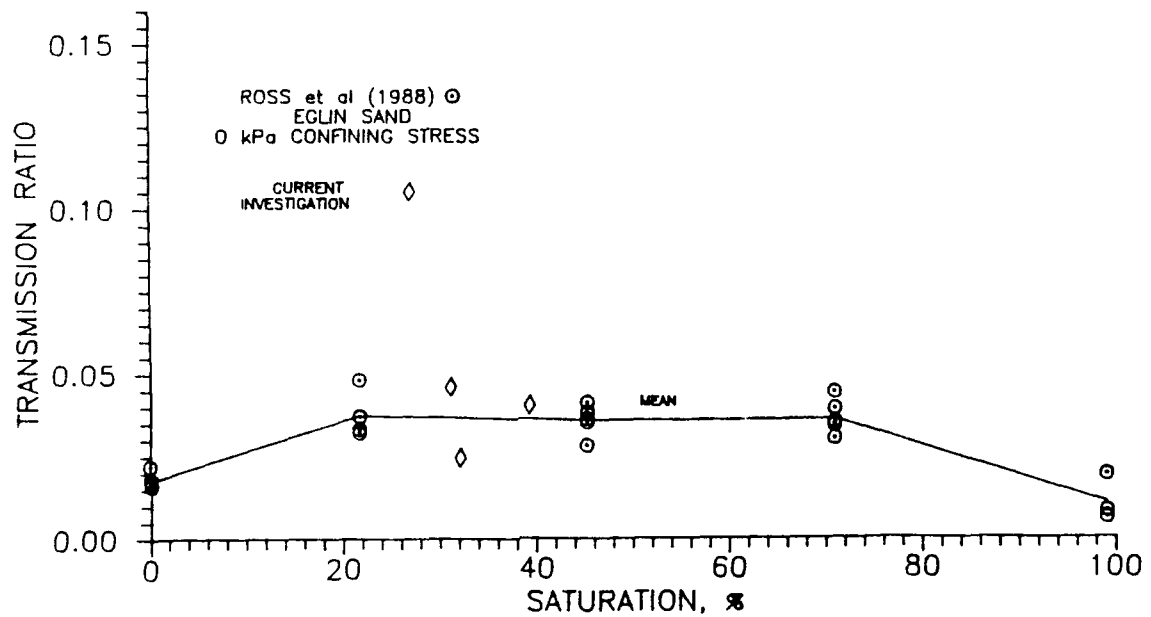


Figure 4.11 Transmission Ratio Versus Saturation for Eglin Sand Under 310 kPa Confining Stress



a.



b.

Figure 4.12 Results For Eglin Sand Obtained by Ross et al. (1988) and Results for Samples Compacted Moist Using Sample Container in Current Investigation a. Wave Velocity, b. Transmission Ratio

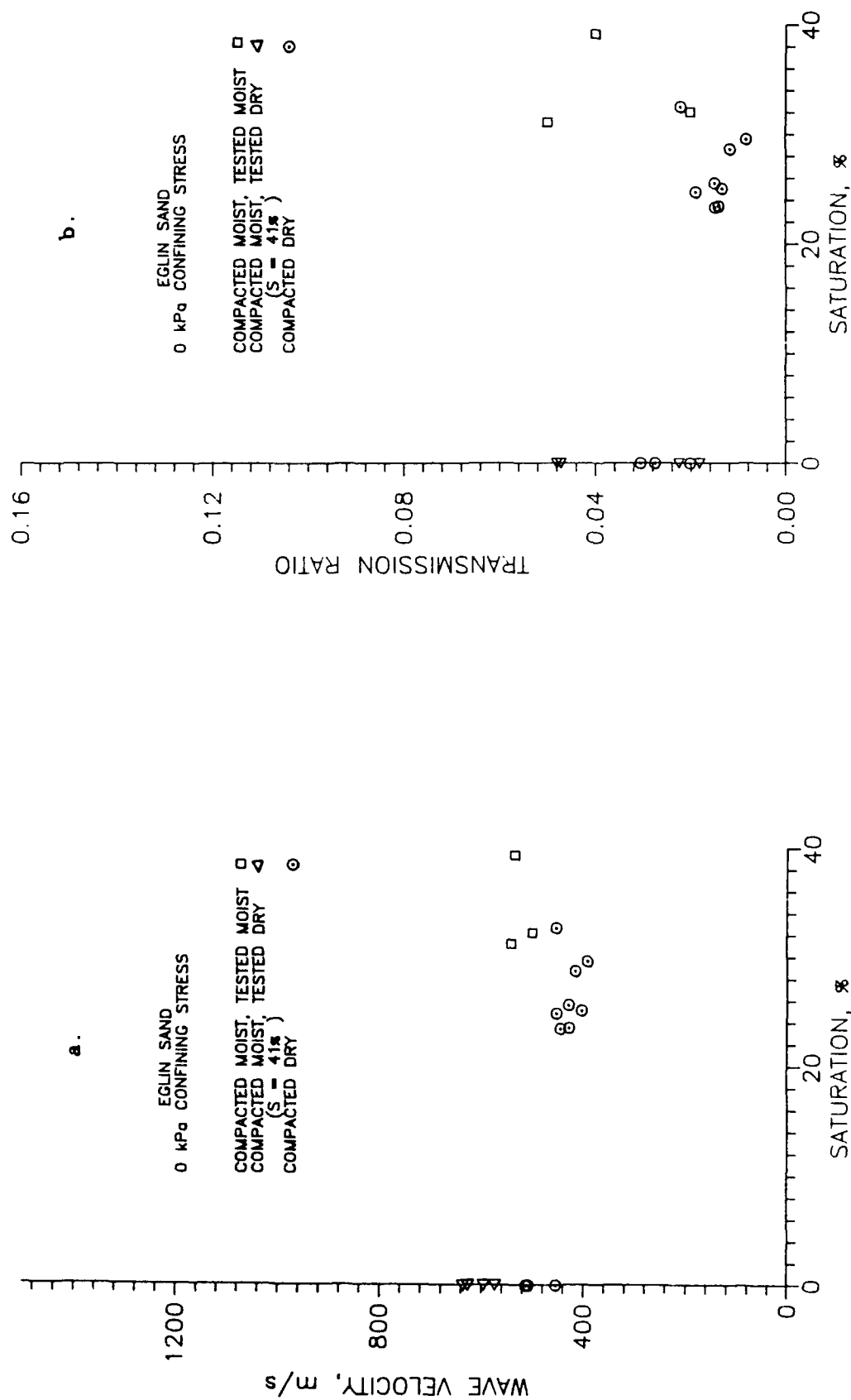


Figure 4.13 Comparison of Egline Sand Samples Compacted and Tested Both Moist and Dry a. Wave Velocity, b. Transmission Ratio

constrained modulus. These predictions were then compared with the wave velocities obtained from the SHPB tests.

A typical strip-chart recorder stress-time history is shown in Figure 4.14. The secant constrained modulus was determined for the tests by measuring the displacement between axial loads of 4.45 kN (2,200 kPa) and 31.14 kN (15,000 kPa) divided by the sample strain.

Tables 4.7 and 4.8 list the values of constrained modulus for initial loading and reloading conditions for various saturation levels. The relationships between constrained modulus and saturation are presented in Figure 4.15 for the Ottawa sand, and Figure 4.16 for the Eglin sand.

#### D. CAPILLARY PRESSURE-DESATURATION CURVES

Capillary pressure-desaturation curves were determined for each sand according to ASTM D2325. The results are presented in Figures 4.17 and 4.18 for the Ottawa and Eglin sands.

Both sands desaturate with a small increase in capillary pressure (less than 2 kPa), making it difficult to determine the displacement pressure. The moisture in the 20-30 Ottawa sand displaces at a very low capillary pressure due to the uniformity of the grain size distribution. The Eglin sand has a higher percentage of finer grained particles, making the displacement pressure somewhat higher (less than 7 kPa). The residual saturation level for the 20-30 Ottawa sand is approximately 2 percent, while the Eglin sand has a residual saturation level of approximately 16 percent.

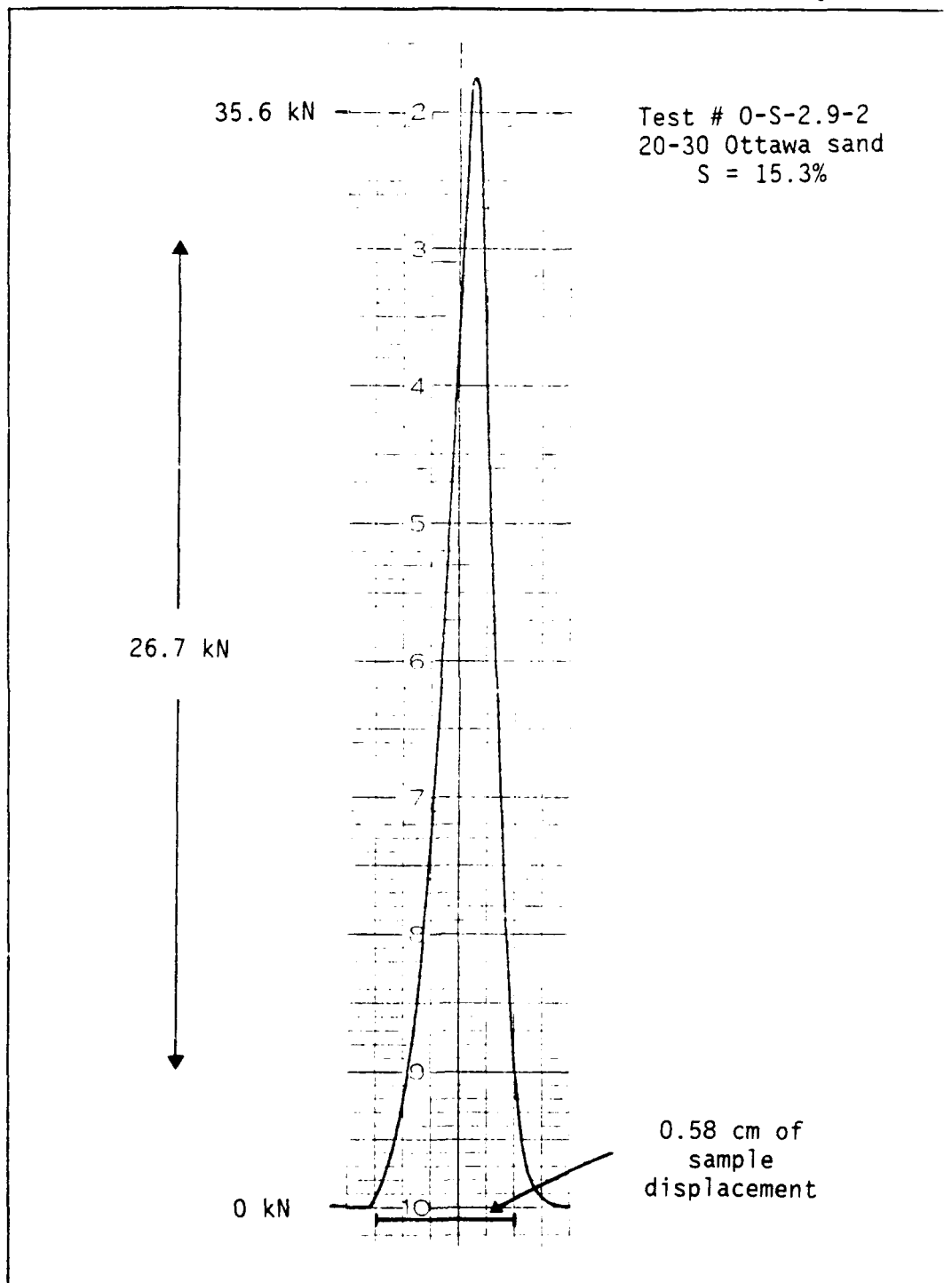


Figure 4.14 Typical Strip-Chart Recorder Load-Time History for Quasi-Static Tests



Table 4.7 Quasi-Static Constrained Modulus Values for 20-30  
Ottawa Sand at Various Saturation Levels

SAMPLE NUMBER	SATURATION (%)	VOID RATIO	D INITIAL (kPa)	D RELOAD (kPa)
0-1	0.0	0.51	611531	698891
0-2	0.0	0.51	627211	698891
4.5-1	7.9	0.51	582407	764414
2-1	11.4	0.51	611531	698891
3-1	14.0	0.51	555937	679475
2.9-2	15.3	0.51	611531	741247
3.7-1	19.1	0.51	596611	723706
2.0-1	39.8	0.51	509609	—

Table 4.8 Quasi-Static Constrained Modulus Values for Eglin  
Sand at Various Saturation Levels

SAMPLE NUMBER	SATURATION (%)	VOID RATIO	D INITIAL (kPa)	D RELOAD (kPa)
0-1	0.0	0.51	436805	661113
0-2	0.0	0.51	394532	643717
5.9-1	23.8	0.51	317680	543581
8.8-1	25.9	0.51	370627	596611
4.4-1	26.0	0.51	370627	568865
2.9-2	27.6	0.51	407688	627211
4.4-2	29.8	0.51	376329	611531
2.2-2	44.6	0.51	339737	543581
2.9-1	46.8	0.51	344522	568865
2.2-1	52.7	0.51	354506	568865
1.5-1	76.2	0.51	344522	555937
1.5-2	76.4	0.51	382204	643717

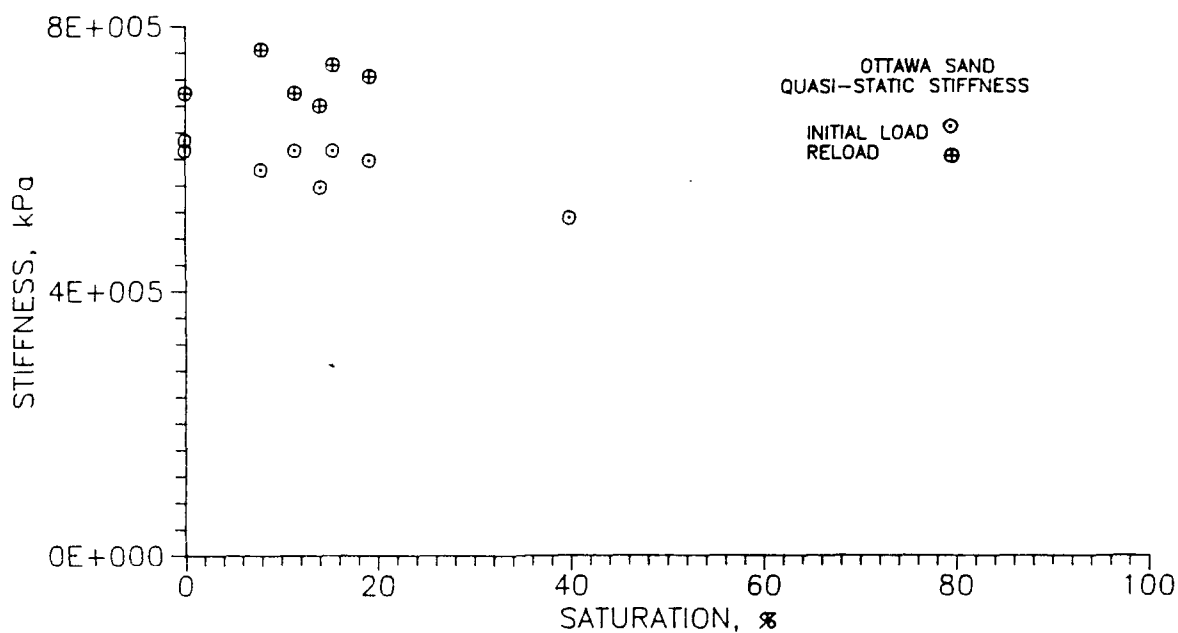


Figure 4.15 Quasi-Static Constrained Modulus Versus Saturation for 20-30 Ottawa Sand

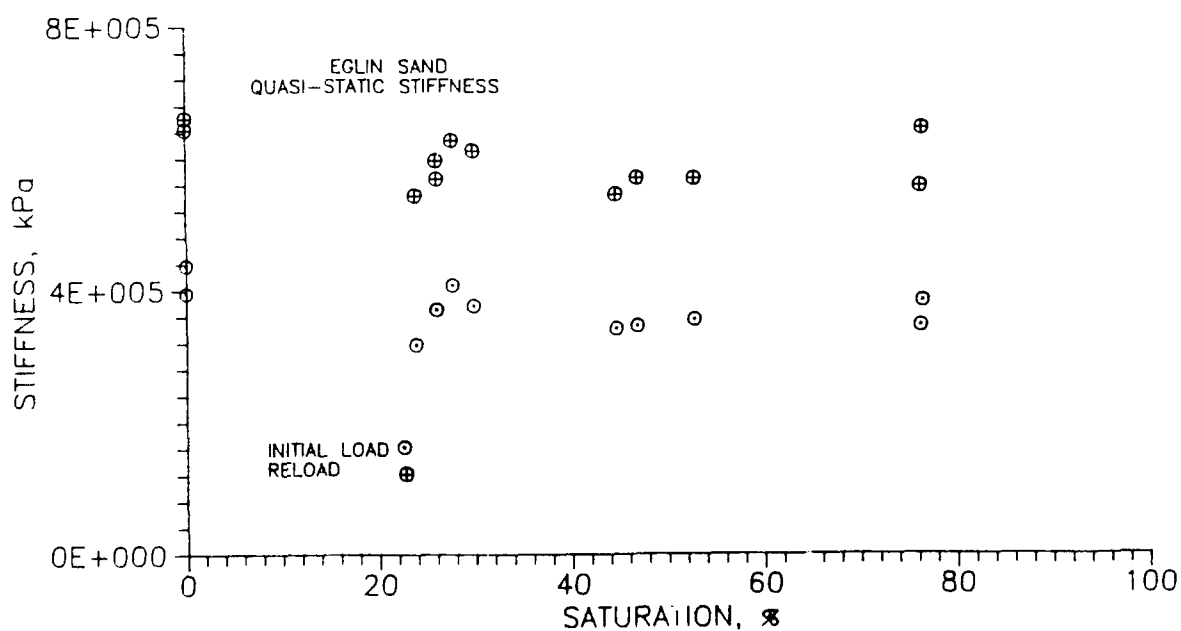


Figure 4.16 Quasi-Static Constrained Modulus Versus Saturation for Eglin Sand

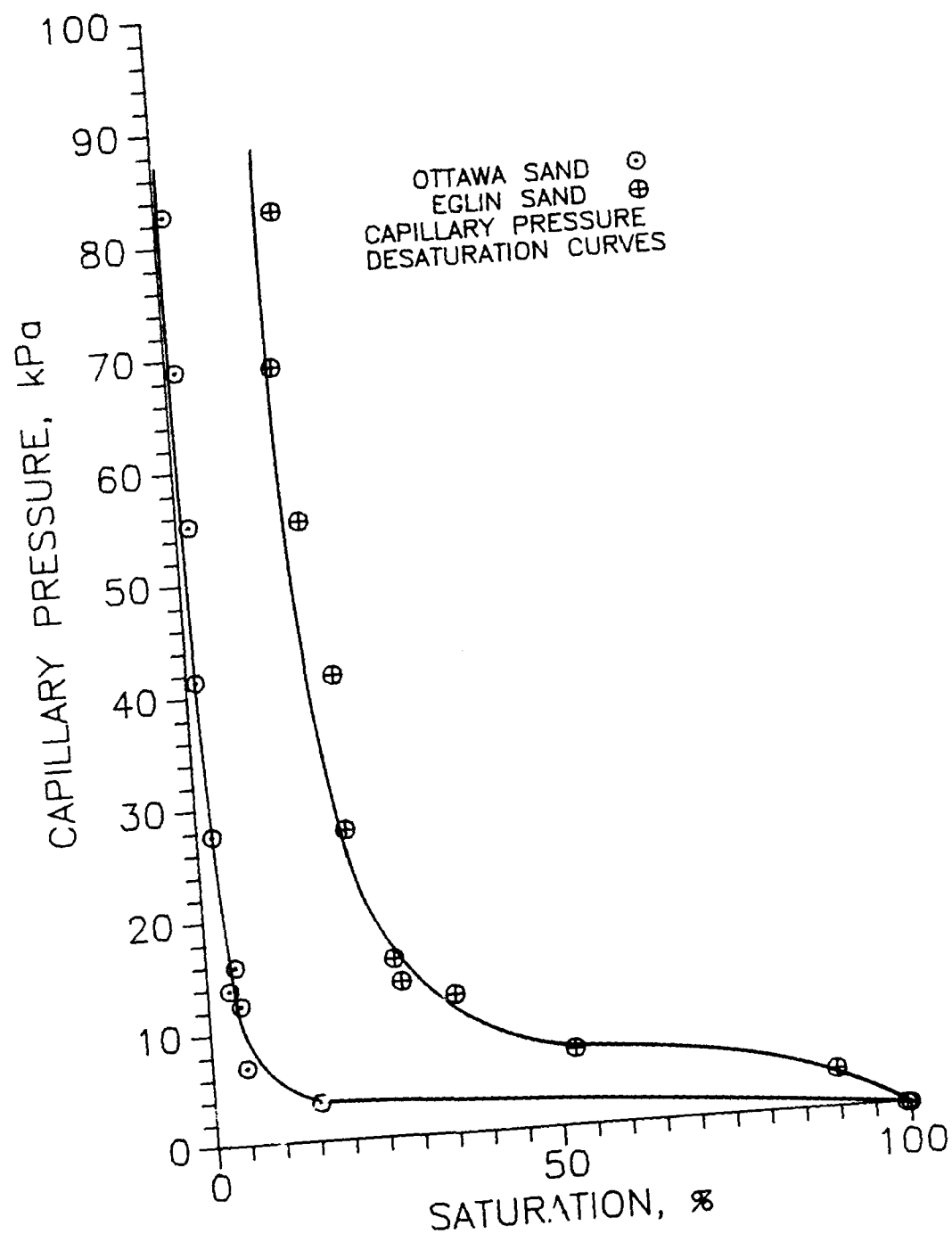


Figure 4.17 Capillary Pressure-Desaturation Curve for 20-30 Ottawa and Eglin sands

## V. ANALYSIS OF RESULTS

### A. PRESENT INVESTIGATION

#### 1. General Observations

The wave velocity, stress transmission and quasi-static confined compression tests all seem to show the same trend as saturation is increased. In general, the values of wave velocity, stress transmission and quasi-static constrained modulus decrease slightly as the saturation level increases up to approximately 80 percent. Above this saturation level the dynamic test results show an increase in wave velocity and stress transmission. This may occur because the compressive wave front begins to travel through the water phase as saturation is increased during the high strain testing. This effect was theorized by Whitman (1970) and discussed in Chapter 2. Quasi-static stiffness tests on both sands have shown that the constrained modulus also decreases with increasing saturation. The variation in stiffness which occurred with changes in saturation was as much as 20 percent.

Comparing the dynamic tests results performed under different triaxial confining stresses shown in Figures 4.4 through 4.11, it appears that the confining stress increases the wave velocity and stress transmission. At high confining stresses, the wave velocity and transmission ratio still decreases with increasing saturation

levels. Therefore, confining stress has shifted the results without affecting the general trends observed. Based on the two confining stresses used, wave velocity varies with the total applied stress (confining and dynamic stress) based on the following equations for the 20-30 Ottawa and Eglin sands, respectively:

$$V_c = 47.3 \sigma^{0.5} \quad (R^2 = 0.85) \quad (5.1)$$

$$V_c = 5.7 \sigma^{0.3} \quad (R^2 = 0.94) \quad (5.2)$$

There is no definitive reason for the scatter obtained in this investigation, though several conclusions can be drawn. Since it occurs in both the dynamic and quasi-static test results the scatter is not a function of the strain rate. Comparing tests performed with 310 kPa confining stress with tests performed with zero confining stress, it appears that there is no variation in the scatter recorded. Sand type also has little effect as similar amounts of scatter occur for both the Ottawa and Eglin sands. Based on the above observations, the amount of scatter obtained may be due to sample preparation differences, interparticle variations within the compacted sand specimens or end effects between the pressure bars and the sand sample. Nimmo and Akstin (1988) express their concern that changes in humidity or temperature in the room where compaction takes place may affect the particle arrangement of sand specimens. From Figures 2.18 through 2.22, similar scatter was recorded by Ross et al. (1988).

Sample preparation errors were minimized by compacting, saturating and desaturating several samples simultaneously through the course of this investigation. Sample preparation was closely

controlled, resulting in a mean void ratio of 0.514, and a standard deviation of 0.010 for all specimens prepared.

It should be noted that there were no tests performed on the Eglin sand between saturation levels of zero and 23 percent. The residual saturation level as shown in Figure 4.17 prevented the Eglin sand from being desaturated below this value.

## 2. Prediction of Wave Velocity based on Quasi-Static Modulus

Compressive stress wave velocity can be predicted through equation 2.3 if the constrained modulus and total density of the soil are known. In order to determine if there are any strain rate effects in loading the Ottawa and Eglin sands, quasi-static moduli were used to predict the wave propagation velocities for each sand at various saturation levels. Because there was no data obtained under any other condition, this analysis is limited to dynamic tests performed at zero confining stress.

Figures 5.1 and 5.2 show the relationship between the wave velocities and transmission ratios determined from SHPB testing and those predicted by quasi-static modulus for 20-30 Ottawa sand. Figures 5.3 and 5.4 show the same relationships for the Eglin sand. The predicted values for transmission ratio were determined by equation 2.7 using the acoustic impedance of the steel and soil. The

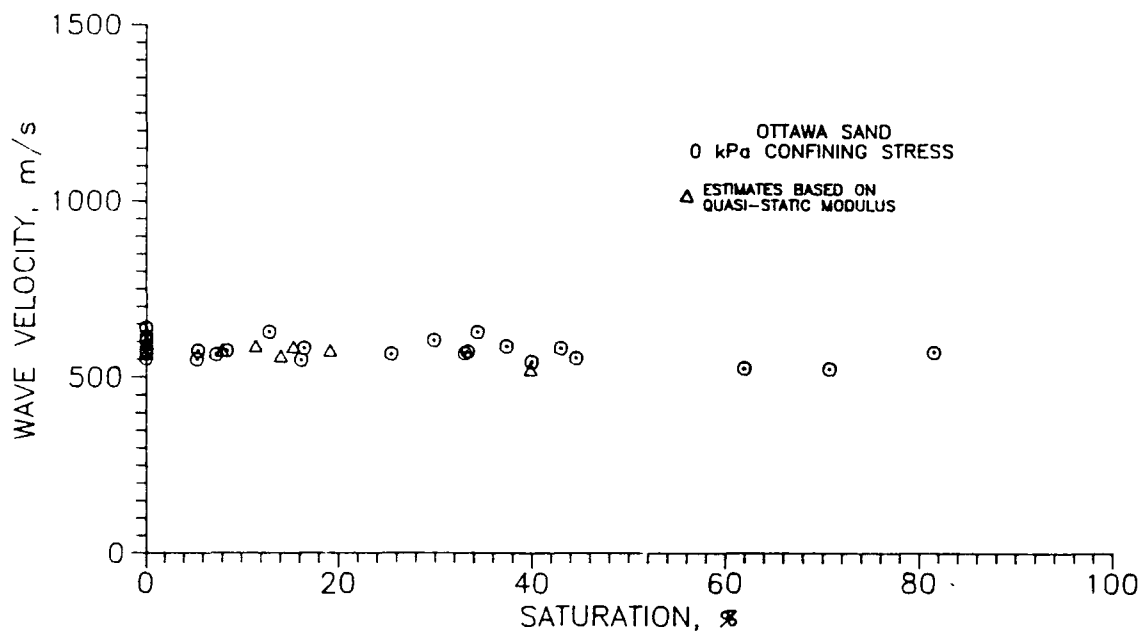


Figure 5.1 Wave Velocity Versus Saturation Results with Values Based on Quasi-Static Modulus for 20-30 Ottawa Sand Under Zero Confining Stress (Compacted Dry)

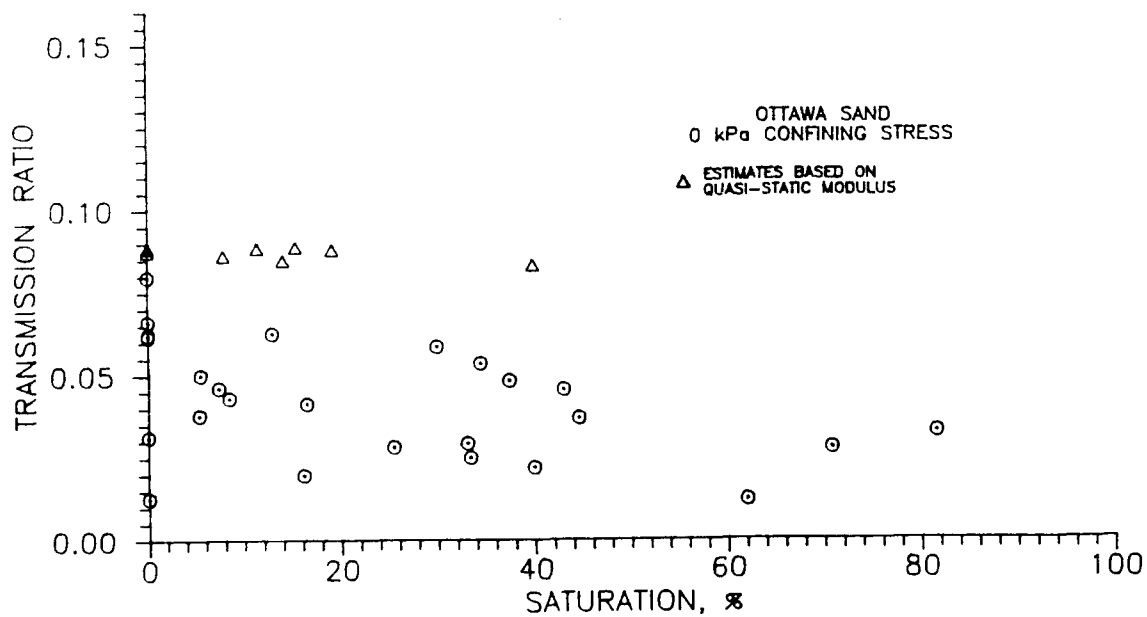


Figure 5.2 Transmission Ratio Versus Saturation Results with Values Based on Quasi-Static Modulus for 20-30 Ottawa Sand Under Zero Confining Stress (Compacted Dry)

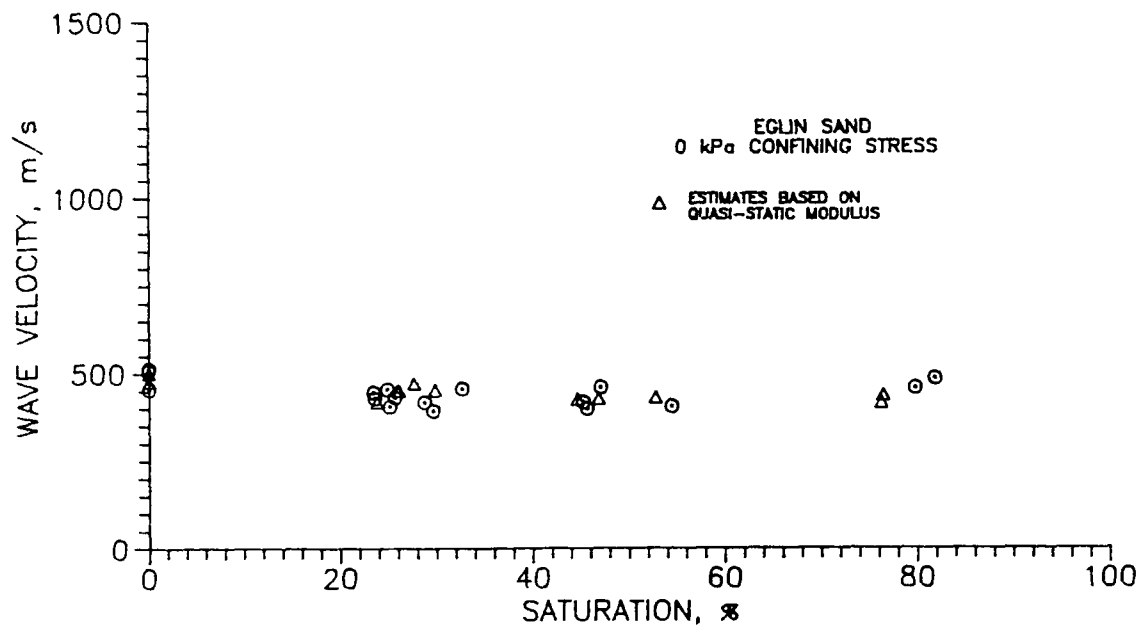


Figure 5.3 Wave Velocity Versus Saturation Results with Values Based on Quasi-Static Modulus for Eglin Sand Under Zero Confining Stress (Compacted Dry)

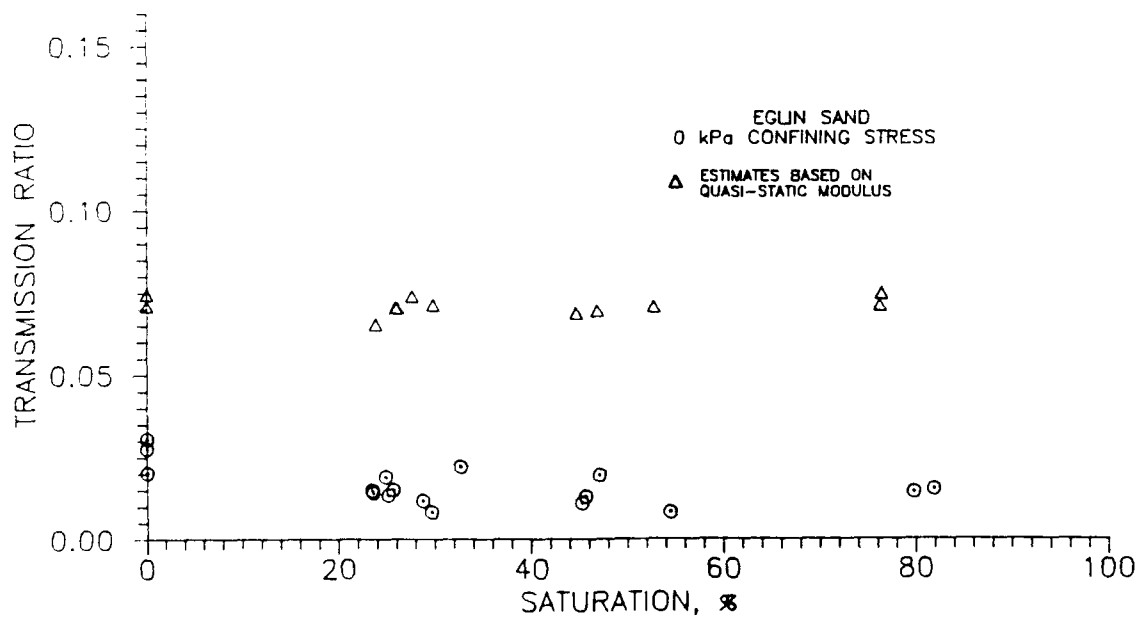


Figure 5.4 Transmission Ratio Versus Saturation Results with Values Based on Quasi-Static Modulus for Eglin Sand Under Zero Confining Stress (Compacted Dry)



acoustic impedance of the soil was calculated based on the predicted wave velocity and total density for each test.

The wave velocity values predicted from the quasi-static modulus are very similar to the experimentally determined dynamic values for both the Ottawa and Eglin sands. This would seem to show that the rate of loading does not affect the constrained modulus for either of the sands.

The predicted values of transmission ratio for both the Ottawa and Eglin sands are two to three times larger than the actual values obtained from SHPB testing. Equation 2.7, used to predict the transmission ratio values, is based on the assumption that no attenuation of the compressive wave occurs as it passes through the soil. The experimental results in Figures 5.2 and 5.4 show that a significant amount of attenuation occurs through the two sands.

### 3. Prediction of Wave Velocity based on Constant Modulus

If the capillarity of an unsaturated sand contributes to an increase in intergranular stress within the sand, an increase in wave propagation velocity would be expected due to the increase in modulus. If there is little contribution due to capillarity, a simple model can be developed to predict the wave velocity. The dry dynamic modulus (or as explained in the previous section, the dry quasi-static modulus) and the total density of the sand at a particular saturation level can be used in equation 2.3 to predict the wave velocity at any saturation level. Figures 5.5 through 5.8 show the wave velocity results obtained from the SHPB for each sand under the two confining

stresses. Also placed on the figures are the predicted wave velocities based on the average dry dynamic modulus for each sand and confining stress determined from equation 2.3. For the saturation levels used in this investigation, the model predicts the experimental results satisfactorily. Equation 2.3 shows that the water phase has little influence on the modulus of the soil, but influences the wave velocity through an increase in total density.

The transmission ratio can also be estimated from this model in the same manner described in the previous section. But it is of little use since equation 2.7 does not take attenuation effects into consideration.

#### 4. Constrained Modulus in Terms of $(\sigma - u_a)$ and $(u_a - u_w)$

Fredlund and Morgenstern (1976) presented equation 2.13, discussed in Chapter 2, which relates the volumetric strain of the soil structure,  $\epsilon_v$ , to the normal strain components. This is expressed by:

$$\epsilon_v = C_t d(\sigma - u_a) + C_w d(u_a - u_w) \quad (2.13).$$

This equation demonstrates that the strain is related to the stress components  $(\sigma - u_a)$  and  $(u_a - u_w)$  through the compressibility of the soil due to the solid and water phases.

A similar relationship can be determined between the stress components and the wave velocity of a compression wave propagating through soil. From equation 2.3 the compressive wave velocity is a function of the constrained modulus and the total density of the soil

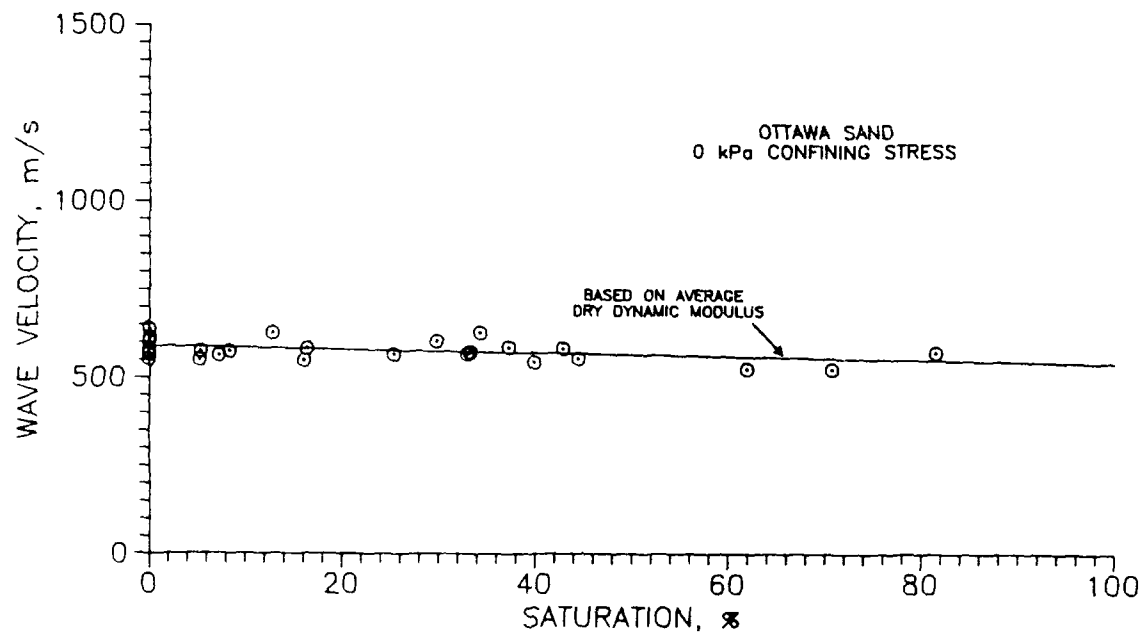


Figure 5.5 Wave Velocity Versus Saturation Model Based on Constant Modulus for 20-30 Ottawa Sand under Zero Confining Stress (Compacted Dry)

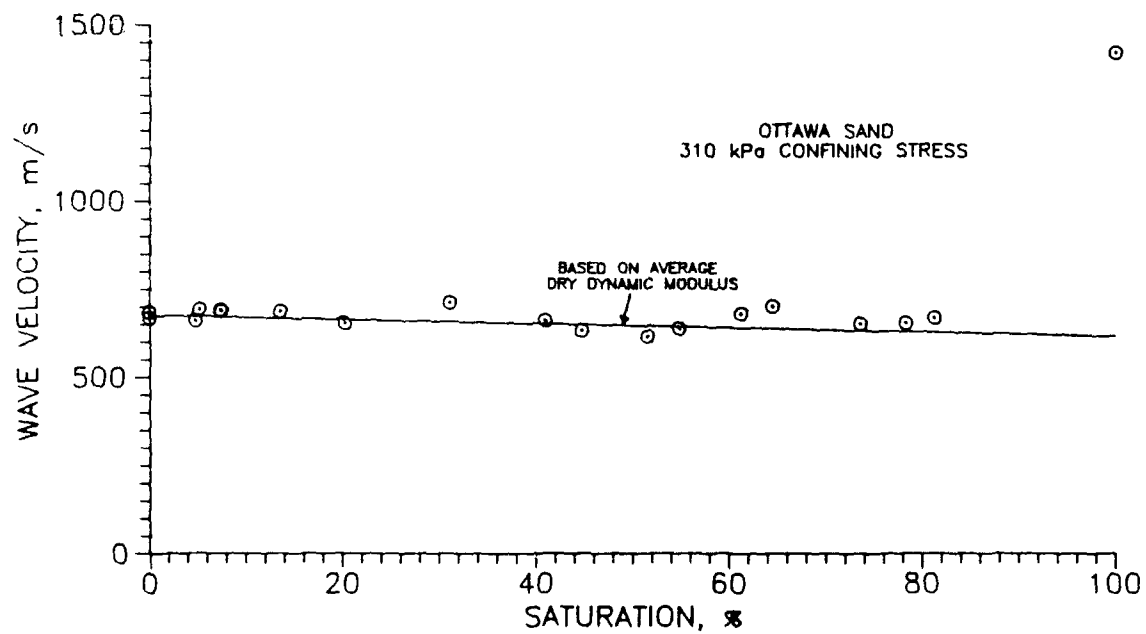


Figure 5.6 Wave Velocity Versus Saturation Model Based on Constant Modulus for 20-30 Ottawa Sand under 310 kPa Confining Stress (Compacted Dry)

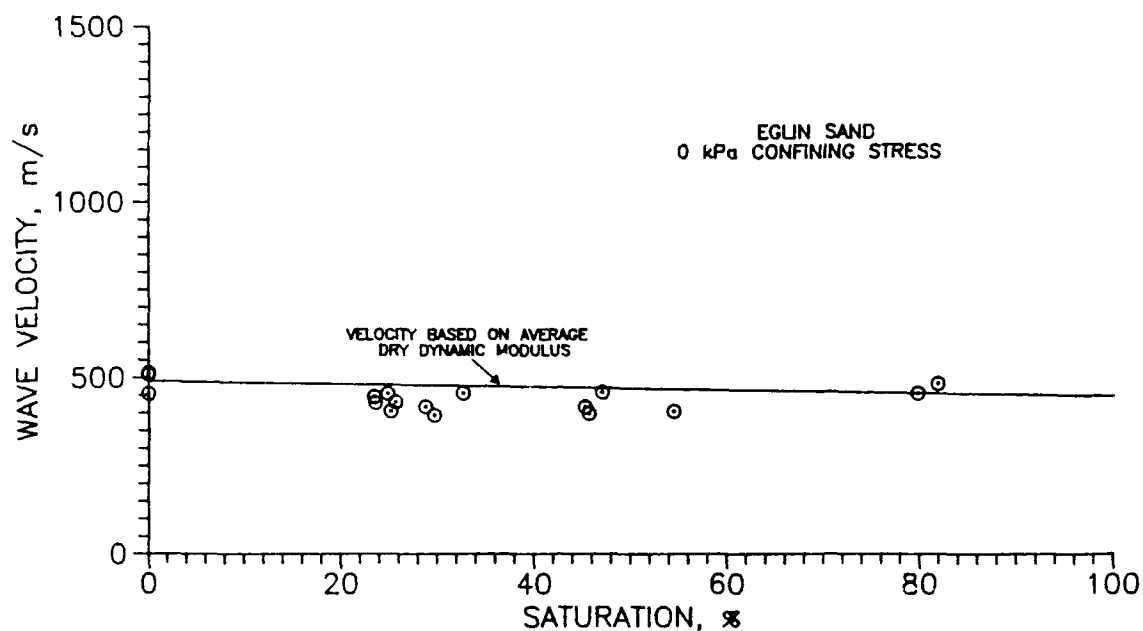


Figure 5.7 Wave Velocity Versus Saturation Model Based on Constant Modulus for Eglin Sand Under Zero Confining Stress (Compacted Dry)

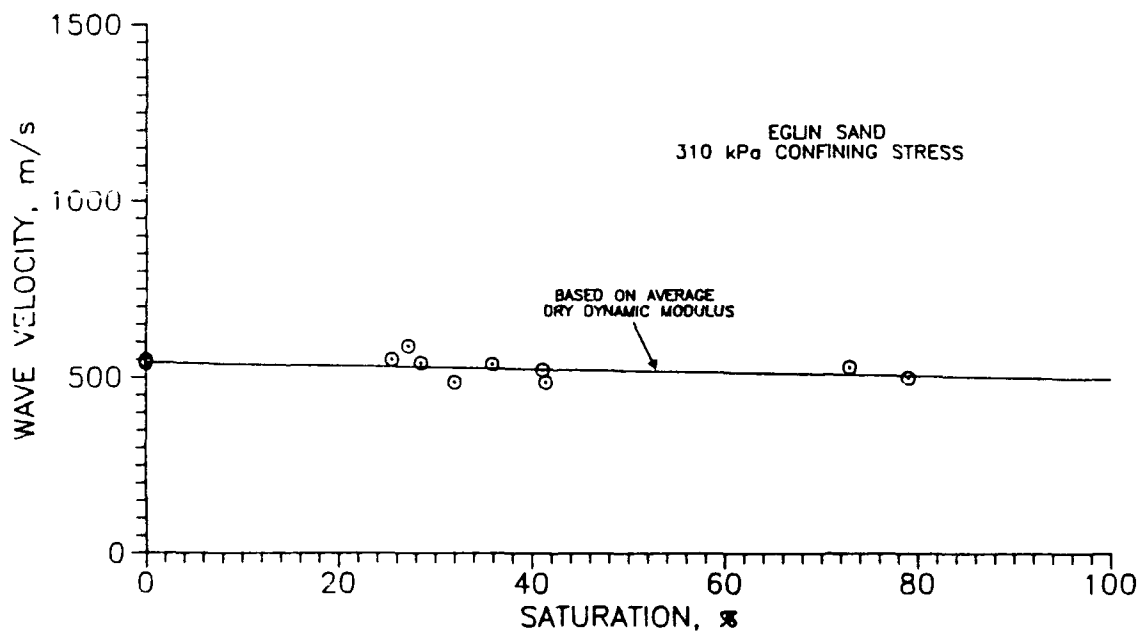


Figure 5.8 Wave Velocity Versus Saturation Model Based on Constant Modulus for Eglin Sand Under 310 kPa Confining Stress (Compacted Dry)

under confined compression. From equation 2.13 above, the modulus is a function of stress and strain, therefore the wave velocity squared multiplied by the total density ( $V_c^2 \rho_t$ ) is a function of the stress and strain within the soil. The relationship between wave velocity and stress is not a constitutive equation, but it is useful in relating the wave velocity to the stress components ( $\sigma - u_a$ ) and ( $u_a - u_w$ ).

Figures 5.9 and 5.10 present the constrained modulus ( $V_c^2 \rho_t$ ) (in kPa) as a function of the two stress components for both the Ottawa and Eglin sands. The total stress used in this analysis,  $\sigma$ , is the sum of the confining stress,  $\sigma_o$ , and dynamic stress,  $\sigma_D$ . The dynamic stress component is the average stress within the sample due to the dynamic loading. This value was calculated based on the SHPB incident and transmitted stress and the acoustic impedance of the steel and sand. The capillary pressure values used in the figures were based on the saturation levels of the sands prior to testing, and capillary pressure-desaturation curves given in Figure 4.17. The constrained modulus was determined from the average wave velocity through the sample and the total soil density.

Based on a linear regression analysis, the outline of the best-fit planes through the data is also presented. These best-fit planes can be used in predicting the modulus of the sand based on the applied stress and pore pressure conditions of the soil. Table 5.1 contains the equations for both of the best-fit planes presented.

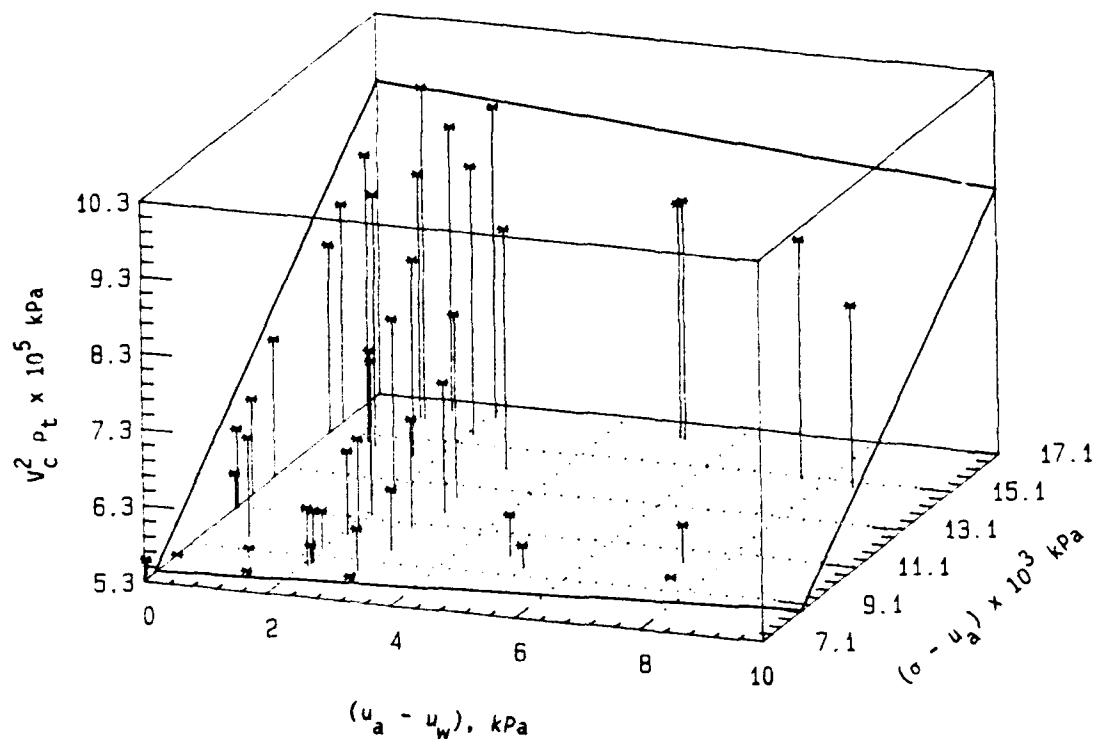


Figure 5.9 Constrained Modulus Versus  $(\sigma - u_a)$  and  $(u_a - u_w)$  for 20-30 Ottawa Sand (Compacted Dry)

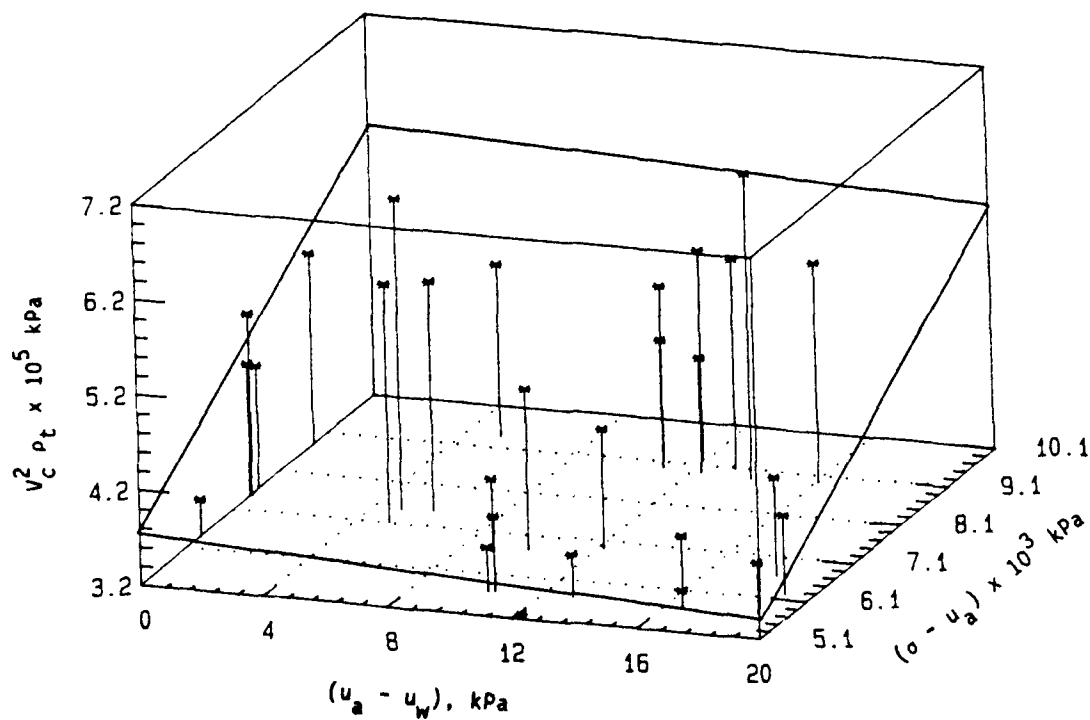


Figure 5.10 Constrained Modulus Versus  $(\sigma - u_a)$  and  $(u_a - u_w)$  for Eglin Sand (Compacted Dry)

Table 5.1 Equations for Multiple Regression Analysis Planes for  
Ottawa and Eglin Sands Based on Total Peak Applied Stress, Pore  
Pressure and Constrained Modulus

---

20-30 Ottawa Sand:

$$V_c^2 \rho_t = (2.024 - 0.056 * (u_a - u_w) + 0.0004 * (\sigma - u_a)) \times 10^5$$

$$R^2 = 0.901 \qquad s = 0.42$$

Eglin Sand:

$$V_c^2 \rho_t = (1.510 - 0.016 * (u_a - u_w) + 0.0004 * (\sigma - u_a)) \times 10^5$$

$$R^2 = 0.522 \qquad s = 0.63$$


---

From the slopes of the best fit lines in Figures 5.9 and 5.10, it appears that the pore pressure component,  $(u_a - u_w)$  has little influence on the value of constrained modulus. When the pore water pressure is altered due to a change in saturation, the constrained modulus appears to be relatively unaffected. As the total stress,  $(\sigma - u_a)$  increases, the constrained modulus generally increases, which is in agreement with the theory for stress-strain conditions under confined compression (see Figure 2.12). When the samples are compacted dry, Fredlund's theory supports the conclusion that the pore water has little influence in changing the values of constrained modulus for the ranges of saturation used in this investigation.

## B. COMPARISON WITH THE RESULTS OBTAINED FROM PREVIOUS INVESTIGATIONS

### 1. Effects of Confining Stress

Figure 5.11 shows the results obtained by Hardin (1961) and Stoll and Ebeido (1965). Also shown are the results obtained in this investigation for dry 20-30 Ottawa sand under a confining stress of

310 kPa. The results obtained by Stoll and Ebeido show a considerable amount of scatter, but the wave velocities are greater than those obtained by Hardin. This follows theoretical predictions that a soil with some lateral constraint will have a higher modulus at higher stress levels resulting in higher wave velocities. The results obtained in this investigation have higher wave velocities than either of the other two sets of data. This was expected because the samples in this investigation were not allowed to strain laterally, and were subjected to larger dynamic stresses.

Using high stress, confined compression tests, Hendron (1963) determined that the constrained modulus varies with confining stress to the one-third power. From equation 2.3, the wave velocity would then be expected to be proportional to confining stress to the one-sixth power. This result is the same as that predicted by Duffy and Mindlin (1957) and Richart et al. (1970), based on a theoretical packing of spheres. Based on this relationship, the predicted wave velocities are lower than that obtained in the current investigation. There are several reasons for this difference. First, Hendron did not use 20-30 Ottawa or Eglin sands in his investigation. Differences in sand type may be responsible for the difference between the wave velocities obtained in this investigation and that based on Hendron's work. Also, equation 2.3 was developed for determining the wave velocity for a material which is within its elastic range.



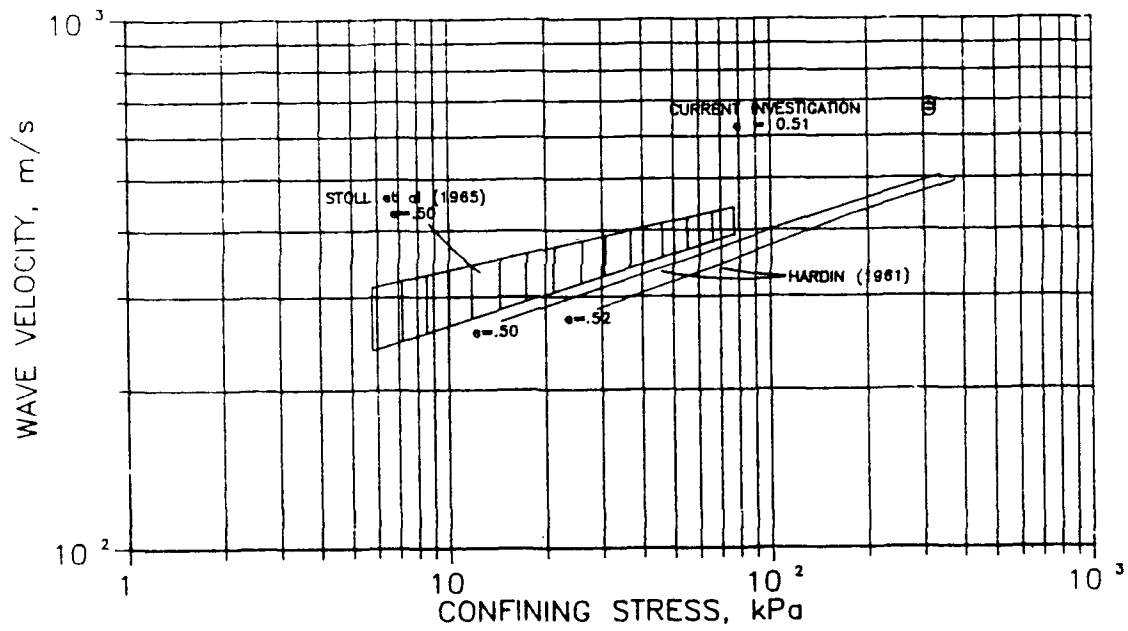


Figure 5.11 Confining Stress Versus Wave Velocity for Results Obtained by Hardin (1961), Stoll et al. (1965), and the Current Investigation for 20-30 Ottawa Sand (Compacted Dry)

## 2. Effects of Saturation

In this investigation it was found that the saturation levels between zero and 80 percent do not greatly influence the values of wave propagation velocity, transmission ratio or quasi-static stiffness for 20-30 Ottawa and Eglin sands compacted dry. If compacting a sample at different moisture contents is influential in determining the wave velocity parameters and static stiffness, the results obtained by Calhoun and Kraft (1966), Hendron et al. (1969), Wu et al. (1984), and Ross et al. (1988) should be similar because all samples were compacted moist to a particular saturation level prior to testing. Because the samples were compacted dry in this investigation, the results obtained would be expected to be different. As discussed in Chapter 2, the results obtained by Ross et al. (for constrained modulus) and Wu et al. (for shear modulus) show the greatest increase in stiffness occurs at intermediate saturation levels. The results obtained by Calhoun and Kraft, and Hendron et al. are very different. Soil type may be influential in the trends observed, but Wu et al. performed shear wave propagation tests on both sandy and silty soils and obtained similar trends. From the summary given in Chapter 2, all of the these researchers have compacted their samples by different methods. Based on the study by Mulilis et al. (1977), the method of sample compaction is a consideration which is as important as the amount of moisture used during compaction. The disparity in results obtained by the previous researchers may be attributed to both variations in sample preparation, and the types of testing apparatus used. The results obtained in this investigation

may also be attributed to the sample compaction process. It is apparent that before the variations in saturation levels can be evaluated, the method of compaction must first be considered.

### 3. Effects of Loading Rate

Whitman (1970) and Jackson et al. (1980) have concluded that loading rate effects in dry granular soils are an important consideration for rise times of less than one millisecond. The data obtained in this research shows that for the Ottawa and Eglin sands, compacted dry, then saturated, then desaturated, there are no rate effects occurring between samples loaded quasi-statically and those loaded with rise times of 15 microseconds (see Figures 5.1 through 5.3). The differences in results may be a function of the types of sand used and the high dry densities used in this investigation.

### 4. Model Comparisons

#### a. Whitman (1970)

Equation 2.14 presented by Whitman (1970) relates the compressive wave velocity to the dry soil modulus, specific gravity and saturation level. Wave velocities have been computed from this equation based on the dry moduli of the Ottawa and Eglin sands under both confining stresses. The results are presented along with the experimental data from this investigation in Figures 5.12 through 5.15. As shown in the figures, the model proposed by Whitman

accurately describes the experimental data. Figure 5.13 shows that the model is still accurate at almost complete saturation.

Whitman's model shows that at lower saturation levels there is little contribution by the water phase in changing the modulus of the soil. Whitman's model takes into account the increase in wave velocity as saturation levels approach 100 percent, which is an improvement over the previous model at higher saturation levels. It is interesting to note that at lower saturation levels, the results of this model are almost identical to the previously described model, which is based on constant dry modulus.

b. Anderson and Hampton (1980)

The model presented by Anderson and Hampton (1980) was developed to determine the compressive wave velocities through gassy sediments. Presented in Figures 5.16 and 5.17 are results based on the model along with the data obtained in this investigation for the Ottawa and Eglin sands under zero confining stress. The velocity data is presented as a ratio of the moist wave velocity divided by the average dry wave velocity for each sand.

Figures 5.16 and 5.17 show that the model does not accurately represent the data obtained in this investigation. The model predicts the wave velocity results to be much lower than those determined experimentally.

This model is based on a modified rule of mixtures for soil particles suspended in a fluid and was developed for the determination of wave velocities in soft ocean sediments. The accuracy of the model

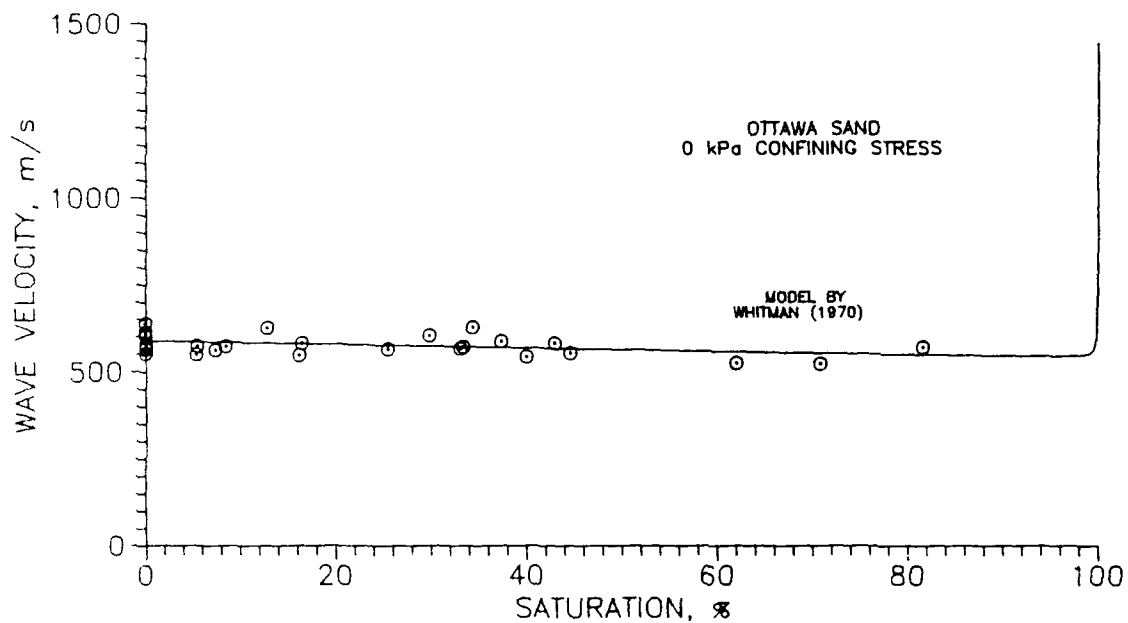


Figure 5.12 Wave Velocity Versus Saturation Results with Model Proposed by Whitman (1970) for 20-30 Ottawa Sand Under Zero Confining Stress (Compacted Dry)

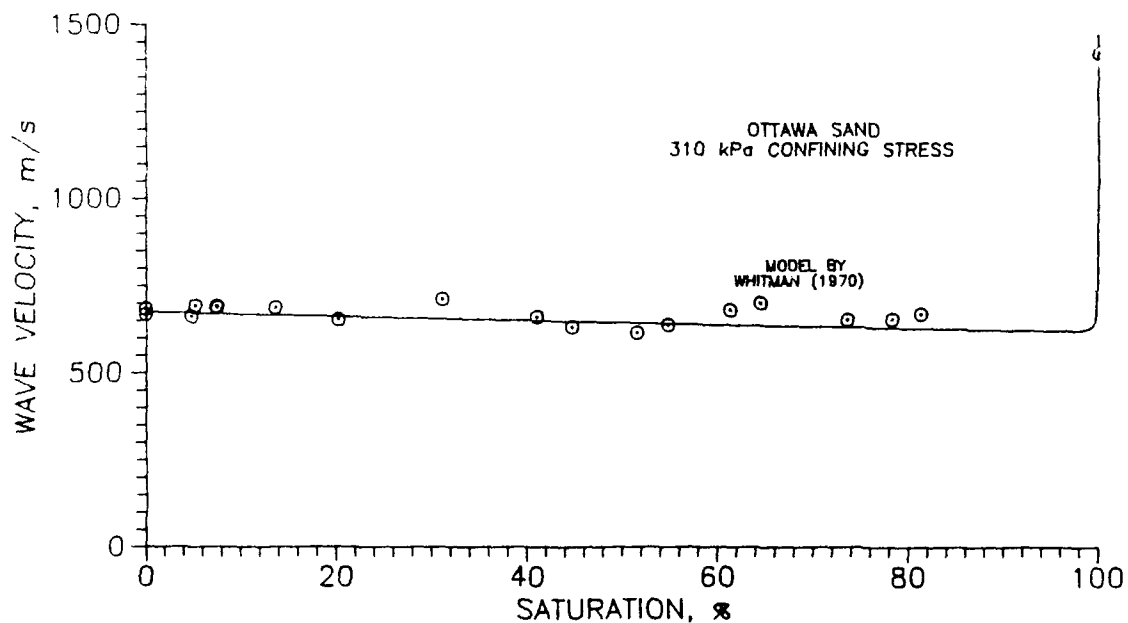


Figure 5.13 Wave Velocity Versus Saturation Results with Model Proposed by Whitman (1970) for 20-30 Ottawa Sand Under 310 kPa Confining Stress (Compacted Dry)

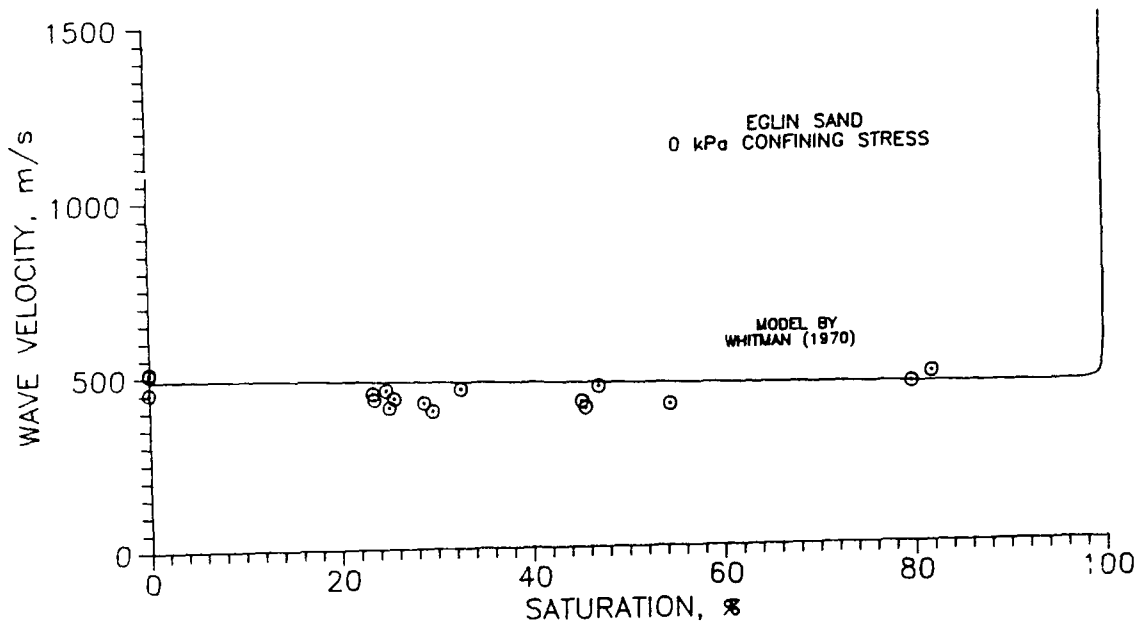


Figure 5.14 Wave Velocity Versus Saturation Results with Model Proposed by Whitman (1970) for Eglin Sand Under Zero Confining Stress (Compacted Dry)

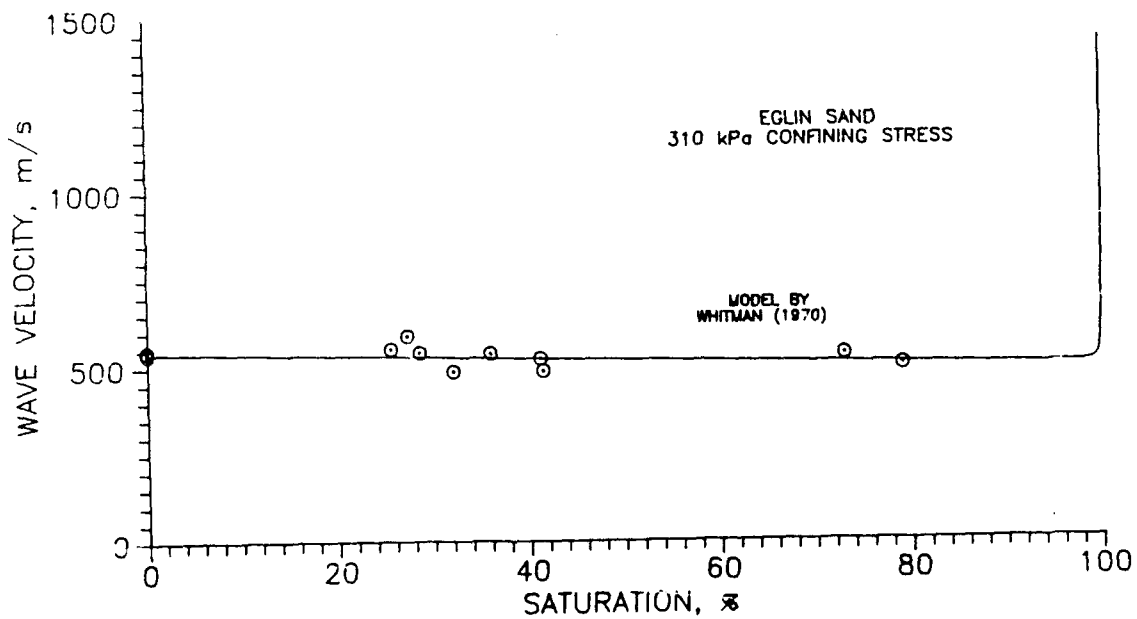


Figure 5.15 Wave Velocity Versus Saturation Results with Model Proposed by Whitman (1970) for Eglin Sand Under 310 kPa Confining Stress (Compacted Dry)

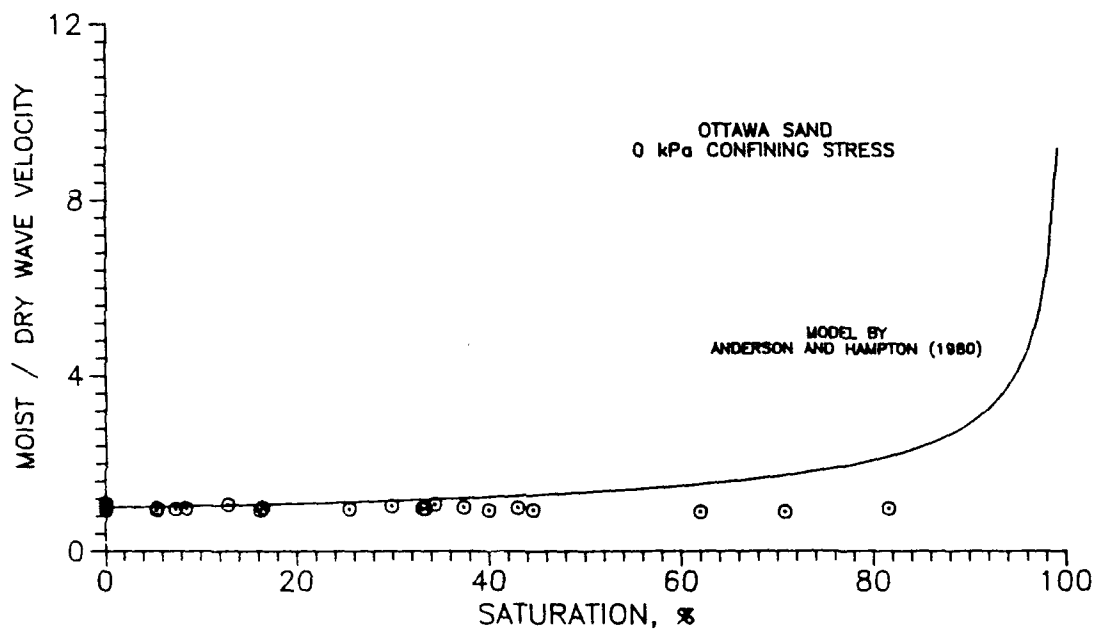


Figure 5.16 Wave Velocity Versus Saturation Results with Model Proposed by Anderson and Hampton (1980) for 20-30 Ottawa Sand Under Zero Confining Stress (Compacted Dry)

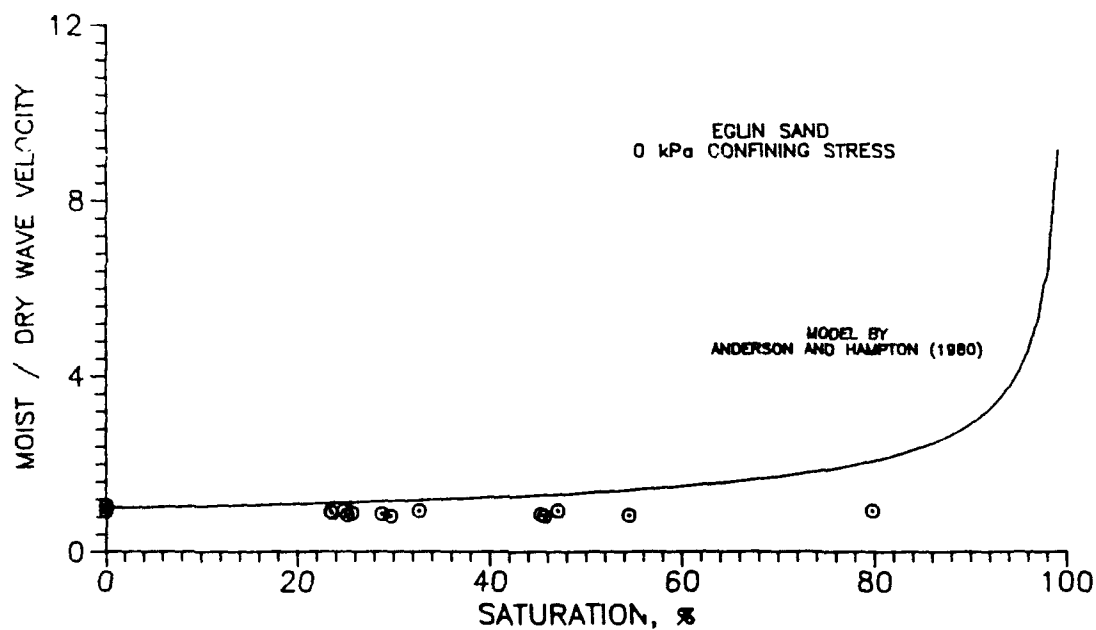


Figure 5.17 Wave Velocity Versus Saturation Results with Model Proposed by Anderson and Hampton (1980) for Eglin Sand Under Zero Confining Stress (Compacted Dry)

increases as the saturation levels approach 100 percent. The differences at lower saturation levels occur because the compressibility of the dry soil in the model is dependent on the compressibility of air. This combined compressibility will be very low, therefore the predicted wave velocities are very low. Since the saturation levels used in this investigation are well below 100 percent, this model does not fit the data with sufficient accuracy.

#### 5. Results obtained by Ross et al. (1988)

All testing performed by Ross et al. (1988) and that performed in this investigation utilized the same SHPB, soil types, saturation ranges, and dry densities. The general trends for wave velocity, stress transmission and quasi-static modulus tests performed by Ross et al. (given in Figures 2.18 through 2.22), are considerably different than those obtained in this investigation. Figures 5.18 and 5.19 show the values of wave velocity and stress transmission ratio obtained for Eglin sand by Ross et al. Also on the figures are the results obtained in this investigation. A similar relationship occurs with quasi-static modulus. The difference in results could be due to differences in the sample containers used, or the moisture content of the sand during compaction. All other factors were consistent in both investigations.

The sample container used by Ross et al. was a thick-walled steel specimen container designed to prevent lateral expansion. Figures 4.12a and b show that when samples were compacted moist in the specimen cell used in this investigation, the wave velocities are



similar to those obtained by Ross et al., and are markedly higher than those obtained in this investigation when the samples were compacted dry, then brought to the same saturation level. The results obtained by both investigations for dry compacted samples show similar results and scatter for values of wave propagation velocity and stress transmission ratio. This would seem to rule out any possibility for differences in sample containers being responsible for the differences in trends observed.

Based on the above discussion, the only differences in sample preparation techniques which could account for the difference in trends is that Ross et al. compacted the samples moist, while in this investigation they were compacted dry then brought to the same saturation level. It appears that there is something inherent in the compaction process which is causing differences to occur when relating velocity, transmission ratio and quasi-static constrained modulus to saturation level using different compaction techniques.

From the discussion in Chapter 2, several investigators have concluded that sample compaction procedures create differences in the behavior of the soil during testing. Changes in liquefaction potential (Mulilis et al., 1977), cyclic stability (Ladd, 1977) and permeability (Juang and Holtz, 1986; Nimmo and Askin, 1988), have been attributed to variations in the sand fabric or grain orientations created during the compaction process.

The energy compaction curve presented by Ross (1989) shown in Figure 2.11 shows that variations in saturation level of moist sands during compaction will affect the energy required to compact a sample

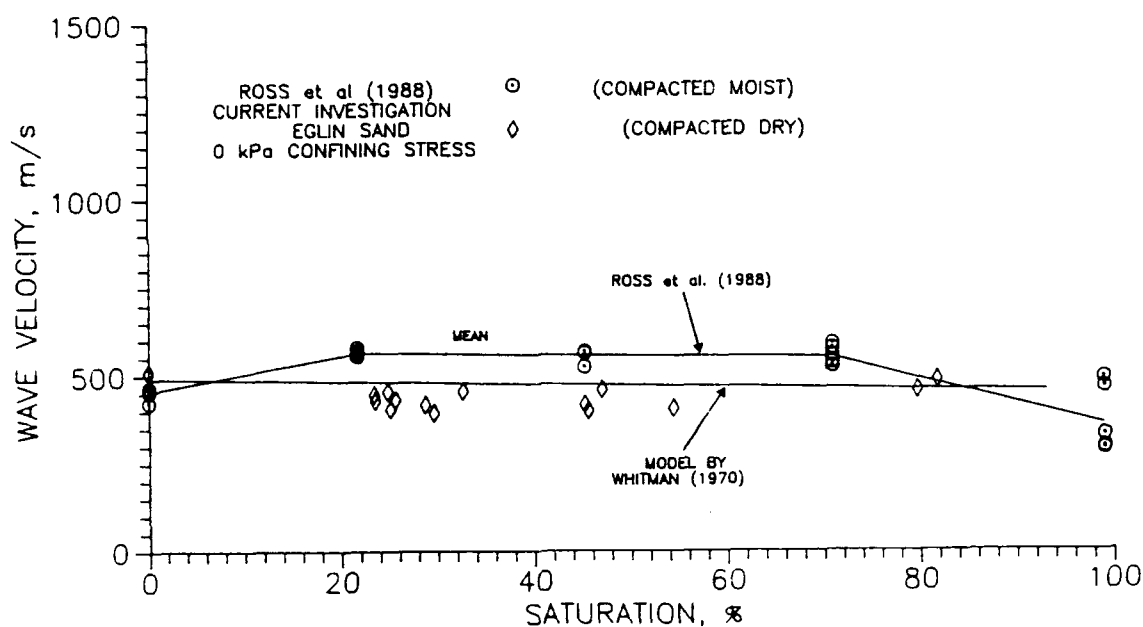


Figure 5.18 Wave Velocity Values Obtained by Ross et al. (1988) and in the Current Investigation for Eglin Sand Under Zero Confining Stress

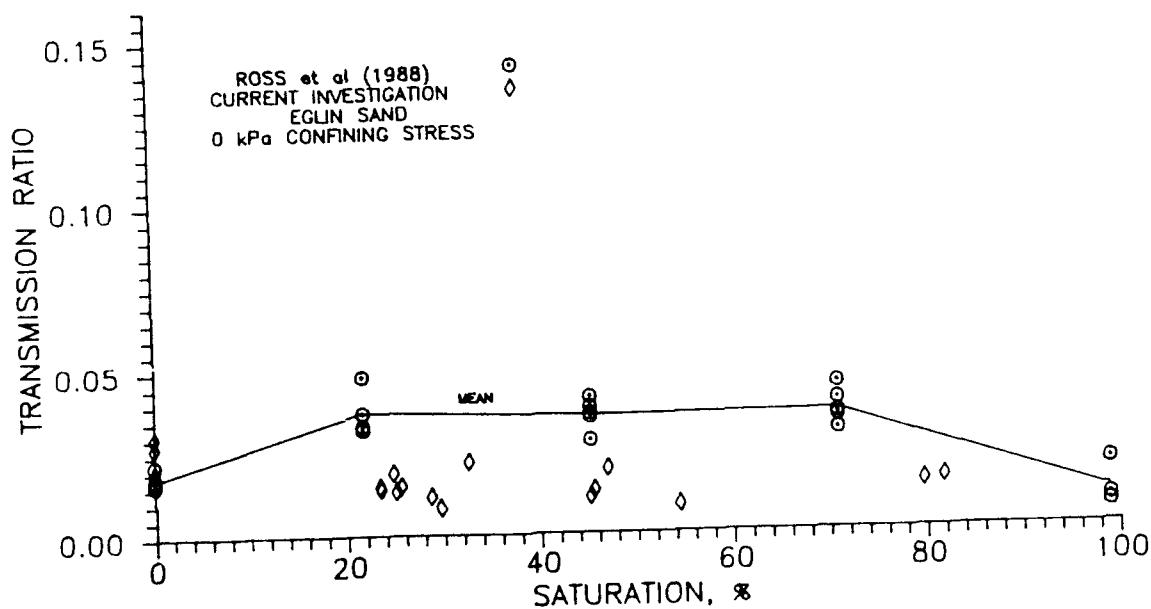


Figure 5.19 Stress Transmission Ratio Results Obtained by Ross et al. (1988) and in the Current Investigation for Eglin Sand Under Zero Confining Stress

to a constant dry density. If this energy variation is due to capillary forces between the sand particles, the theory by Ladd (1977) would predict that the most random fabric should occur during compaction when the capillary stress is a maximum. From Figure 2.11, this occurs between saturation levels of 20 to 40 percent. From the results presented by Ross et al. (Figures 2.18 through 2.24), the maximum wave velocity, stress transmission and constrained modulus values occur when the capillary stress in the soil is high. It may be concluded that the more random fabric creates higher values of wave propagation velocity, stress transmission and quasi-static constrained modulus.

Based on the studies by Juang and Holtz (1986) and Nimmo and Askin (1988), sands compacted dry have a larger range of pore sizes than sands compacted moist. For sands compacted moist to the same void ratio, the distribution of pore sizes is more uniform and generally smaller than when compacted dry. Based on the results obtained by Ross et al. (1988) this uniform distribution of pore sizes makes the sand less compressible under quasi-static and dynamic loading conditions.

For the samples of Eglin sand compacted moist, oven dried, then tested on the SHPB, Figure 4.13a shows the values of wave velocity are somewhat higher than the average values obtained for specimens compacted and tested dry. The transmission ratio results did not appear to be effected as much by the procedure as shown in Figure 4.13b. If the wave velocity results are correct, there may be a difference in fabric between samples compacted moist and dry, and

once the fabric is formed, it will not change once the moisture is removed.

It is also possible that sands compacted under various moisture contents will have different amounts of lateral (or confining) stress "locked in", that is, the sand is being overconsolidated by different amounts depending on the molding water content. This will effectively increase the stress within the sample. As discussed in Chapter 2, cyclic loading has been shown to change the value of  $K_0$  for sands and silts (Drnevich et al., 1967; D'Appolonia et al., 1969; Lambe and Whitman, 1969; Youd and Craven, 1975). There is also a small amount of data suggesting values of  $K_0$  vary under static confined compression for samples molded under different water contents (Hendron et al., 1969).

From this investigation it has been found that total applied stress varies with wave velocity to the second or third power, depending on sand type. Hardin (1961) has shown that based on his experimentation, confining stress is proportional to wave velocity to the fourth power, while Duffy and Mindlin (1957) and Richart et al. (1970) show that confining stress is proportional to wave velocity to the sixth power when based on the theoretical packing of spheres. From these relationships, a small increase in confining stress will cause a very large increase in wave velocity. If the amount of lateral confining stress stored in a sand is dependent on moisture content during compaction, a small change will cause large changes in wave velocity and transmission ratio.

Figure 5.20 shows the results obtained in this investigation for the Eglin sand under both zero and 310 kPa confining stress. Also in the figure are the results obtained by Ross et al. (1988) for Eglin sand under zero confining stress. It may be concluded that at intermediate saturation levels, the samples prepared by Ross et al. contain an "equivalent" confining stress locked in the soil with a value near 310 kPa. In order to quantify the actual values of equivalent confining stress, controlled tests must be performed to measure the change in confining stress during the compaction process.

One of the objectives on this investigation was to determine how fluctuations in saturation level will affect compressive stress wave velocity and stress transmission. It appears that based on the study performed by Ross et al. (1988), and the current investigation, the moisture content during compaction is very important in determining the dynamic properties of an unsaturated sand. From this investigation it was found that capillarity in itself does not appear to greatly affect the dynamic or static stiffness of sands. Therefore, when sands are compacted dry, variations within the saturation ranges used in this study will not greatly effect soil stiffness under static or dynamic conditions. It is the moisture content at which a sand is compacted that appears to influence the fabric and grain orientation of a sand, or change it's stress state. Based on a limited amount of data, the grain orientations or the stress state will remain within the sand, independent of changes in saturation level over time.

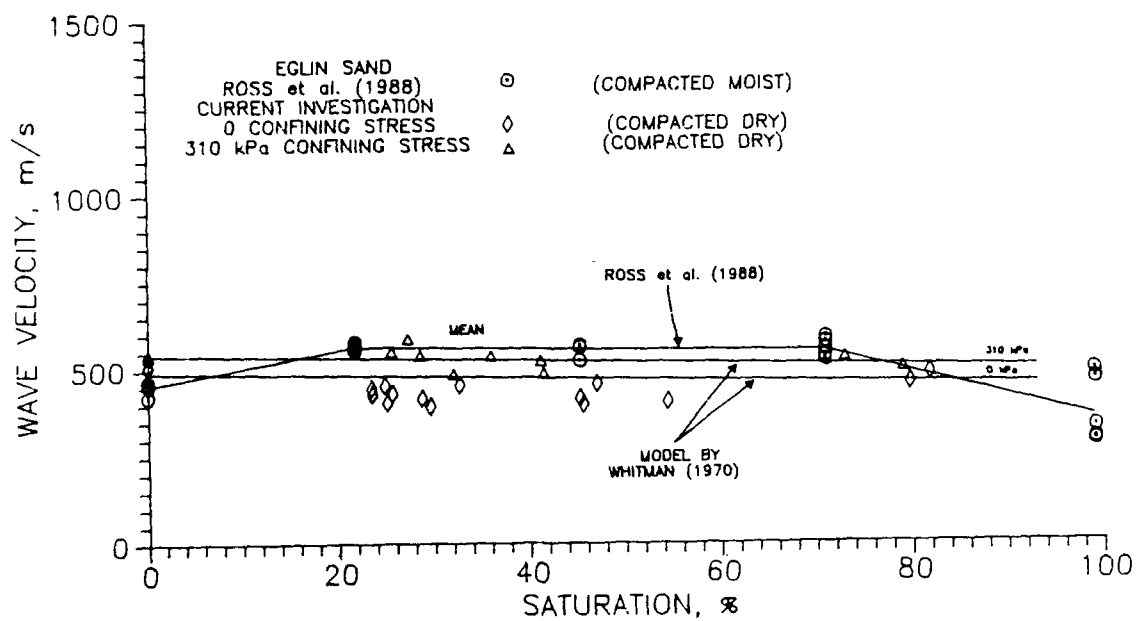


Figure 5.20 Wave Velocity Values Obtained by Ross et al. (1988)  
 and in the Current Investigation for Eglin Sand Under Zero and 310 kPa  
 Confining Stress

## VI. SUMMARY, CONCLUSIONS AND RECOMMENDATIONS

### A. SUMMARY

This investigation has studied the effects of saturation level and compaction technique on the parameters of compressive stress wave propagation in sands. Many soils in the field are in an unsaturated state, so research in this area is useful in understanding soil-structure interaction due to blast or impact loadings.

Dynamic wave propagation tests were performed utilizing a split-Hopkinson pressure bar, which applied high strain, short duration compressive loadings to the sand specimens. Values of wave propagation velocity and stress transmission ratio were measured for two sand types. Samples were prepared by compacting the sand dry to a constant density, then saturating, and then desaturating the samples by use of a pressure plate apparatus. Saturation levels were varied from zero to 82 percent. During testing, specimens were allowed to strain one-dimensionally under triaxial confining stress of either zero or 310 kPa. Quasi-static compression tests were also performed to determine the relationship between the results obtained dynamically and under quasi-static conditions.

For the range of saturation studied, the test results show that the values of wave velocity and stress transmission ratio decrease slightly with an increase in saturation for both confining

stresses used. Values of quasi-static constrained modulus vary in a similar manner. The results obtained for wave propagation velocity are closely predicted by Whitman's (1970) model given in equation 2.14.

The trends obtained in this investigation are much different than that presented by Ross et al. (1988) for the same soil types and dry densities. Their tests were performed on the same apparatus as in this investigation, but the samples were compacted moist to the required saturation levels. Changes in liquefaction potential (Mulilis et al., 1977), cyclic strength (Ladd, 1977), and permeability (Juang and Holtz, 1986; Nimmo and Askin, 1988) have been attributed to variations in compaction technique. Research also suggests that the method of sample compaction may also effect the amount of lateral or confining stress stored within the sand structure (Drnevich et al., 1967; D'Appolonia et al., 1969; Lambe and Whitman, 1969; Youd and Craven, 1975). It appears from the current investigation that the moisture content of the sand during compaction is very influential in determining the values of wave velocity, transmission ratio and quasi-static constrained modulus for sands. In particular, compacting samples at different moisture contents may influence the fabric and grain orientation of the sand or change the stress state in the sand.

## B. CONCLUSIONS

The objective of this study is to determine how moisture content during compaction, saturation level, and confining stress affect the values of wave velocity, stress transmission ratio and



quasi-static constrained modulus. From this experimental laboratory investigation performed on 20-30 Ottawa and Eglin sands, several conclusions can be made.

The most significant conclusion reached is that the sand compaction process is very influential in determining the values of wave velocity, stress transmission, and quasi-static constrained modulus. Ross et al. (1988) determined that sands which are compacted moist at intermediate saturation levels have values of wave velocity, stress transmission, and stiffness which can be as much as 20 percent higher than those compacted dry or very wet. When the 20-30 Ottawa and Eglin sands were compacted dry, then saturated, then desaturated in this investigation, the saturation level appeared to have little influence on the compressive stress wave parameters and quasi-static stiffness. It appears that when the sand is compacted dry, fluctuations in saturation level will not greatly effect the dynamic wave propagation parameters or quasi-static stiffness.

From this investigation and that performed by previous researchers, there are at least two possible reasons why compaction technique affects the static and dynamic parameters of sands. First, compacting sands at different saturation levels may effect the fabric and grain orientation of the sand particles. Secondly, it is also possible that variable amounts of lateral stress is stored within the sand during the compaction process, depending on the quantity of moisture in the sand during compaction. Even with these possible explanations, no definitive conclusions can be drawn from this investigation as to why the static and dynamic properties of the sands used in this investigation are affected by the compaction process.

Sand samples were compacted dry in this investigation to show the influence of moisture on the compaction process. Though it is not common practice to compact sands in the field in this manner, the results obtained based on this compaction method, and that performed by Ross et al. (1988) has shown that the stiffness of the soil is very dependent on the moisture content used. This infers that conventional field compaction methods of adding water during compaction will affect the stiffness of the sand. When laboratory data is used to predict the behavior of a sandy soil, it is very important that the samples be compacted in the same manner, and at the same moisture content as will be used in the field.

Increasing the confining stress around the sand increases the values of compressive wave velocity and stress transmission ratio. The wave velocity varies with confining stress to the one-third power for 20-30 Ottawa sand and to the one-half power for Eglin sand at the particular dry densities used in this study. For both confining stresses used, wave velocity and stress transmission decrease slightly with increasing saturation for samples compacted dry, saturated, then desaturated by use of the pressure plate method.

The theory presented by Fredlund (1986) accurately predicted that the capillary pressures developed in the sands which were compacted dry, then saturated, then desaturated would have little influence on the stiffness. The equation proposed by Bishop et al. (1960) for determining the change in effective stress in an unsaturated soil did not predict the variations in wave velocity, stress transmission and quasi-static stiffness for sands compacted in the same manner. The theory for effective stress presented by Bishop

et al. does predict the trends obtained by Ross et al. (1988). It should be noted though that this investigation has shown that trends obtained by Ross et al. (1988) are largely due to the compaction process.

### C. RECOMMENDATIONS

From the results of this investigation and a review of the pertinent literature, the following recommendations for further research on wave propagation in moist sands are made.

- Study how sand grain fabric is affected by changes in moisture content and the compaction process.
- Determine the relationship between changes in lateral and axial stress with changes in moisture content during compaction.
- Perform wave propagation tests on sands compacted by several different methods to determine how wave velocity and stress transmission ratio results change.
- Develop an analytical or empirical method for predicting wave velocity and stress transmission ratio for different compaction techniques and saturation levels.

## VII. REFERENCES

- ASTM (1987). Annual Book of ASTM Standards. American Society for Testing and Materials, Philadelphia, PA.
- Anderson, A. L. and Hampton, L. D. (1980). "Acoustics of Gas-Bearing Sediments, I. Background, and II. Measurements and Models." Journal of the Acoustic Society of America, Vol. 67, No. 6, 1865-1903.
- Balakrishna Rao, H. A. (1975). "One-Dimensional Compression of Partially Saturated Soils." Report No. AFWL-TR-73-177, Air Force Weapons Laboratory, Kirtland AFB, NM.
- Bishop, A. W., Alpan, I., Blight, G. E., and Donald, I. B. (1960). "Factors Controlling the Strength of Partially Saturated Cohesive Soils." Conference on Shear Strength of Cohesive Soils, ASCE, 503-532.
- Bishop, A. W. and Blight, G. E. (1963). "Some Aspects of Effective Stress in Saturated and Partially Saturated Soils." Geotechnique, Vol. 13, No. 3, 177-197.
- Calhoun, D. E., and Kraft, D. C. (1966). "An Investigation of the Dynamic Behavior of a Partially Saturated Silt with Applications to Shock-Wave Propagation." Technical Report No. AFWL-TR-65-176, Air Force Weapons Laboratory, Kirtland AFB, NM.
- Corey, A. T. (1986). Mechanics of Immiscible Fluids, 2nd Ed. Water Resources Publications, Littleton, CO.
- D'Appolonia, D. J., Whitman, R. V., and D'Appolonia, E. (1969). "Sand Compaction with Vibratory Rollers." Journal of the Soil Mechanics and Foundation Engineering Division, ASCE, Vol. 95, No. SM1, 263-284.
- Davies, R. M. (1948). "A Critical Study of the Hopkinson Pressure Bar." Philosophical Transactions of the Royal Society of London, Series A, Vol. 240, 375-457.
- Dowding, C. H. (1985). Blast Vibration Monitoring and Control. Prentice-Hall, Inc., Englewood Cliffs, N.J.
- Drnevich, V. P., Hall, J. R., Jr., and Richart, F. E., Jr. (1967). "Large Amplitude Vibration Effects on the Shear Modulus of Sand." Contract Report No. DA-22-079-eng-340 NWER Subtask 13.009, U.S. Army Engineer Waterways Experiment Station, CE, Vicksburg, MS.
- Duffy, J., and Mindlin, R. D. (1957). "Stress-Strain Relations and Vibrations of a Granular Medium." Applied Mechanics Division, ASME, Vol. 24, 585-593.

Felice, C. W. (1986). "The Response of Soil to Impulse Loads Using the Split-Hopkinson Pressure Bar Technique." AFWL-TR-85-92, Air Force Weapons Laboratory, Air Force Systems Command and Kirtland Air Force Base, NM.

Felice, C. W., Gaffney, E. S., Brown, J. A., and Olsen, J. M. (1987). "Dynamic High Stress Experiments on Soil." Geotechnical Testing Journal, GTJODJ, Vol. 10, 192-202.

Fletcher, E. B. and Poorooshasb, H. B. (1968). "Response of a Clay to Low Magnitude Loads Applied at a High Rate." Proceedings of the International Symposium on Wave Propagation and Dynamic Properties of Earth Material, Univ. of New Mexico, 781-786.

Foster, C. R. (1962). "Field Problem: Compaction." Foundation Engineering, G.A. Leonards (ed), McGraw-Hill, New York, NY, 1000-1024.

Fredlund, D. G. (1979). "Appropriate Concepts and Technology for Unsaturated Soils." Second Canadian Geotechnical Colloquium, Canadian Geotechnical Journal, Vol. 16, No. 1, 121-139.

Fredlund, D. G. (1986). "Soil Mechanics Principles that Embrace Unsaturated Soils." Proceedings of the Eleventh ICSMFE, San Francisco, Vol. 2, 465-472.

Fredlund, D. G., and Hasan, J. U. (1979). "One-Dimensional Consolidation Theory: Unsaturated Soils." Canadian Geotechnical Journal, Vol. 1, No. 3, 521-531.

Fredlund, D. G., Hasan, J. U., and Filson, H. L. (1980). "The Prediction of Total Heave." Fourth International Conference on Expansive Soils, Denver, CO, 1-17.

Fredlund, D. G., and Morgenstern, N. R. (1976). "Constitutive Relations for Volume Change in Unsaturated Soils." Canadian Geotechnical Journal, Vol. 13, No. 3, 261-276.

Fredlund, D. G., and Morgenstern, N. R. (1977). "Stress State Variables for Unsaturated Soils." Journal of Geotechnical Engineering, ASCE, Vol. 103, No. GT5, 447-466.

Hardin B. O. (1961). "Study of Elastic Wave Propagation and Damping in Granular Materials." Presented to the University of Florida, Gainesville, Fl, in partial fulfillment of the requirements for the degree of Doctor of Philosophy.

Hardin B. O., and Richart, F. E., Jr. (1963). "Elastic Wave Velocities in Granular Soils." Journal of the Soil Mechanics and Foundation Engineering Division, ASCE, Vol. 89, No. SM1, 33-65.

Hendron, A. J. (1963). "The Behavior of Sand in One-Dimensional Compression." Thesis presented to the University of Illinois, Urbana,

IL, in partial fulfillment of the requirements for the degree of Doctor of Philosophy.

Hendron, A. J., Davisson, M. T., and Parolao, J. F. (1969). "Effect of Degree of Saturation on Compressibility of Soils from the Defence Research Establishment, Suffield." P.O. No. WESBPJ-68-67, U.S. Engineer Waterways Experiment Station, CE, Vicksburg, MS.

Holtz, R. D., and Kovacs, W. D. (1981). An Introduction to Geotechnical Engineering. Prentice-Hall, Englewood Cliffs, NJ.

Hopkinson, B. (1914). "A Method of Measuring the Pressure Produced in the Detonation of High Explosives or by the Impact of Bullets." Philosophical Transactions of the Royal Society of London, Series A, Vol. 213, 437-456.

Hryciw, R. D., and Dowding, C. H. (1987). "Cone Penetration of Partially Saturated Sands." Geotechnical Testing Journal, GTJODJ, Vol. 10, No. 3, 135-141.

Jackson, J. G., Jr., Ehrgott, J. Q., and Rohani, B. (1980). "Loading Rate Effects on Compressibility of Sand." Journal of Geotechnical Engineering, ASCE, Vol. 106, No. GT8, 839-852.

Jennings, J. E. B., and Burland, J. B. (1962). "Limitations to the Use of Effective Stresses in Partially Saturated Soils." Geotechnique, Vol. 12, No. 2, 125-144.

Juang, C. H., and Holtz, R. D. (1986). "Fabric, Pore Size Distribution, and Permeability of Sandy Soils." Journal of Geotechnical Engineering, ASCE, Vol. 112, No. 9, 855-868.

Klute, A. (1986). "Water Retention: Laboratory Methods." Methods of Soil Analysis, Part I. Physical and Mineralogical Methods. 2nd Ed. Soil Science Society of America, Publishers, Madison, WS, 635-661.

Kolbuszewski, J.J. (1948). "An Experimental Study of Maximum and Minimum Porosities of Sands." Proceedings of the Fourth International Conference for Soil Mechanics and Foundation Engineering, Rotterdam, Netherlands, Vol. 2, pp. 158-165.

Kolsky, H. (1949). "An Investigation of the Mechanical Properties of Materials at Very High Rates of Loading." Proceedings of the Physical Society, Section B, Vol. 62, 676-700.

Kolsky, H. (1963). Stress Waves in Solids. Dover Publications, Inc., New York, NY.

Ladd, R. S. (1977). "Specimen Preparation and Cyclic Stability of Sands." Journal of Geotechnical Engineering, ASCE, Vol. 103, No. GT6, 535-547.

Lambe, T. W., and Whitman, R. V. (1969). Soil Mechanics. John Wiley and Sons, New York, NY.

Lindholm, U. S. (1971). Techniques in Metals Research, R. F. Bunshah (ed), Vol. 5 Part I. Interscience, New York, NY.

Martin, J. W. (1957). "Correlation of Sonic Engineering Properties of Soils through Use of the Soniscope." Presented to M.I.T. in partial fulfillment of the requirements for the degree of Master of Science.

Matyas, E. H., and Radhakrishna, H. S. (1968). "Volume Change Characteristics of Partially Saturated Soils." Geotechnique, Vol. 18 No. 4, 432-448.

McWhorter, D., and Sunada, D. K. (1977). Groundwater Hydrology and Hydraulics. Water Resources Publications, Littleton, CO.

Moore, P. J. (1963). "Report No. 21: One-Dimensional Compression and Wave Propagation." Contract No. DA-22-079-eng-224, U.S. Army Engineer Waterways Experiment Station, CE, Vicksburg, MS.

Mulilis, J. P., Seed, H. B., Chan, C. K., Mitchell, J. K., and Arulanandan, K. (1977). "Effects of Sample Preparation Technique on Sand Liquefaction." Journal of Geotechnical Engineering, ASCE, Vol. 103, No. GT2, 91-108.

Nicholas, T. (1982). Impact Dynamics, Zukas, J. A., Nicholas, T., Swift, H. F., Greszczuk, L. B., Curran, D. R. (eds). John Wiley and Sons, New York, NY.

Nimmo, J. R., and Akstin, K. C. (1988). "Hydraulic Conductivity of a Sandy Soil at Low Water Content After Compaction by Various Methods." Journal of the Soil Society of America, Vol. 52, 303-310.

Richart, F. E., Jr., Hall, J. R., Jr., and Woods, R. D. (1970). Vibrations of Soils and Foundations. Prentice-Hall, Inc., Englewood Cliffs, NJ.

Rinehart, J. S. (1975). Stress Transients in Solids. HyperDynamics, Santa Fe, NM.

Ross, C. A. (1989). Unpublished Data. Engineering and Services Laboratory, AF Engineering and Services Center, Tyndall AFB, FL.

Ross, C. A., Nash, P. T., and Friesenhahn, C. J. (1986). "Pressure Waves in Soils Using a Split-Hopkinson Pressure Bar." ESL-TR-86-29 Engineering and Services Laboratory, AF Engineering and Services Center, Tyndall AFB, FL.

Ross, C. A., Thompson, P. Y., and Charlie, W. A. (1988). "Moisture Effects on Wave Propagation in Soils." ASCE/EMD Specialty Conference, Blacksburg, VA.

Stoll, R. D., and Ebeido, I. A. (1965). "Shock Waves in Granular Soil." Journal of the Soil Mechanics and Foundation Engineering Division, ASCE, Vol. 91, No. SM4, 107-125.

Weidlinger, P., and Matthews, A. T. (1964). "Shock and Reflection Phenomena in a Nonlinear Medium." Paper presented at the ASCE Structural Engineering Conference, New York, NY.

Whitman, R. V. (1970). "The Response of Soils to Dynamic Loadings." Contract No. DA-22-079-eng-224, U.S. Army Engineer Waterways Experiment Station, CE, Vicksburg, MS.

Whitman R. V., Miller, E. T., and Moore, P. J. (1964). "Yielding and Locking of Confined Sand." Journal of the Soil Mechanics and Foundation Engineering Division, ASCE, Vol. 90, No. SM4, 57-84.

Whitman, R. V., Roberts, J. E., and Mao, S. (1960). "Report 4: One-Dimensional Compression and Wave Velocity Tests." Contract No. DA-22-079-eng-224, U.S. Army Engineer Waterways Experiment Station, CE, Vicksburg, MS.

Wood, A. B. (1930). A Textbook of Sound. McGraw Hill, New York, NY.

Wu, S., Gray, D. H., and Richart, F. E. (1984). "Capillary Effects on Dynamic Modulus of Sands and Silts." Journal of Geotechnical Engineering, ASCE, Vol. 110, No. 9, 1188-1203.

Youd, T. L., and Craven, T. N. (1975). "Lateral Stress in Sands During Cyclic Loading." Journal of Geotechnical Engineering, ASCE, Vol. 101, No. GT2, 217-221.